DOE/MC/29228 -- 5641
(DE97002275)

Selective Methane Oxidation Over Promoted Oxide Catalysts

Topical Report
September 8, 1992 - September 7, 1996

Work Performed Under Contract No.: DE-FG21-92MC29228

For
U.S. Department of Energy
Office of Fossil Energy
Morgantown Energy Technology Center
P.O. Box 880
Morgantown, West Virginia 26507-0880

By
Zettlemoyer Center for Surface Studies
and Department of Chemistry
Lehigh University
Bethlehem, Pennsylvania 18015

Disclaimer

SELECTIVE METHANE OXIDATION OVER PROMOTED OXIDE CATALYSTS

TABLE OF CONTENTS

SELECTIVE METHANE OXIDATION OVER PROMOTED OXIDE CATALYSTS

LIST OF FIGURES

SELECTIVE METHANE OXIDATION OVER PROMOTED OXIDE CATALYSTS

LIST OF TABLES

SELECTIVE METHANE OXIDATION OVER PROMOTED OXIDE CATALYSTS

EXECUTIVE SUMMARY

Kamil Klier and Richard G. Herman
Lehigh University, Bethlehem, PA 18015

The objective of this research was to selectively oxidize methane to C_2 hydrocarbons and to oxygenates, in particular formaldehyde and methanol, in high space time yields using air at the oxidant under milder reaction conditions that heretofore employed over industrially practical oxide catalysts. The research carried out under this U.S. DOE-METC contract was divided into the following three tasks:

Task 1. Maximizing Selective Methane Oxidation to C_2^+ Products Over Promoted SrO/La_2O_3 Catalysts.

Task 2. Selective Methane Oxidation to Oxygenates.

Task 3. Catalyst Characterization and Optimization.

Under Task 1, it was found that surface doping the strongly basic SrO/La_2O_3 catalyst with sulfate by impregnation doubled the catalytic activity toward C_2 hydrocarbon formation at temperatures as low at 500°C, and at the same time significantly improved the selectivity toward the C_2 hydrocarbon products. The selectivity is at least partly controlled by the level of methane converted to products and the availability of oxygen. The most active and selective catalyst consisted of 1 wt% SO_4^{2-}/1 wt% SrO/La_2O_3 that operated in the 500-700°C temperature range to convert a CH_4/air = 1/1 reactant mixture at 0.1 MPa and gas hourly space velocity (GHSV) = 70,000 ℓ/kg catalyst/hr to C_2 hydrocarbons.

Under Task 2, high surface area silica-supported vanadia catalysts have been prepared and shown to exhibit the highest productivities toward formaldehyde formation from CH_4/air = 1.5/1.0 reactant mixtures at 580-639°C. The catalysts contained the equivalent of 1-5 wt% V_2O_5 impregnated into Cab-O-Sil, with the 1 wt% V_2O_5/SiO_2 catalyst exhibiting the highest selectivity toward formaldehyde. Using the concept that methane can be activated to form methyl radicals that could be stabilized on a catalyst surface long enough to be hydrolyzed by steam to form methanol, a dual bed catalyst system was designed. In this configuration, the first catalyst bed consisted of the 1 wt% SO_4^{2-}/1 wt% SrO/La_2O_3 catalyst and the second bed was typically the 1 wt% V_2O_5/SiO_2 catalyst. Using a steam-containing reactant mixture, e.g. CH_4/air/steam = 1.5/1.0/0.2 at 0.1 MPa and ≈70,000 ℓ/kg catalyst/hr, high productivity of both formaldehyde and methanol was obtained, along with higher yields of C_2 hydrocarbons.

Indeed, it was found that even over the single bed V_2O_5/SiO_2 catalyst, both the space time yield of and selectivity toward formaldehyde were improved by the presence of steam in the methane/air reactant mixture, and an attractive feature of the product mixture was the low quantity of carbon dioxide produced. Space time yields of >1.2 kg CH_2O/kg catalyst/hr have been achieved. High surface area V_2O_5-SiO_2 xerogel catalysts were synthesized that exhibited high space time yields of methanol at 625-650°C, but they tended to form more CO_2 than the impregnated catalysts.

Characterization studies carried out under Task 3 greatly aided in providing an understanding of the functioning of the catalysts. Chemical and *in situ* laser Raman studies of the $SO_4^{2-}/SrO/La_2O_3$ catalysts demonstrated that carbonate build-up on the catalysts under low temperature and/or low flow rate conditions led to at least partial deactivation of the catalysts. However, this deactivation was reversible by increasing the reaction temperature above 580°C and using a moderate GHSV. *In situ* laser Raman studies of vanadia catalysts with a variety of supports demonstrated that highly reducible vanadium, e.g. on SnO_2, led to deep oxidation of the methane to form CO_2. The study also showed that methane alone could not reduce the surface vanadia species and suggested that V=O is not the active site for the initial activation of the methane molecule. NMR and XRD studies of the V_2O_5-SiO_2 xerogel catalysts indicated that in low vanadium-containing catalysts, dispersed tetrahedral V acts as the active and selective site for methane conversion, while high vanadium-containing catalysts contain crystalline V_2O_5 that leads to deep oxidation of methane to form CO_2. Thus, selective formation of formaldehyde and methanol occurs with fairly low loading of vanadium on silica catalysts.

Although low productivity of CO_2 has been achieved over vanadia/silica catalysts, improved product selectivities of these processes are still needed. Optimization of the catalysts and the engineering of the processes developed here still need to be carried out, especially in regard to the direct synthesis of methanol from methane.

Principal accomplishments for the development of catalyst systems that produce high space time yields of C_2 hydrocarbons, formaldehyde, and methanol by the direct, selective oxidation of methane include the following:

- the 1 wt% $SO_4^{2-}/SrO/La_2O_3$ promoted catalyst developed here produced over 2 kg of C_2 hydrocarbons/kg catalyst/hr at 550°C,
- V_2O_5/SiO_2 catalysts have been prepared that produce up to 1.5 kg formaldehyde/kg catalyst/hr at 630°C with low CO_2 selectivities, and
- a novel dual bed catalyst system has been designed and utilized to produce over 100 g methanol/kg catalyst/hr at 600°C with the presence of steam in the reactant mixture.

SELECTIVE METHANE OXIDATION OVER PROMOTED OXIDE CATALYSTS

PROJECT OBJECTIVES

The objectives of this research were centered on the selective partial oxidation of methane, either by oxidative coupling of methane to C_2 hydrocarbons (Equations 1-3) or selective oxidation of methane to oxygenates, in particular formaldehyde and methanol as represented by Equations 4 and 5. Air, rather than nitrous oxide, was utilized as the oxidizing gas at high gas hourly space velocity, but mild reaction conditions (500-700°C, 1 atm total pressure). All of the investigated processes were catalytic, aiming at minimizing difficult to control gas phase reactions.

$$2CH_4 + 1/2O_2 \rightleftarrows C_2H_6 + H_2O \quad (1)$$

$$2CH_4 + O_2 \rightleftarrows C_2H_4 + 2H_2O \quad (2)$$

$$2CH_4 + 2CO_2 \rightleftarrows C_2H_4 + 2CO + 2H_2O \quad (3)$$

$$CH_4 + O_2 \rightleftarrows CH_2O + H_2O \quad (4)$$

$$CH_4 + 1/2O_2 \rightleftarrows CH_3OH \quad (5)$$

Oxide catalysts were chosen for this research, and they were generally surface doped with small amounts of acidic dopants or redox dopants. For example, it was proposed and shown that the very basic SrO/La_2O_3 catalyst that is active in the formation of methyl radicals, and therefore of C_2^+ hydrocarbon products, could be doped with sulfate to increase further its activity and selectivity to C_2 hydrocarbon products.

The research carried out under this U.S. DOE-METC contract was divided into the following three tasks:

Task 1. Maximizing Selective Methane Oxidation to C_2^+ Products Over Promoted SrO/La_2O_3 Catalysts.

Task 2. Selective Methane Oxidation to Oxygenates.

Task 3. Catalyst Characterization and Optimization.

Task 1 dealt with the preparation, testing, and optimization of acidic promoted lanthana-based catalysts for the synthesis of C_2^+ hydrocarbons. Task 2 aimed at the formation and optimization of promoted catalysts for the synthesis of oxygenates, in particular formaldehyde and methanol. Task 3 involved analysis and characterization of the most promising catalysts so that optimization can be achieved.

INTRODUCTION

Perspectives on the Development of Active Oxide Catalysts for the Direct Selective Oxidation of Methane

Currently, methane (as natural gas) is utilized as the feedstock resource for synthesizing methanol, part of which is subsequently converted to formaldehyde. In this process, methane is first converted to synthesis gas (H_2 + CO) by steam reforming over nickel-based catalysts, as represented by Step 1 shown in Equation 6.

$$CH_4 \overset{1}{\Rightarrow} CO/H_2 \overset{2}{\Rightarrow} CH_3OH \overset{3}{\Rightarrow} CH_2O \qquad (6)$$

Step 1 is a high temperature process, e.g. carried out at 850°C, that is energy intensive. In the three-step process, methanol is the formaldehyde precursor, and approximately 60% of the cost of this precursor arises from the high temperature steam reforming of methane to produce synthesis gas (Step 1). Thus, there is a significant economic incentive to develop a one-step direct conversion of methane to methanol and/or formaldehyde that would by-pass methane reforming (Step 1).

Since much more research has been carried out for the direct conversion of methane to formaldehyde than for the direct synthesis of methanol, an historical perspective is presented here to demonstrate the progress made and the opportunities that arise in achieving the selective oxidative conversion of methane to oxygenates over heterogeneous metal oxide catalysts. The primary oxidative conversion processes that methane undergoes are shown in Equations 1,4,5,7,8. All of these reactions are thermodynamically favorable, but Reaction 2 is the most favored of these oxidation processes. Thus, selective formation of formaldehyde (and methanol) can be viewed as a problem in controlling the kinetics of these reactions. The approach taken here is centered upon developing a selective oxide catalyst that is active at moderate reaction temperatures.

$$CH_4 + 2\,O_2 \Rightarrow CO_2 + 2H_2O \qquad (7)$$
$$CH_4 + 0.5\,O_2 \Rightarrow CO + H_2 \qquad (8)$$
$$2CH_4 + 0.5\,O_2 \Rightarrow C_2H_6 + H_2O \qquad (1)$$
$$CH_4 + O_2 \Rightarrow CH_2O + H_2O \qquad (4)$$
$$CH_4 + 0.5\,O_2 \Rightarrow CH_3OH \qquad (5)$$

Intimately involved with the selective formation of formaldehyde and methanol is the suppression of secondary reaction processes. At high temperatures, secondary reactions readily occur, especially those involving further reaction with free radicals. In the case of formaldehyde, direct oxidation to form CO can also occur, as represented by Equation 9. To prevent reactions such as this from occurring, moderate temperatures and quick removal

of reaction products from the synthesis zone of the reactor, i.e. short residence times, are approaches to be taken.

$$CH_2O + 0.5\,O_2 \Rightarrow CO + H_2O \quad (9)$$

The emphasis in this report and in our research is placed on the space time yields of products achieved in continuous flow reactors over heterogeneous catalysts, *not* on the %yields, although these latter quantities are sometimes reported, especially with respect to C_2 coupling products. There are many publications in this area of research, and those quoted here are principally those reporting first results or significant increases in the productivity of products synthesized directly from methane.

Methane Conversion *via* Coupling to C_2 Hydrocarbons

Saturated linear hydrocarbons, particularly methane, are major components of natural gas. While methane makes an excellent gaseous fuel, it is desirable to convert it to higher molecular weight products for transportation, storage, and for utilization as chemical feedstocks. The principal desired reactions were previously given in Equations 1, 2, 4, and 5. As pointed out, another reaction of potential interest is CO_2-induced coupling of methane to form ethene, as shown in Equation 3.

After Keller and Bhasin published their research results for methane coupling over a decade ago [1], many laboratories have been striving to develop efficient methane conversion catalysts and technologies for selective formation of C_2 hydrocarbons. At present, there is no commercial technology for processes of the type represented by Equations (1)-(5)] above, despite the sizeable patent and open literature on this subject. Various aspects of the state of the art of methane oxidation, including early developments, have been reviewed by Foster in 1985 [2], Gesser et al. in 1985 [3], Pitchai and Klier in 1986 [4], Scurrell in 1987 [5], Lee and Oyama in 1988 [6], Hutchings et al. in 1989 [7], Amenomiya et al. in 1990 [8], Lunsford in 1990 and 1991 [9,10], Mackie in 1991 [11], Hamid and Moyes in 1991 [12], Forlani and Rossini in 1992 [13], Krylov in 1993 [14], and Zhang et al. in 1994 [15]. Therefore, the literature will not be extensively reviewed here. Upon analysis of the available data, it was pointed out that the catalytic C_2 coupling reaction is a high temperature reaction, usually carried out in the 700-800°C range, and apparently has an upper limit of ≈25% yield [13].

Progress in Direct Formaldehyde Synthesis Before 1986

Although intensive research has been carried out recently on the direct oxidative conversion of methane to oxygenates, the field has not been extensively reviewed. Therefore, the research results reported in the literature for the direct conversion of methane

to formaldehyde will be summarized here. Since much less research has been directed toward the direct conversion of methane to methanol, available literature reports will be given when methanol and formaldehyde are co-products (discussed below) and when our results are discussed later in this report.

The direct synthesis of formaldehyde has long been of interest, and it had been reported that during World War II, formaldehyde was industrially produced from methane in Eastern Europe [16]. In one process carried out in Copsa Mica, Romania [16], the synthesis reaction utilized a trace amount of NO as "catalyst" and produced CH_2O from methane/air = 1.0/3.7 mixtures (with recycle) at 400-600°C and atmospheric pressure in a silica/alumina ceramic-lined furnace. With four furnaces at the plant, 18 metric tons/month of formaldehyde (100% basis) were produced during World War II and at least until 1947. A small amount of methanol was formed as a side product.

Toward the end of World War II, a catalytic process was being developed by Germany at the Hibernia Stickstoffwerke at Herne using 0.5 wt% Ag_2O/BaO_2 supported on unglazed porcelain clips (10/90 wt%) [16], where the reactant mixture consisted of 30 vol% ozonized oxygen and 70 vol% dry coke oven gas, which resulted in ≈49% CH_4 in the final mixture. Demonstration runs of up to six weeks were made using typical catalyst volumes of 242 ℓ, and it was reported that up to ≈30 g CH_2O/ℓ catal/hr (corresponding to ≈25% conversion of methane to formaldehyde with total gas hourly space velocity (GHSV) = 100 ℓ/ℓ catal/hr) could be produced at 80-120°C with the non-uniformly heated catalyst bed [16]. However, the typical flow rate employed was 8 ℓ/ℓ catal/hr that resulted in a productivity of ≈1.2 g CH_2O/ℓ catal/hr.

Little further research was carried out on the direct synthesis of formaldehyde until 1970, when insight into the selective oxidation of methane to formaldehyde was provided by Cullis et al. [17] who were investigating metal catalysts dispersed on oxide supports. It was found that the product selectivity was switched from deep oxidation products toward formaldehyde by addition of pulses of chloromethane and dichloromethane to the methane/oxygen reactant mixture over a Pd/ThO_2 catalyst. Mann and Dosi observed similar behavior upon injection of halomethanes, especially with dichloromethane, into the reactant stream over Pd/Al_2O_3 catalysts [18]. Although the halogens exhibited a significant promotional effect, the productivity of formaldehyde over both of these catalysts was low.

In the early 1970s, two patents claimed high space time yields of oxygenates over MoO_3-containing catalysts. In 1971, Dowden and Walker reported [19] very significant space time yields of methanol and formaldehyde over a catalyst consisting of 5% $(MoO_3)_3 \bullet Fe_2O_3$ supported on an alumina/silica (Al_2O_3/SiO_2 = 25/75) catalyst that had been sintered at 1000°C to obtain a surface area of 0.1 m^2/g. With a CH_4/O_2 = 96.9/3.1 vol% reactant mixture at 439°C and 5.3 MPa with GHSV of 46,000 hr^{-1}, the methane conversion level was 2.1% and the observed productivities of formaldehyde and methanol were 100 and 869 g/kg catal/hr, respectively. It is noted that this was a high pressure process. It was

reported that these productivities were achieved by quenching the products just below the catalyst bed to <200°C by injection of water.

In 1975, it was disclosed by Stroud [20] that adding a small quantity of ethane to the methane reactant was beneficial for oxygenate production over a $CuO \bullet MoO_3$ catalyst, but at the same time, the oxygen conversion must be <75%. For example, with a reactant stream consisting of $CH_4/C_2H_6/O_2/N_2 \approx 89.5/5.9/3.3/1.3\%$ at 485°C, 2 MPa, and with GHSV = 46,700 hr^{-1}, 109.4 and 356.5 g/kg catal/hr of formaldehyde and methanol were produced, respectively, corresponding to molar selectivities of 13.1 and 10.0%. Other products included some C_2 oxygenates, C_2H_4, CO, and CO_2 [20].

In the early 1980s, it was found that silica (Cab-O-Sil) supported MoO_3 catalysts produced formaldehyde, methanol, and CO (with little or no CO_2) at 550-600°C and <0.1 MPa from $CH_4/N_2O/H_2O$ mixtures (typically ≈ 0.20-0.25/1/1) [21-24]. For example, Liu et al. [23] showed that with a $CH_4/N_2O/H_2O$ reactant mixture with partial pressures of 75/280/260 torr, respectively, at 594°C with GHSV = 4387 ℓ/kg catal/hr, 17.44 g/kg catal/hr of formadehyde with 49.5% selectivity (6.0% CH_4 conversion) along with 2.93 g/kg catal/hr of methanol (plus CO and CO_2) were produced over a MoO_3/Cab-O-Sil catalyst. Using O_2 as the oxidant in CH_4-rich reactant gas mixtures containing 3.11 mol% H_2O over a 5 wt% $MoO_3/SiO_2 \bullet Al_2O_3$ catalyst, Pitchai and Klier obtained a similar space time yield of CH_2O (≈9 g/kg catal/hr) at 600°C but no methanol [4]. A comparison of the formaldehyde productivities achieved in these quoted studies is shown in Figure 1.

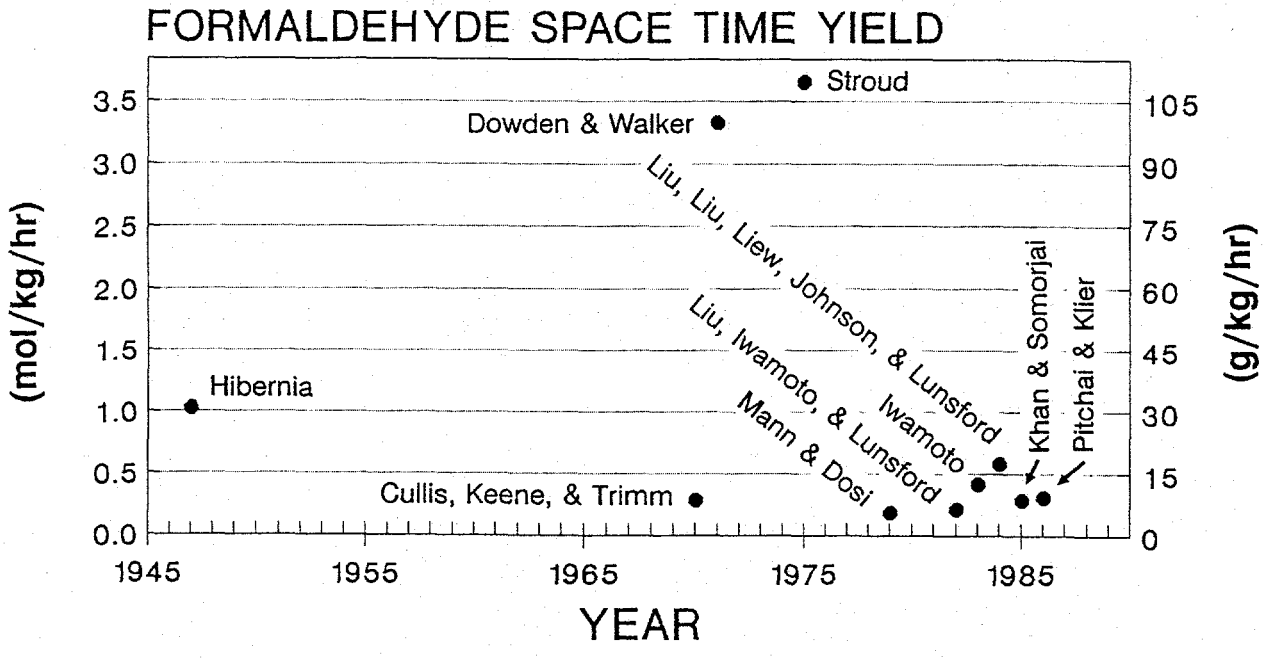

FIGURE 1. Space time yields reported up to 1986 for the direct synthesis of formaldehyde *via* methane oxidation over heterogeneous catalysts in continuous flow reactors.

Liu et al. [23] provided particular insight into the mechanism of the activation of methane and conversion to oxygenates by proposing a mechanism, based on catalytic results (with N_2O as the oxidant in the presence of steam), electron spin resonance, and infrared spectroscopic evidence obtained with MoO_3/SiO_2 catalysts, in which $^{\bullet}CH_3$ reacted with the surface $Mo^{5+}O^{2-}$ moiety to form surface CH_3O^- species, as shown in Equations 10-14.

$$Mo^{5+} + N_2O \Rightarrow Mo^{6+}O^- + N_2 \quad (10)$$

$$Mo^{6+}O^- + CH_4 \Rightarrow Mo^{6+}OH^- + {}^{\bullet}CH_3 \quad (11)$$

$$Mo^{6+}O^{2-} + {}^{\bullet}CH_3 \Rightarrow Mo^{5+}OCH_3^- \quad (12)$$

$$Mo^{5+}OCH_3^- + Mo^{6+}O^{2-} \Rightarrow Mo^{4+} + Mo^{5+}OH^- + CH_2O \quad (13)$$

$$Mo^{6+}OH + Mo^{5+}OH^- \Rightarrow Mo^{5+} + Mo^{6+}O^{2-} + H_2O \quad (14)$$

As indicated, it was proposed that O^- was the reactive form of oxygen that abstracted a hydrogen from CH_4 to yield a methyl radical that subsequently formed the methoxide species. It was pointed out that reaction of the methoxide species with water in the reactant stream should yield methanol, although some studies did not detect methanol among the products formed [4]. Comparative studies of methane oxidation over MoO_3-based catalysts using N_2O and O_2 as oxidizing agents indicated that the partial oxidation products were favored by high CH_4/O_2 molar ratios but low CH_4/N_2O molar ratios [4]. The literature on selective oxidation of methane was reviewed up to 1985 by Pitchai and Klier [4], and mechanistic schemes proposed by others were also discussed.

Formaldehyde Catalyst Development After 1986

MoO_3/SiO_2 Catalysts. Significant improvements in the productivity of direct formaldehyde synthesis from methane were made after 1986. Much of the research effort continued with MoO_3-containing catalysts, but vanadia-based catalysts were also explored. The usual support for these catalysts was high surface area Cab-O-Sil, which is a silica that is particularly free of impurities, but other supports were investigated as well.

Using a CH_4/O_2 = 9/1 reactant mixture at 0.1 MPa and 650°C over Na-free MoO_3/SiO_2 catalysts (e.g. Cab-O-Sil or acid-washed (to remove alkali impurities) silica gel containing 1.8 wt% Mo), Spencer obtained [25] space time yields of formaldehyde as high as 95.4 mol/kg catal/hr (with GHSV = 5000 hr^{-1}, 6.9% CH_4 conversion was achieved with 25% selectivity to CH_2O). It was shown that as the methane conversion level was increased, e.g. by increasing temperature and/or decreasing GHSV, the formaldehyde selectivity decreased, but the CO selectivity increased and CO_2 remained approximately 10% of the product slate. It was demonstrated that small quantities of sodium tended to poison the promotional behavior of Mo on the silica support and suppressed methane conversion and formaldehyde selectivity. The experimental data fit the model in which sodium inhibited the direct oxidation of methane to formaldehyde but promoted the oxidation of formaldehyde to carbon monoxide [26]. This inhibiting effect of sodium on a 7 wt% MoO_3/Cab-O-Sil

catalyst was confirmed under low methane conversion conditions (<0.13%) by Kennedy et al. [27] when O_2 (CH_4/O_2 = 28/1) was used as the oxidant at 550°C. From the experimental data, Spencer proposed [25] that CO_2 and CH_2O were formed by parallel pathways over the Na-free MoO_3-promoted catalysts.

The structure of the molecularly dispersed surface molybdenum oxide species on SiO_2 has recently been determined by the application of several *in situ* spectroscopic methods. At elevated temperatures and in the presence of oxygen, *in situ* X-ray absorption near-edge spectroscopy (XANES) measurements revealed that the surface molybdenum oxide species on SiO_2 possess a coordination that is between tetrahedral and octahedral [28]. Corresponding *in situ* Raman and extended X-ray absorption fine structure spectroscopy (EXAFS) measurements demonstrated that the surface molybdenum oxide species on SiO_2 was present as an isolated species [28,29]. *In situ* infrared studies employing ^{18}O-labelling further showed that the surface molybdenum oxide species on SiO_2 possesses only one terminal Mo=O bond [30].

The preparation method and the nature of the silica support were shown not to affect the molecular structure of the isolated surface molybdenum oxide species on SiO_2 [31]. However, the presence of alkali impurities decreased the number of isolated surface molybdenum oxide species and formed new alkali molybdate compounds [32]. Corresponding temperature programmed reduction studies showed that alkali molybdate compounds generally decreased the amount of reducible oxygen available in the catalysts. The methane oxidation reactivity was found to correlate with the isolated surface molybdenum oxide species that did not form alkali molybdate compounds, which revealed that the oxygen associated with the alkali molybdate compounds was not readily available for methane oxidation.

In situ Raman studies of the MoO_3/SiO_2 catalysts under methane oxidation reaction conditions were also obtained in order to determine the influence of the reaction environment on the surface molybdenum oxide species. These studies demonstrated that the isolated surface molybdenum oxide species was essentially unchanged by the methane oxidation reaction environment [32]. There was no direct evidence for the formation of a Mo-OCH_3 species that may have been present in trace quantities, and consequently not detected. The Mo-OCH_3 species could also not be directly detected with *in situ* Raman spectroscopy during methanol oxidation [31]. However, the isolated surface molybdenum oxide species was not stable during *methanol oxidation*, and this resulted in the formation of microcrystalline MoO_3 particles that aggregated, perhaps due to the formation of Mo-OCH_3, i.e. the formation of mobile Mo-OCH_3 species might induce the agglomeration of surface molybdenum oxide species and crystallization of MoO_3 on SiO_2. The relative stability of isolated surface molybdenum oxide species on SiO_2 during *methane oxidation* suggests that such intermediate species are less stable during this reaction. It has also been proposed that the active state of the molybdenum oxide species in MoO_3/SiO_2 catalysts employed for methane oxidation may be in the form of silicomolybdic acid species, $H_4SiMo_{12}O_{40}$ [33].

Recent *in situ* Raman studies by Banares et al. [34] showed that this species can be formed by exposing the MoO_3/SiO_2 catalyst to water-saturated air at room temperature for an extended period of time, but it was shown that this species was not stable above 300°C and decomposed to form isolated surface molybdenum oxide species. The decomposition of bulk silicomolybdic acid species at 300°C has also been reported by Rocchicciolil-Deltcheff et al. [35]. Thus, silicomolybdic acid species are not stable at the much higher temperatures employed for methane oxidation, i.e. ≥500°C.

V_2O_5/SiO_2 Catalysts. In contrast to the proposal that CO_2 and CH_2O were formed by parallel pathways from CH_4/O_2 over MoO_3-based catalysts [25], Spencer and Pereira [36] proposed that over V_2O_5/SiO_2 catalysts a sequential pathway leads to CO_2 formation, i.e.

$$CH_4 \Rightarrow CH_2O \Rightarrow CO \Rightarrow CO_2. \qquad (15)$$

The V_2O_5/SiO_2 (Cab-O-Sil) catalyst appeared to be more active than the MoO_3/SiO_2 catalyst, although the extrapolated data for the two catalysts at 575°C were similar, e.g. 32.5% CH_2O selectivity at 3% methane conversion. The sequential pathway over the V_2O_5/SiO_2 catalyst was consistent with the very low selectivities for CO_2 at low methane conversion levels and higher CO_2 selectivities at high CH_4 conversions observed over this catalyst.

Iwamoto, using N_2O in the presence of water as the oxidant instead of oxygen, also found that 2% V_2O_5/SiO_2 was a more active catalyst than 2% MoO_3/SiO_2 for oxidation of methane, and at 450°C a 92.7% selectivity to CH_2O was observed (0.5% CH_4 conversion to yield 1.12 g CH_2O/kg catal/hr) [37]. However, upon increasing the temperature to 550°C with the $CH_4/N_2O/H_2O/He$ = 1/2/4.7/2.3 reactant mixture at GHSV = 1800 ℓ/kg catal/hr, the activity of the catalyst increased to 11.2% CH_4 conversion, but the selectivity toward CH_2O decreased to 12.7% (but with a higher CH_2O productivity of 3.4 g/kg catal/hr) because of the formation of methanol.

During this same period of time, Lee and Ng [38] also investigated methane oxidation over 2 wt% vanadia-promoted SiO_2, $TiSiO_2$, and TiO_2 catalysts. The V_2O_5/SiO_2 catalyst was the most active of those investigated and gave the highest selectivity and productivity for formaldehyde. It was observed that N_2O was a much better oxidant than O_2, in terms of both activity and CH_2O selectivity, under the reaction conditions employed. With a reactant mixture of $CH_4/N_2O/He$ = 1/4/2 with GHSV = 4800 ℓ/kg catal/hr over a 2 wt% V_2O_5/SiO_2 catalyst, a high space time yield of 132.2 g CH_2O/kg catal/hr was obtained at 600°C and 0.1 MPa. This productivity occurred with a high methane conversion level of 31.5% and a formaldehyde selectivity of 51.0% (plus 35.4% CO and 13.6% CO_2). However, upon increasing the reaction temperature to 650°C, the CH_2O productivity dropped to zero. Under similar reaction conditions (600°C), a 1.7 wt% MoO_3/SiO_2 catalyst was appreciably less active (7.5% CH_4 conversion) and selective (42.7% CH_2O) than the corresponding vanadia catalyst, yielding 20.1 g CH_2O/kg catal/hr [38].

Recently, the molecular structure of the vanadium oxide species on the surface of 1 to 10 wt% V_2O_5/SiO_2 catalysts has been determined by *in situ* solid state ^{51}V NMR, Raman spectroscopy, and EXAFS/XANES studies. Comparison of the ^{51}V NMR spectra of the V_2O_5/SiO_2 catalysts to reference compounds with well-defined structures demonstrated that the surface vanadium oxide species possessed a tetrahedral structure contained one terminal V=O bond and three bridging V-O-Si bonds [39]. Similar conclusions were obtained from EXAFS/XANES measurements [40]. Raman studies were consistent with the above structure and also showed that the surface vanadium oxide species on SiO_2 were present as isolated moieties [39,41].

In situ Raman studies of the V_2O_5/SiO_2 catalysts have now been carried out in the current research, and the influence of the methane oxidation reaction conditions on the isolated surface vanadium oxide species was monitored. It was shown that during methane oxidation at 500°C, the isolated surface vanadium oxide species were not altered by the reaction environment (no shift nor diminution in the intense of the 1034 cm^{-1} V=O line) and no V-OCH_3 species were directly detected, and these results will be presented and discussed later in this report.

Double Redox Catalysts. A different approach to catalyst development was taken wherein double redox cations, e.g. Cu/Fe, were doped into high surface area [42] and low surface area supports [42,43]. For example, Anderson and Tsai synthesized a lattice-substituted Fe-ZSM-5 zeolite that was ion exchanged with Cu^{2+} and carried out methane oxidation studies with N_2O as the oxidant [42]. With CH_4/N_2O = 80/20 at 342°C and GHSV = 431,000 hr^{-1}, 6.2 C% of the product was CH_2O (at 1.12% CH_4 conversion). However, it was reported [48] that 50 C% of the product was CH_3OH, with the remainder being CO_2 (35%) and CO (8.5%). Decreasing the GHSV led to a slightly higher methane conversion but lower selectivity toward CH_2O and CH_3OH.

Sojka et al. [43,44] also utilized redox couples as methane oxidation catalysts, where low surface area ZnO (e.g. 0.5 m^2/g) was employed as the support and air was used as the oxidant. The concept was to predominantly activate oxygen on one reactive center, e.g. $Cu^{1+/2+}$ while the second center would activate methane to form stabilized methyl radicals, e.g. on $Fe^{3+/2}$ or $Sn^{4+/2+}$. Of those investigated, the best catalyst consisted of $Cu^{1+}/Fe^{3+}/ZnO$ = 1/1/98. As the reaction temperature was increased with this catalyst, the conversion of methane increased while the formaldehyde selectivity decreased. An optimum temperature of 750°C was observed for the formation of CH_2O in terms of productivity. At this temperature and at 0.1 MPa, a CH_4/air = 1/1 reactant mixture with GHSV = 70,000 ℓ/kg catal/hr produced 76 g CH_2O/kg catal/hr [44]. The methane conversion was low (2.5%), as was the formaldehyde selectivity (10%). The cationic dopants were found to be surface-enriched as Coulombic pairs and to function by switching the selectivity toward CH_2O and away from CO_2 at lower temperatures (<700°C) and away from C_2 hydrocarbons at higher temperatures (>700°C). A schematic model of the catalyst is shown in Figure 2.

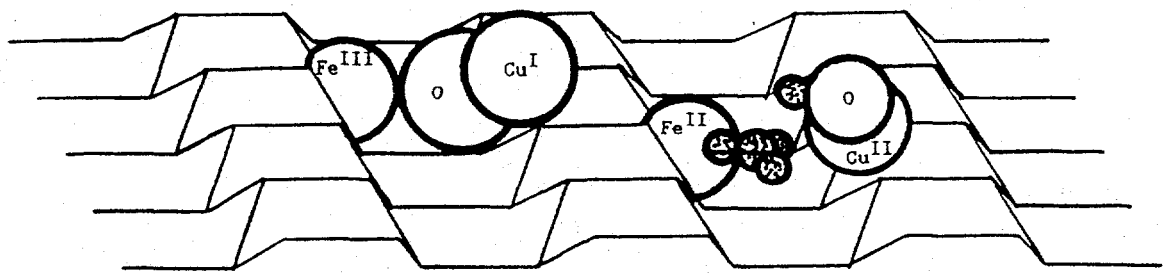

$CH_3{}^{\oplus}Fe^{2+}$ $\quad -H^{\oplus} \rightarrow \quad CH_3O^{\ominus} \quad -H^{\ominus} \rightarrow \quad H_2CO$

$HO^{\ominus}Cu^{2+}$

FIGURE 2. Schematic of the active ZnO surface containing Cu^{1+}/Fe^{3+} Coulombic redox pairs doped into the ZnO matrix.

While undoped ZnO exhibited only low activity, Hargreaves et al. [45] demonstrated that a low surface area (≈3 m^2/g) unpromoted C_2 coupling catalyst, i.e. MgO prepared by calcination of magnesium hydroxycarbonate, could be induced to produce formaldehyde as the principal product by controlling the reaction conditions. With a CH_4/O_2/diluent = 6/1/6 reactant mixture at 850°C and 0.1 MPa, the oxygen consumption was controlled by varying the flow rate in the range of GHSV = 1,000-48,000 hr^{-1}. At high O_2 conversion (>70%), CO_2 was the dominant product, while in the range of about 10-70% O_2 conversion, CO was the principal product formed. However, at low levels of O_2 conversion in the range of 3-5%, formaldehyde was formed with ≈60% selectivity, with CO ≈ CO_2 ≈ 20%. Hargreaves et al. [45] proposed that the product selectivity for the partial oxidation of methane was controlled by the balance between methyl radical coupling and oxidation, which was guided by the abundance of O_2 through the reaction zone. It was subsequently pointed out that the maximum in the CH_2O selectivity pattern shown [45] corresponded to a formaldehyde productivity of 9 mol (270 g)/ℓ catal/hr [46] (bulk density of the catalysts was not given).

Double Bed Catalysts. Another reaction engineering approach to produce high space time yields of CH_2O was taken by Sun et al. [47], where a double catalyst bed was utilized to enhance the productivity of CH_2O. The concept of this experiment is shown in Figure 3, where the first catalyst consisted of 1 wt% SrO/La_2O_3, a very active methyl radical generator that oxidatively produces C_2 hydrocarbons from methane [48,49], while the second bed consisted of 2 wt% MoO_3/SiO_2 that is envisioned to trap the $^{\bullet}CH_3$ species long enough for reaction with activated oxygen on the surface of the catalyst, see Equations 8-11. Indeed, by using the dual bed configuration, CH_4 conversion was increased by two orders of magnitude at 630°C, while the CH_2O space time yield was tripled, as shown in Table 1 [47].

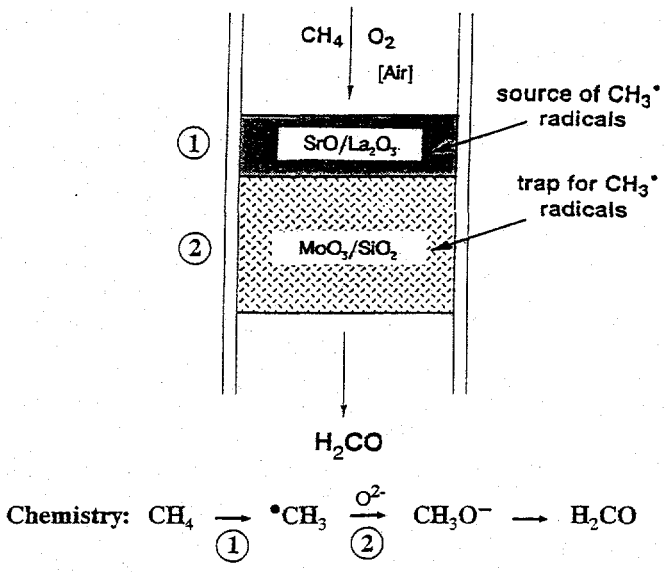

FIGURE 3. Schematic drawing of the double bed catalyst configuration for the oxidative conversion of methane to formaldehyde.

TABLE 1. Methane conversion, formaldehyde space time yield (STY), and formaldehyde selectivity from CH_4/Air = 1.5/1.0 at ambient pressure and with GHSV = 70,000 ℓ/kg cat/hr over a single bed 2 wt% MoO_3/SiO_2 catalyst and a double bed consisting of 1 wt% SrO/La_2O_3||2 wt% MoO_3/SiO_2 catalysts [47].

Temperature (°C)	CH_4 Conv. (mol%)	H_2CO STY (g/kg catal/hr)	H_2CO Sel. (C atom%)
• MoO_3/SiO_2 (0.100 g)			
595	0.02	10.8	100
630	0.08	37.9	100
665	0.24	39.7	31.5
• SrO/La_2O_3 || MoO_3/SiO_2 (0.025 g/0.100 g)			
525	0.4	2.3	1.0
560	3.1	18.8	1.3
595	5.4	62.1	2.4
630	8.2	129.0	3.3
665	11.3	52.4	1.0

It is clear from the data in Table 1 that a small amount of the SrO/La_2O_3 catalyst activated a large quantity of methane, and, indeed, the available oxygen was nearly completely consumed and converted to products. Formation of C_2 hydrocarbons was observed, and the quantity and selectivity of these increased with temperature. At the same time, the CO_2 selectivity progressively decreased. A *mechanically mixed* bed of the two catalysts produced almost no formaldehyde, which appeared to be converted to CO, in contrast to the double bed configuration [47].

SiO_2 as a Catalyst. As previously pointed out, most of the catalysts investigated for the conversion of methane to formaldehyde have been silica-supported catalysts. It has been shown that at least some silicas can activate methane, and under some reaction conditions formaldehyde is observed as a product [25,50-55]. Various forms of SiO_2 are available, and as pointed out eariler, the fumed silica Cab-O-Sil is a common form utilized as a catalyst support because it is of rather high purity. A comparison of Cab-O-Sil with a silica gel (Grace 636 gel) in terms of methane conversion and product selectivity has been carried out at 730°C [56], and the experimental results are shown in Table 2. Blank reactor runs with no catalyst showed negligible conversion of methane.

TABLE 2. Methane Conversion, Formaldehyde Space Time Yield (STY), and Product Selectivities From CH_4/Air = 1.5/1.0 at Ambient Pressure and 730°C with GHSV = 70,000 ℓ/kg cat/hr Over Cab-O-Sil (EH-5) and Silica Gel (Grace 636) Catalysts [56].

Silica	CH_4 Conv. (mol%)	H_2CO STY (g/kg/hr)	Selectivity (C mol%)			
			CH_2O	C_2 HC	CO	CO_2
Cab-O-Sil	0.31	75.7	46.0	39.1	--	14.9
Gel	1.36	267.0	38.8	11.4	41.8	8.0

The data in Table 2 show that the silica gel was much more active than the Cab-O-Sil, although both were high surface area materials, i.e. 385 and 480 m^2/g, respectively. Both silicas produced significant quantities of formaldehyde, but both also formed C_2 hydrocarbons. Over metal oxide promoted silicas, methyl radicals are stabilized long enough to react with activated oxygen to form oxygenates so that hydrocarbon synthesis is minimal or even eliminated. Lowering the reaction temperature to 630°C led to 100% formaldehyde selectivity (0.05 mol% CH_4 conversion) over the Cab-O-Sil catalyst, yielding 24.3 g CH_2O/kg catal/hr, as shown later in this report.

As the above discussion shows, between 1986 and 1992 progress was made in increasing the space time yield of formaldehyde formed directly from methane over oxide catalysts, and a comparison of these results is shown in Figure 4. It is noted that the later investigations utilized air or oxygen, rather than oxidants such as N_2O, as the oxidizing component of the reactant mixture.

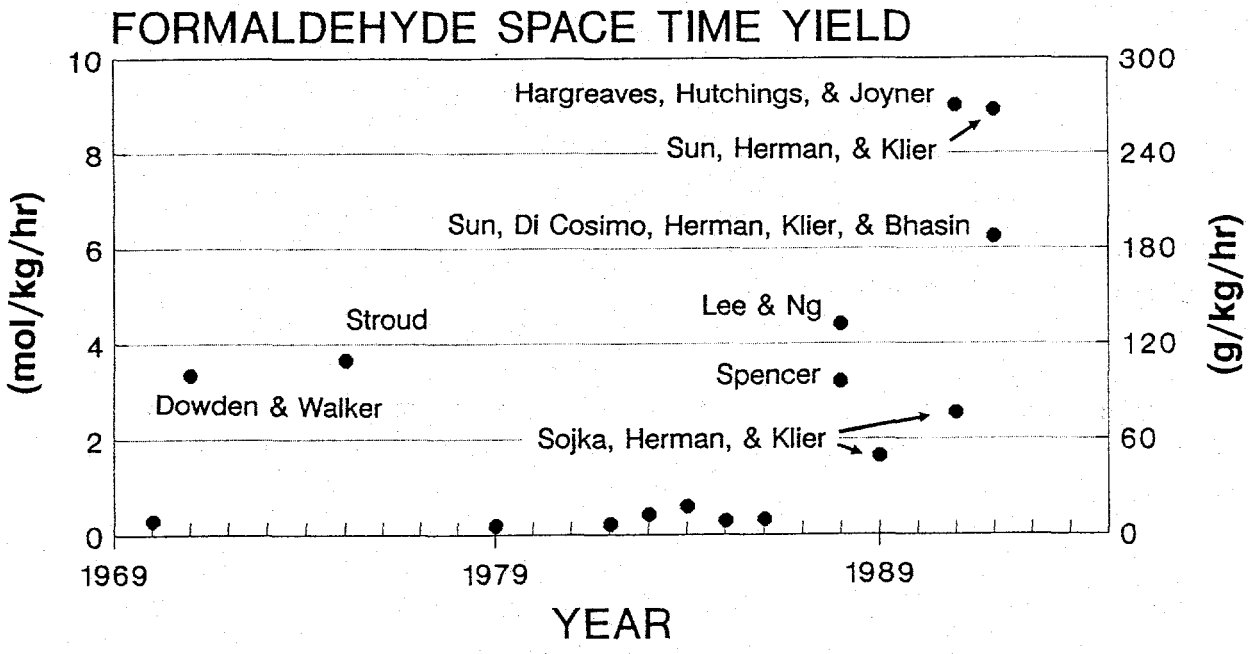

FIGURE 4. Comparison of space time yields of formaldehyde achieved recently by direct methane oxidation over heterogeneous catalysts in continuous flow reactors.

There are a number of ways to manipulate reaction conditions so that high % yields, e.g. elevated temperatures with very small catalyst beds, or space time yields, e.g. by employing high GHSV, are obtained. For example, it was shown that a silica gel catalyst was more active than Cab-O-Sil (Table 2), and to increase the space time yield of formaldehyde even more over the silica gel catalyst, the reaction temperature was increased to 780°C and the reactant gas flow was increased stepwise to GHSV = 560,000 ℓ/kg cat/hr [56]. Under these conditions, only 0.68 mol% CH_4 conversion was obtained, but the space time yield of 812.8 g CH_2O/kg catal/hr was achieved. The observed product selectivity (C atom%) was 28.0% CH_2O, 7.2% ethene, 31.6% ethane, 30.0% CO, and 3.2% CO_2.

RESULTS AND DISCUSSION OF THE TASKS

TASK 1. Maximizing Selective Methane Oxidation to C_2^+ Products Over Promoted SrO/La_2O_3 Catalysts

As pointed out in the Introduction, it is desirable to convert methane to higher molecular weight products for transportation, storage, and for utilization as chemical feedstocks. For the latter application, the C_2 hydrocarbons are especially attractive.

While the catalytic oxidative coupling paths, presented as Equations (1) and (2) on page 3, show considerable promise, it is evident from previously reported examples that the reaction conditions are still quite severe with the catalysts developed to-date, in particular that the reaction temperature, in the range 650-800°C, is still too high. Reactions leading to oxygenates (e.g. Equations (4) and (5) on page 3) are more difficult to conduct selectively, but they have been identified as being very desirable, particularly the oxidation to methanol [57], and this research direction is the basis for Task 2. The standard free energies of all the oxidations represented by these equations are negative over a wide range of temperatures, establishing a thermodynamic driving force for these reactions even at room temperature should an effective catalyst be found. More practical considerations led us to seek a catalyst that would work in the desirable temperature range of 350-650°C.

One of the most active catalysts for the oxidative coupling reactions (1) and (2) is SrO-doped La_2O_3 [48,49]. However, both of these oxide components are strong bases, and it has been reported that the catalyst is poisoned by CO_2 (58), which is a significant factor since CO_2 is a complete oxidation product formed as an undesirable side product during the partial oxidation of methane. Herein, it is reported that doping of the SrO/La_2O_3 catalyst by small amounts of sulfate results in a significant (up to two-fold) enhancement of activity for oxidative coupling, reduction of the effect of CO_2 poisoning and carbonate formation, and the ability to achieve the methane coupling reaction at steady state at high rates at temperatures below 600°C.

I. Experimental Procedures

Catalyst Preparation and Analyses. A large batch of the basic 1 wt% SrO/La_2O_3 catalyst was prepared by AMOCO Oil Co. using the procedure described in References [48,49], and two portions of this batch were sent to us for independent testing. Characterization of the samples by X-ray powder diffraction (XRD) showed the presence of predominantly the hexagonal (ASTM 5-602) form of La_2O_3. However, some lanthanum hydroxide ($La(OH)_3$, ASTM 36-1481) was also observable in the XRD pattern, probably because of the hygroscopic nature of La_2O_3, in addition to a small amount of cubic (ASTM

22-369) La_2O_3. After activation in flowing Ar at 700°C, only hexagonal La_2O_3 was detected by XRD. This was also the case for catalyst samples tested in flowing CH_4/O_2 mixtures to temperatures as high as 850°C.

The surface areas of the catalysts were determined with a Micrometrics Instrumental Corp. Model Gemini-2360 BET instrument using N_2 adsorption after pretreatment in flowing N_2 at 250°C for at least 2 hr. The 1 wt% SrO/La_2O_3 catalyst had a surface area of 6.5 m^2/g *as received.* Chemical analyses were performed by Galbraith Laboratories, Inc.

The sulfated SrO/La_2O_3 catalysts were prepared by the incipient wetness impregnation technique. The appropriate amount of $(NH_4)_2SO_4$ was dissolved in deionized water, the measured quantity of SrO/La_2O_3 was added, and the slurry was continuously stirred with a magnetic stirrer until dryness was achieved. This was followed by drying the solid overnight at 120°C and calcination in air at 600°C for 4 hr. Prior to catalytic testing, the samples were activated *in situ* under flowing air (or O_2) at 500°C for 1 hr unless stated otherwise. The content of sulfate added to the 1 wt% SrO/La_2O_3 varied as nomially 0.5, 1.0, 2.0, and 4.0 wt% SO_4^{2-} of the total weight of catalyst. The gases used in this study were zero grade purity and were used without further purification.

Catalytic Testing. To determine the activity and selectivity of the catalysts, fixed-bed continuous-flow 9 mm OD (7 mm ID) or 13 mm OD (11 mm ID) quartz reactors that narrowed to 4 mm OD (2 mm ID) at the outlet were used with 0.100-0.125 g of catalyst. The system had two independently controlled inlet gas lines, and standard reactant mixtures of CH_4/air (1/1 or 1.5/1) were employed at ambient pressure (0.1 MPa). The gas hourly space velocity (GHSV) was typically 70,000 ℓ/kg cat/hr. Usually each test was carried out at steady state methane conversion for 1-3 hr. In determining the effect of reaction temperature on the methane conversion and product selectivity, the usual procedure was to employ the following temperature sequence: 500, 550, 600, 650, 700, 650, 600, 550, and 500°C. Each temperature was maintained for 2-10 hr, and the data points shown in the figures are usually the averages of 3-15 product analyses.

The principal products analyzed by on-line automated sampling of the exit gas using gas chromatography (Hewlett-Parkard 5890 GC controlled by an integrator and a PC using ChromPerfect software) were CO_2, C_2 hydrocarbons ($C_2H_6 + C_2H_4$), C_3 hydrocarbons ($C_3H_8 + C_3H_6$), CO, and H_2O. The C_3 products were generally not included in the product mixture reported since they were present in only trace quantities. Condensable water-soluble products, i.e. formaldehyde in particular, were collected in two water-filled scrubbers in series, the first was kept at room temperature and the second at 0°C. Formaldehyde was quantitatively determined by the modified Romijn's iodometric titration method [59], which has been well-established as a reliable method for determining small amounts of formaldehyde in aqueous solutions. In the present research, the carbon mass balance was always better than 90% and usually better than 95%.

II. Activity and Selectivity of the SrO/La_2O_3 Catalyst

To determine the degree of reproducibility of catalyst testing of the AMOCO Oil Co. SrO/La_2O_3 catalyst, four different portions of the catalyst were tested by three different researchers. The catalytic tests of the 1 wt% SrO/La_2O_3 catalyst were carried out with a CH_4/air = 1/1 reactant mixture at 0.1 MPa and with GHSV = 70,000 ℓ/kg catal/hr over the range of temperatures of 500-700°C. During the testing, the temperature was increased from 500°C to 700°C, and in two of the tests (solid symbols) the temperature was then decreased stepwise to 500°C. As shown in Figure 5, reproducible catalyst behavior was observed and no deactivation, with the possible exception at 500°C, was apparent.

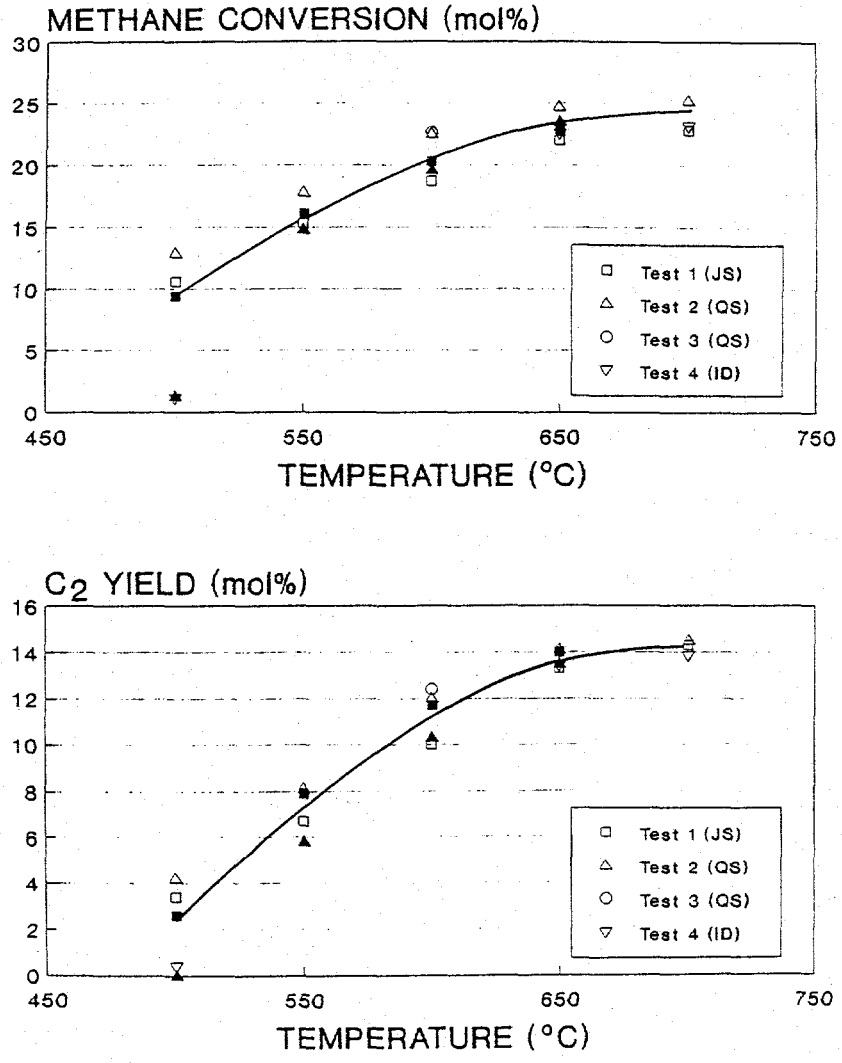

FIGURE 5. Effect of temperature on the conversion of methane and on C_2 hydrocarbon yield (mol%) over the 1 wt% SrO/La_2O_3 catalyst (0.100 g) with CH_4/Air = 1/1 at a total pressure of 0.1 MPa and GHSV = 70,000 ℓ/kg catal/hr. The open symbols represent sequentially increasing reaction temperatures, while the solid filled symbols represent decreasing reaction temperatures.

It was found that this catalyst was active at temperatures as low as 500°C, which is appreciably less that the steam reforming temperature of ≈850°C used to convert methane to synthesis gas. At temperatures higher than 550°C under the reaction conditions employed, over 70% of the oxygen was consumed. Thus, at the higher temperatures studied, the conversion level of methane was limited by the availability of the O_2 reactant. This was a contributing factor to the increasing C_2 hydrocarbon selectivity and %yield (defined as the product of the total C_2 selectivity (mol% ethane + ethene) and the total conversion of methane (mol%)) as the reaction temperature and methane conversion increased.

To further probe the catalytic behavior resulting in increasing C_2 hydrocarbon selectivity with increasing methane conversion, both undoped La_2O_3 and SrO-doped La_2O_3 catalysts were investigated. As shown in Figure 6, as the reaction temperature was increased over undoped La_2O_3 and the SrO/La_2O_3 catalysts, the conversion of methane to products increased. At the same time, the C_2 hydrocarbon selectivity exhibited a direct relationship with the methane conversion level. The data points in this figure are identified in Table 3,

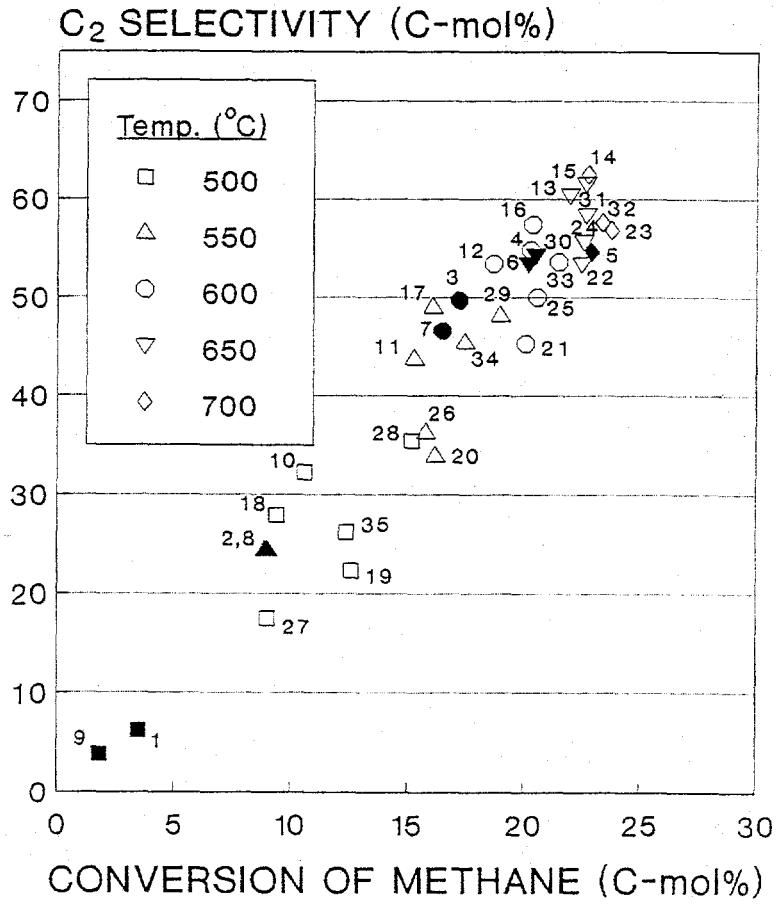

FIGURE 6. The C_2 hydrocarbon selectivity (mol%) as a function of methane conversion over La_2O_3 (filled symbols) and different samples of the 1 wt% SrO/La_2O_3 catalyst (open symbols) with CH_4/Air = 1/1 at 0.1 MPa and GHSV = 70,000 ℓ/kg catal/hr using 0.100 g samples. Also see Table 3.

and it can be determined that the SrO/La_2O_3 catalyst was much more active and selective toward C_2 hydrocarbon formation at the lower reaction temperatures than was the pure La_2O_3 catalyst, i.e. the initial 500°C tests of the two catalysts are represented by data points 10 (10.6% CH_4 conversion) and 1 (3.4% CH_4 conversion), respectively. Accordingly, data points 18 and 9 are the corresponding final tests after completing the temperature cycle and decreasing the reaction temperature back to 500°C for the La_2O_3 and SrO/La_2O_3 catalysts, respectively. At 700°C, the activities of the two catalysts were approximately the same (data points 5 and 14), but the SrO/La_2O_3 catalyst exhibited a higher C_2 hydrocarbon selectivity than did the pure La_2O_3.

TABLE 3. Designation of data points presented in Figure 6 for the testing of different portions (0.100 g) of the pure La_2O_3 and 1 wt% SrO/La_2O_3 catalysts. Different reaction temperatures were utilized, as designated in Figure 6, with a reaction mixture of CH_4/Air = 1/1 at 0.1 MPa with GHSV = 70,000 ℓ/kg cat/hr.

Test No.	Catalyst	Treatment[a]	Data Points
16	La_2O_3	Water Treated[b]	1-9
1	SrO/La_2O_3	As Received (Sample 1)	10-18
9	"	As Received (Sample 2)	19-27
21	"	As Received (HT Pretreat)[c]	28-35

[a]Pretreated in flowing air at 500°C for 1 hr, unless indicated otherwise, after which the gas flow was changed to CH_4/air = 1/1 and testing was carried out beginning at 500°C.

[b]Slurried with distilled water to simulate the doping procedure, dried, and then tested.

[c]Pretreatment consisted of slowly increasing the reactor temperature to ≈700°C in flowing air, maintaining the temperature for 1 hr, cooling to 500°C, maintaining this temperature for 1 hr, and then proceeding with the testing experiment.

III. Promotion of the SrO/La_2O_3 Catalyst by Sulfate Doping

Effect of Sulfate Concentration. The SrO/La_2O_3 catalyst was surface doped with sulfate using an aqueous $(NH_4)_2SO_4$ solution as described in the Experimental Procedure section. The effect of sulfate content on the catalytic behavior of the 1 wt% SrO/La_2O_3 catalyst was examined at 500 and 550°C with a reactant mixture of CH_4/air = 1/1 with $p_{(total)}$ = 0.1 MPa and GHSV = 70,000 ℓ/kg catal/hr. Upon doping the SrO/La_2O_3 catalyst with a small quantity of sulfate, a large promotional effect on the methane conversion (Figure 7) and C_2 selectivity (Figure 8) was observed. From these figures, it can be seen that adding the sulfate promoter to the catalysts to a 0.5-2 wt% level increased the overall conversion of methane and selectivity to C_2 hydrocarbons by a factor of 1.5-2.0. The curves shown in Figures 7 and 8 tend to show maxima at doping levels of about 1 wt% SO_4^{2-}. Since the methane conversion level was limited by the depletion of the oxygen supply, utilization of higher reaction temperatures tended to flatten the curves for all sulfate doping levels to ≈22-23% CH_4 conversion and ≈50-56% C_2 selectivity.

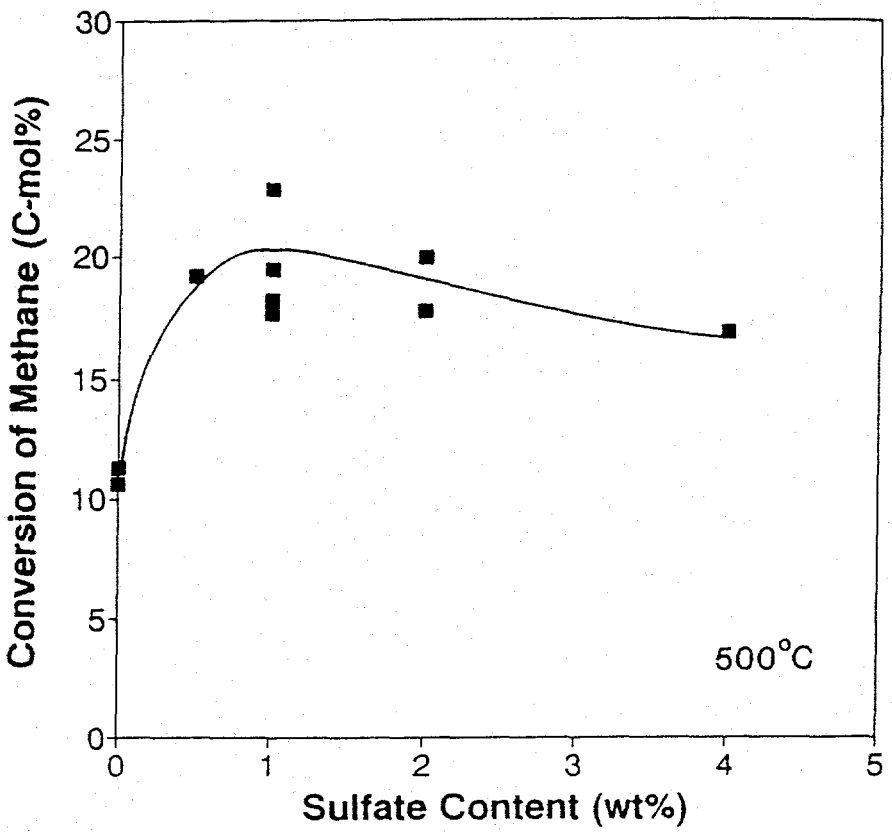

FIGURE 7. Effect of sulfate content on methane conversion at 500°C over the 1 wt% SrO/La_2O_3 Catalyst (0.100 g) with a CH_4/Air = 1/1 reaction mixture at a total pressure of 0.1 MPa and GHSV = 70,000 ℓ/kg catal/hr. Each data point is a catalytic test with a fresh sample.

Figures 7 and 8 demonstrate that the activities and C_2 hydrocarbon selectivities of the SO_4^{2-}-doped catalysts exhibit parallel behavior. Thus, sulfate doping of the catalyst also increased the %yields of the C_2 hydrocarbon products. Indeed, adding 1 wt% SO_4^{2-} to the catalyst increased the %yield at 500°C from 3% to 7.5-11%, e.g. the catalyst showing 45% C_2 selectivity in Figure 8 exhibited a 9% yield for the C_2 hydrocarbons. At this mild reaction temperature, all sulfated catalysts exhibited higher methane conversions and C_2 selectivities than the non-sulfated SrO/La_2O_3 catalyst.

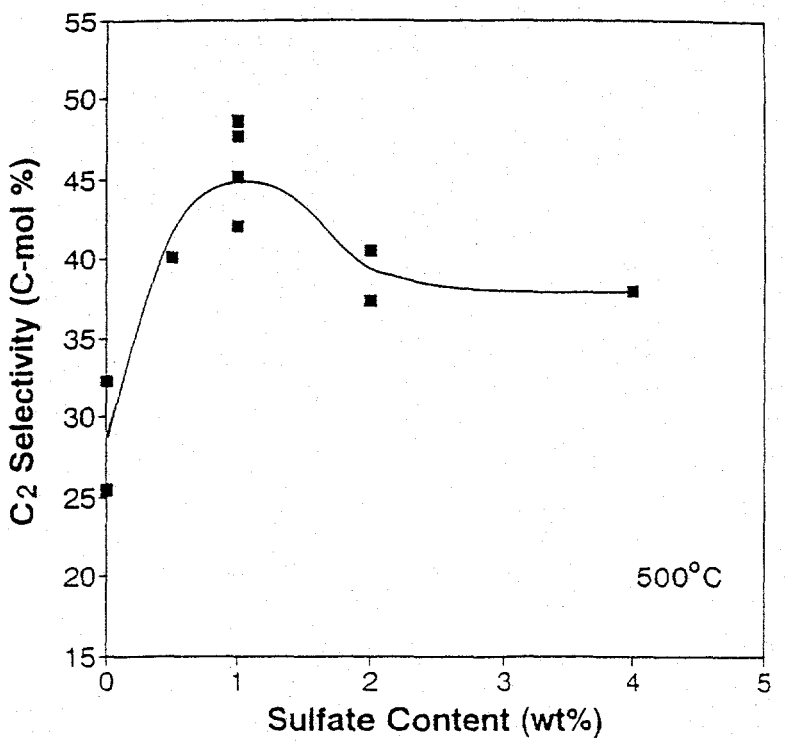

FIGURE 8. Effect of the sulfate content on the C_2^+ hydrocarbon selectivity observed at 500°C over the 1 wt% SrO/La_2O_3 catalyst. The experimental parameters are given in Figure 7.

Catalyst Stability. A fresh sample of the 1 wt% $SO_4^{2-}/SrO/La_2O_3$ catalyst was pretreated at 500°C for 1 hr in air (GHSV ≈ 35,000 ℓ/kg catal/hr) and then tested with CH_4/air = 1/1 with GHSV = 70,040 ℓ/kg catal/hr at 500°C for 1.25 hr. This was followed by a longer term test at 550°C. As shown in Figure 9, the catalyst was stable for over 27 hr in terms of methane conversion and C_2 selectivity (and %yield) during the continuous test. While the level of CH_4 conversion remained steady, the O_2 consumption decreased slightly. This was reflected in the slightly decreasing %yield of CO_2 with time. Toward the end of the experiment, the CO_2/CO ratio = 2.1 ± 0.2. The ethene/ethane molar ratio was approximately 0.75 ± 0.1 during the first 10 hr of testing at 550°C, but the ratio stabilized at 0.68 ± 0.03 during the last 15 hr of the run. During this test, the space time yield of C_2 products was ≈ 1.8 kg (ethene + ethane)/kg cat/hr.

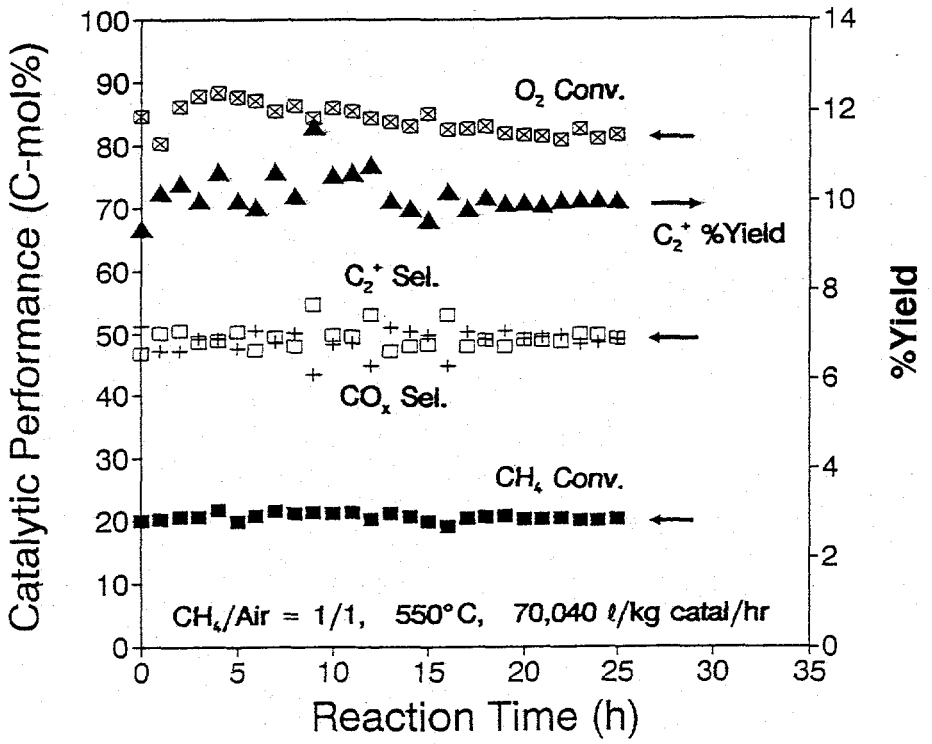

FIGURE 9. Stability test at 550°C of the 1 wt% SO_4^{2-}/1 wt% SrO/La_2O_3 catalyst (0.100 g) with CH_4/Air = 1/1 at a total pressure of 0.1 MPa and GHSV = 70,040 ℓ/kg catal/hr: (a) CH_4 conversion (■); (b) conversion of oxygen (⊠); (c) CO_x selectivity (+); (d) C_2^+ product selectivity (□); and (e) yield of C_2^+ hydrocarbon products (▲).

Effect of Reaction Temperature. The effect of reaction temperature on the conversion of methane and selectivity to C_2 hydrocarbon products was investigated as it had been done for the non-sulfated catalysts, where the temperature was increased stepwise from 500°C to 700°C and then in some cases decreasing the temperature back to 500°C. The results obtained from eleven tests are shown in Figure 10, with further description provided in Table 4.

As shown in Figure 10, the nominal 1 wt% sulfate-promoted SrO/La_2O_3 catalysts exhibited a much higher activity for methane conversion at 500°C than did the nonsulfated catalysts, the data for which are shown in Figure 6. Upon increasing the temperature stepwise to 700°C, the conversion of methane for both types of catalysts increased. However, the extent of the promotional effect of sulfate doping decreased with increasing temperature, and practically no effect at reaction temperatures >650°C was observed. At the high methane conversion levels observed with the $SO_4^{2-}/SrO/La_2O_3$ catalysts, the reactant oxygen was nearly or totally depleted (>85-90%), which limited the oxidative reactions with methane. This, as well as other factors to be discussed later, contributed to the converging catalytic behavior.

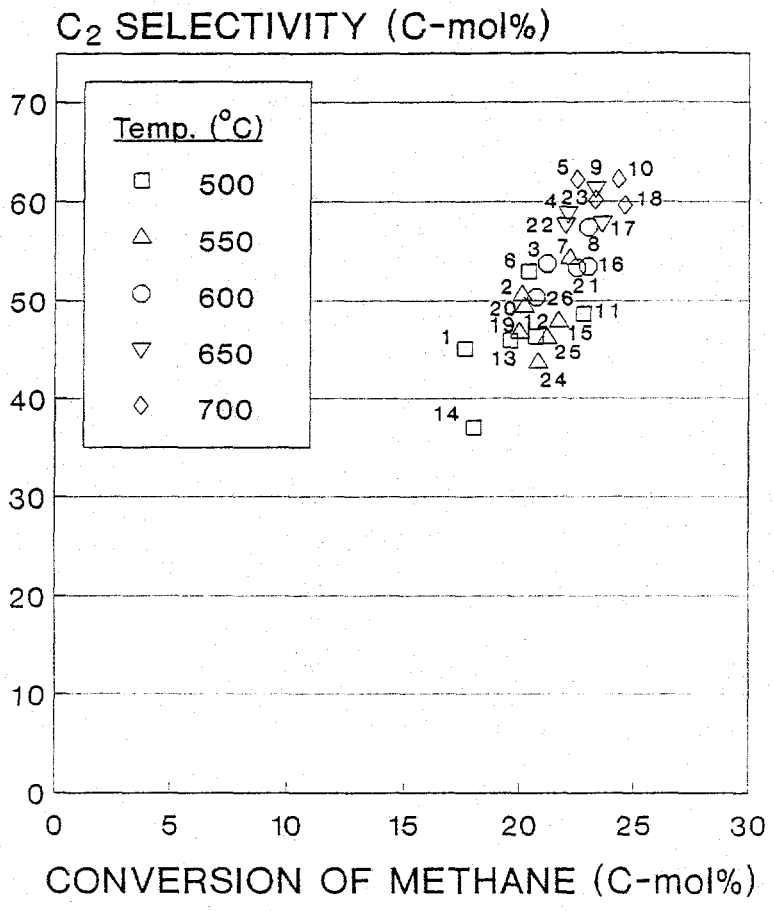

FIGURE 10. The C_2 hydrocarbon selectivity (mol%) as a function of methane conversion over 1 wt% $SO_4^{2-}/SrO/La_2O_3$ catalysts with $CH_4/Air = 1/1$ at 0.1 MPa and GHSV = 70,000 ℓ/kg catal/hr using 0.100 g samples. Also see Table 4.

Upon sequentially decreasing the reaction temperature after the 700°C experiments, approximately identical behavior for the SrO/La_2O_3 and SO_4^{2-}-promoted SrO/La_2O_3 catalysts was observed in terms of activity and C_2 selectivity. In particular, the promoting effect of sulfate was not observable at 500°C after testing at 700°C. To illustrate this, it is pointed out that in terms of %yields of C_2 hydrocarbons, sulfating the SrO/La_2O_3 catalyst (to ≈1 wt%) increased the C_2 %yield at 500°C from 3.4% to 8.0%, but both catalysts exhibited a 2.4% yield at 500°C following the 700°C test. Thus, the promotional behavior of the sulfate had disappeared after completing the temperature cycle. A new pretreatment of the tested catalyst in air at 500°C for one hour did not restore the former enhanced activity obtained at 500°C. As will be described later, the loss of activity is due to partial loss of the sulfate dopant and increasing carbonate content of the catalyst. However, the C_2 selectivity *vs* methane conversion data points for the partially deactivated catalysts, as well as those for the sulfated catalysts containing 0.5, 2, and 4 wt% SO_4^{2-} fall in the same pattern as observed for

TABLE 4. Designation of data points presented in Figure 10 for the testing of different portions (0.100 g) of the 1 wt% $SO_4^{2-}/SrO/La_2O_3$ catalysts at 0.1 MPa with CH_4/Air = 1/1 at GHSV = 70,000 ℓ/kg cat/hr.

Test No.	Treatment[a]	Data Points
3	Prep. 1	1-5
5	Prep. 1	6-10
10	Prep. 1	11
13	Prep. 1	12
14	Prep. 1	13
23	Prep. 1 (HT Pretreat)[b]	14-18
26	Prep. 1	19
27	Prep. 2	20-23
29	Prep. 2	24
30	Prep. 2	25
54	Prep. 4	26

[a]After sulfate doping but prior to being loaded into the reactor, the catalyst samples were calcined in an open air oven for 4 hr at 600°C. After being loaded into the reactor, the samples were then pretreated in flowing air at 500°C for 1 hr, unless indicated otherwise, after which the gas flow was changed to CH_4/air = 1/1 and testing was carried out beginning at 500°C.
[b]Pretreatment consisted of slowly increasing the reactor temperature to ≈700°C in flowing air, maintaining the temperature for 1 hr, cooling to 500°C, maintaining this temperature for 1 hr, and then proceeding with the testing experiment.

the non-sulfated (Figure 6) and 1 wt% $SO_4^{2-}/SrO/La_2O_3$ catalysts (Figure 10), as shown in Figure 11. The 150 data points, each corresponding to a steady state test obtained at different temperatures and with different catalysts, shown in this figure clearly demonstrate that the C_2 selectivity increased as the level of methane conversion increased.

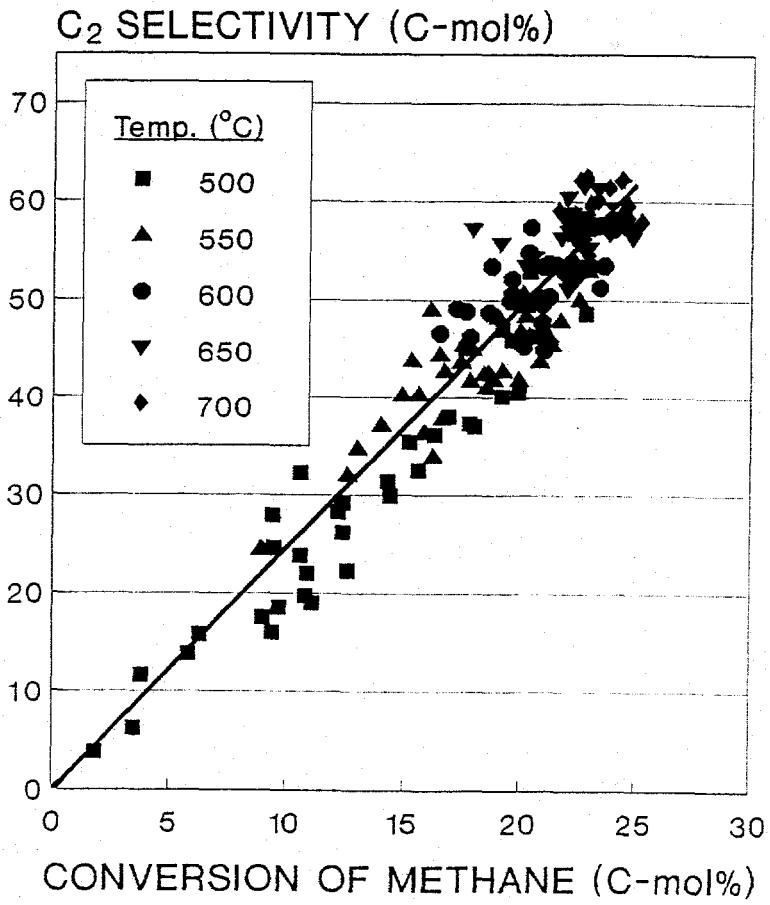

FIGURE 11. The C_2 hydrocarbon yield (mol%) as a function of methane conversion over 31 different catalyst samples comprised of La_2O_3, 1 wt% SrO/La_2O_3, and sulfated SrO/La_2O_3 containing different quantities of SO_4^{2-}. Some of the $SO_4^{2-}/SrO/La_2O_3$ catalysts were pretreated in He or air at 700 or 800°C, and some data points in the 5-20% methane conversion range were obtained with partially deactivated $SO_4^{2-}/SrO/La_2O_3$ catalysts. Testing was carried out with CH_4/Air = 1/1 at 0.1 MPa and GHSV = 70,000 ℓ/kg catal/hr using 0.100 g samples.

In terms of the olefin/paraffin components in the C_2 hydrocarbon product, it was observed that most of the C_2 product was ethane at low conversions. However, as the total C_2 selectivity increased, corresponding to increasing methane conversion, the selectivity to ethene also increased, as shown in Figure 12. A tight correlation is shown in this figure for all 150 catalyst tests to which reference was made in Figure 11.

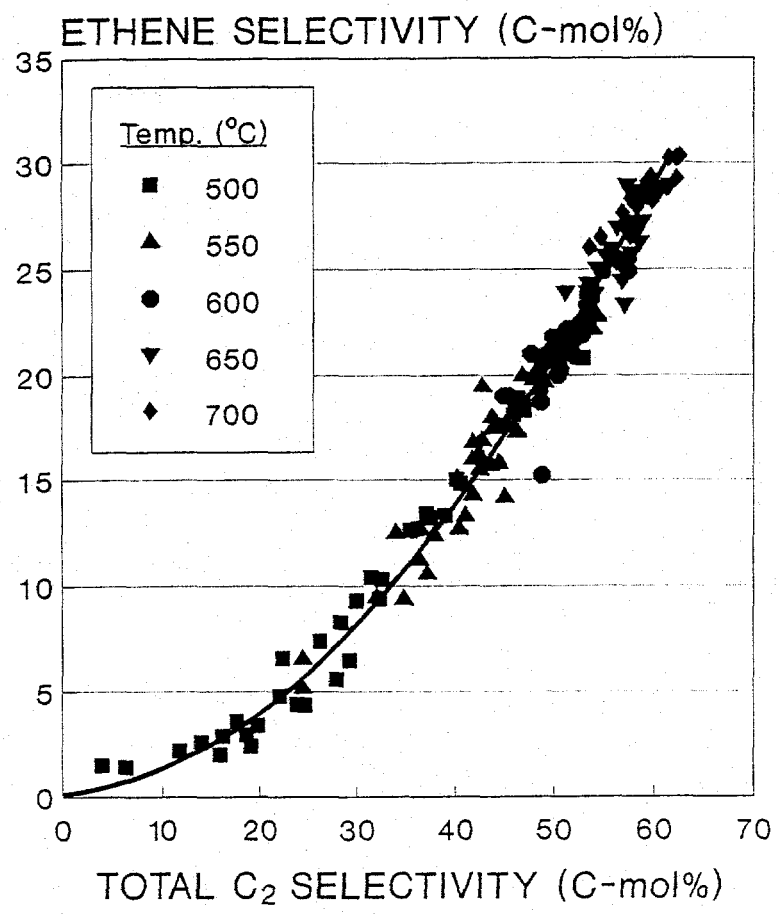

FIGURE 12. The ethene selectivity among the products as a function of C_2 hydrocarbon selectivity (mol%) over La_2O_3, 1 wt% SrO/La_2O_3, and sulfated SrO/La_2O_3 containing different quantities of SO_4^{2-}, as referenced in Figure 11. Testing was carried out with CH_4/Air = 1/1 at 0.1 MPa and GHSV = 70,000 ℓ/kg catal/hr using 0.100 g samples.

IV. Deactivation and Reactivation of $SO_4^{2-}/SrO/La_2O_3$ Catalysts

Effect of Reactant Flow Rate at Moderate Temperature. After the standard pretreatment of the 1 wt% $SO_4^{2-}/SrO/La_2O_3$ catalyst in air at 500°C for 1 hr, the methane conversion reaction was carried out at 550°C at varying GHSV with a constant reactant gas composition of CH_4/Air = 1/1. The reaction started with GHSV = 70,600 ℓ/kg catal/hr, which was then decreased stepwise. As the GHSV was diminished to 4,200 ℓ/kg catal/hr, the CH_4 conversion gradually decreased from 20.8 to 3.9 C-mol%, as shown in Figure 13A (and as now expected, the C_2 selectivity also decreased accordingly). The C_2 %yield also steadily decreased from 9.1 to 0.6 C-mol%.

At this point in the experiment, the gas flow rate was returned to 70,600 ℓ/kg catal/hr, and the steady state conversion reaction was maintained for 7 hr. As shown in Figure 13B,

the methane conversion level remained very low at less than 2.5 during this period of time, and the catalyst was practically deactivated towards C_2 formation. Terminating the methane flow while maintaining the air flow at 550°C for 1 hr, designated as treatment **[1]** in Figure 13B, did not result in reactivation of the catalyst. Indeed, the catalyst was further deactivated for C_2 formation from CH_4/air. Reactivation of the catalyst was achieved by air treatment (GHSV = 35,000 ℓ/kg catal/hr) at 600°C for 4 hr, designated as treatment **[2]** in Figure 13B. As shown in Figure 13B, upon returning to the original testing conditions with CH_4/air = 1/1 at 550°C for 14 hr, ≈22 mol% of the methane was converted to products with 50 C-mol% selectivity to C_2 hydrocarbons (ethene/ethane molar ratio = 0.72). Thus, complete regeneration of the 1 wt% SO_4^{2-}/SOr/La_2O_3 catalyst was accomplished by the 600°C air treatment.

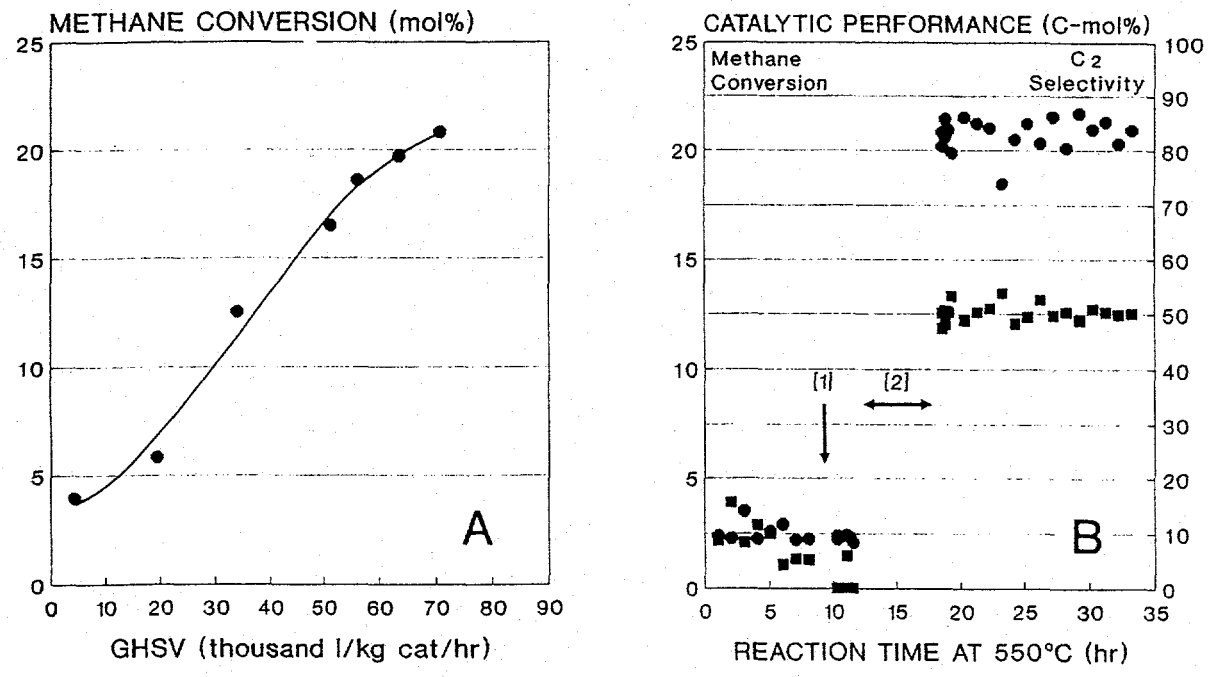

FIGURE 13. **[A]** The effect of decreasing the total reactant flow rate on methane conversion at 550°C over the 1 wt% SO_4^{2-}/1 wt% SrO/La_2O_3 catalyst (0.100 g) with CH_4/air = 1/1 at 1 MPa. **[B]** Catalyst performance at 550°C in terms of methane conversion (●) and C_2 hydrocarbon selectivity (■) upon returning to GHSV = 70,600 ℓ/kg catal/hr, briefly reoxidizing the catalyst during Period [1], and then during Period [2] being subjected to a reactivation treatment of calcination at 600°C for 4 hr in air with GHSV = 35,000 ℓ/kg catal/hr before resuming normal testing with GHSV = 70,600 ℓ/kg catal/hr.

A fresh sample of this same catalyst was pretreated as usual and was then tested with CH_4/air = 1/1 with varying GHSV, as shown for the previous catalyst in Figure 13A. At GHSV ≈ 70,000 ℓ/kg catal/hr, the initial methane conversion was 21.2 mol%, while the total

C_2 selectivity was 46.2 C-mol%. At the lower GHSV of 4,200 ℓ/kg catal/hr, 2.3 mol% CH_4 conversion was observed with a C_2 hydrocarbon selectivity of only 0.1 C-mol%. The reaction was terminated and the catalyst was analyzed for carbonate content, and it was found that the catalyst contained 15.35 wt% CO_3^{2-}. This observation will be discussed later.

A different 1 wt% SO_4^{2-}/1 wt% SrO/La_2O_3 catalyst was prepared and pretreated in air at 500°C for 1 hr. Testing was carried out as described above, beginning with an initial GHSV =70,175 ℓ/kg catal/hr. This catalyst exhibited a lower initial activity than those discussed previously. As the GHSV was diminished stepwise to 17,120 ℓ/kg catal/hr, the CH_4 conversion gradually decreased from 15.38 to 6.79 C-mol%, as shown in Figure 14. Decreasing the GHSV one further step led to a slightly higher conversion of methane.

When the flow rate was increased stepwise, the catalytic behavior changed in the opposite direction to that described above. As shown in Figure 14 (A and B), the conversion level of methane and the C_2^+ selectivity increased with increasing GHSV. In each case, a hysteresis in behavior was observed, where neither the initial methane conversion nor total C_2 selectivity was achieved upon returning to the initial reactant gas flow of GHSV = 70,175 ℓ/kg catal/hr. After completing the reactant gas flow rate cycle, the CH_4 conversion, the C_2^+ selectivity, and the %yield of C_2^+ hydrocarbons had increased to 11.3, 18.3, and 2.1 C-mol%, respectively, while the CO_x product selectivity decreased to 80.0 C-mol%. Thus, the C_2 selectivity was ≈50% of the initial value, while the C_2 %yield was less than half of the original yield obtained at the initial flow rate of GHSV = 70,175 ℓ/kg catal/hr.

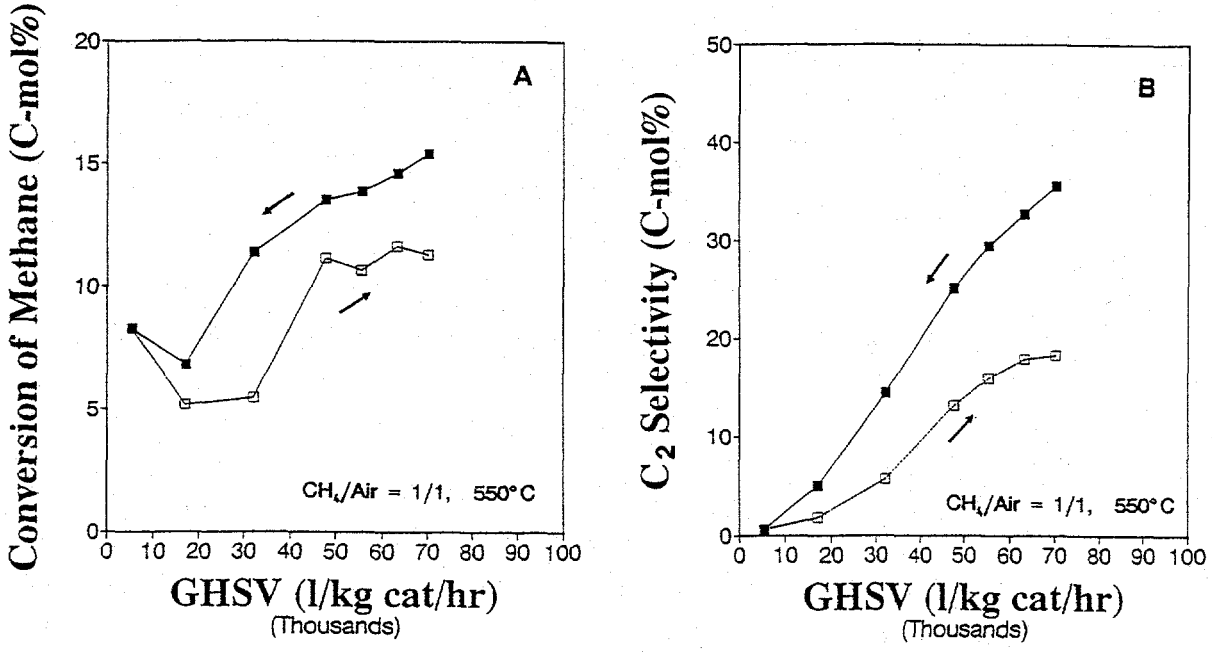

FIGURE 14. Effect of total reactant flow rate on **[A]** methane conversion and **[B]** C_2^+ hydrocarbon selectivity at 550°C over the 1 wt% SO_4^{2-}/1 wt% SrO/La_2O_3 catalyst (0.100 g) with CH_4/air = 1/1 at 0.1 MPa, wherein the reactant mixture GHSV was decreased (■) stepwise from 70,175 to 5,390 ℓ/kg catal/hr and then the procedure was reversed (□).

Study of the Thermal Reactivation of the $SO_4^{2-}/SrO/La_2O_3$ Catalyst. After the experiments described immediately above wherein the gas flow was systematically decreased and then increased to its original value (70,175 ℓ/kg catal/hr), the catalyst was in a partially deactivated state relative to the initial activity and selectivity (Figure 14). To overcome this deactivated state, the reaction temperature was increased stepwise at constant GHSV beginning at 550°C. While gradually and stepwise increasing the temperature to 580°C, the CH_4 conversion slowly increased (Figure 15A), and then upon increasing the temperature further to 585°C, the methane conversion suddenly rose to a much higher activity. Further increasing the reaction temperature from 585°C up to 600°C caused only gradual increases in CH_4 conversion, where the methane conversion was ≈19%.

The sudden increase in methane conversion at 585°C was accompanied by an even more pronounced increase in C_2 hydrocarbon selectivity, as shown in Figure 15B. At 600°C, the C_2 selectivity was ≈43%. The CO_x selectivity pattern was the mirror image of the C_2 selectivity behavior shown in Figure 15B. Upon decreasing the temperature stepwise to 550°C, both the CH_4 conversion and C_2 selectivity decreased somewhat but tended to stabilize at ≈15% and 37%, respectively. These values compare with 15.4% and 35.5% levels observed for the initial test with the fresh catalyst, as shown in Figures 14A and 14B. Thus, the catalyst was regenerated by this higher temperature treatment under reaction conditions. Figures 14 and 15 show together that the SO_4^{2-}-promoted SrO/La_2O_3 catalyst was intrinsically stable under the reaction conditions employed here, and activity suppression arising from utilization of the catalyst at low reaction temperatures was reversible.

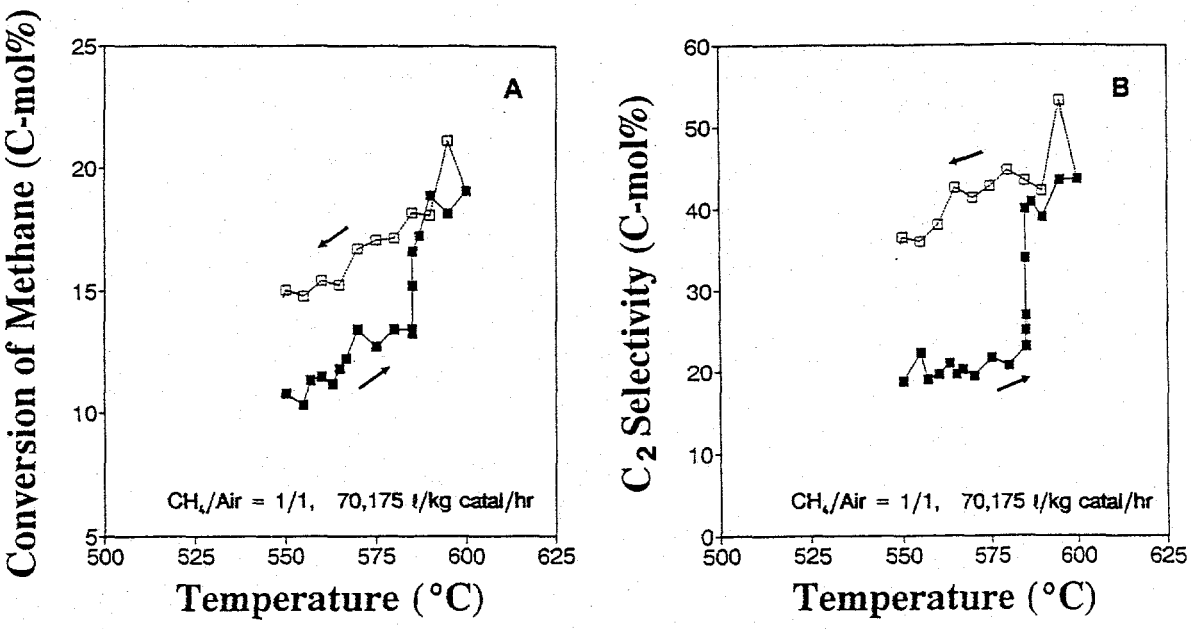

FIGURE 15. Effect of temperature on **[A]** CH_4 conversion and **[B]** C_2^+ selectivity over the partially deactivated 1 wt% $SO_4^{2-}/SrO/La_2O_3$ catalyst (0.100 g) with CH_4/Air = 1/1 at 0.1 MPa and GHSV = 70,175 ℓ/kg catal/hr. The temperature was increased stepwise from 550 to 600°C (■) and then (after the recovery of catalytic performance) decreased to 550°C (□).

V. Effect of the CH_4/Air Reactant Ratio on the Catalytic Activity and Selectivity

Using a portion of the same catalyst as used in the flow rate dependence studies, the effect of the CH4/air reactant ratio was investigated. While the reactant gas flow was kept constant (GHSV = 70,040 ℓ/kg catal/hr) at the reaction temperature of 550°C, the CH_4/air ratio was increased stepwise from 1.0 to 40.8 over the $SO_4^{2-}/SrO/La_2O_3$ catalyst. As the amount (and partial pressure) of methane increased relative to oxygen (CH_4/O_2 = 5-204), the conversion of methane decreased significantly, i.e. from ≈15 to less than 0.5 C-mol% as shown in Figure 16. The drop in the activity was especially large upon increasing the CH_4/air ratio from 1 to ≈3, which yielded about a 4.5-fold decrease in the CH_4 conversion.

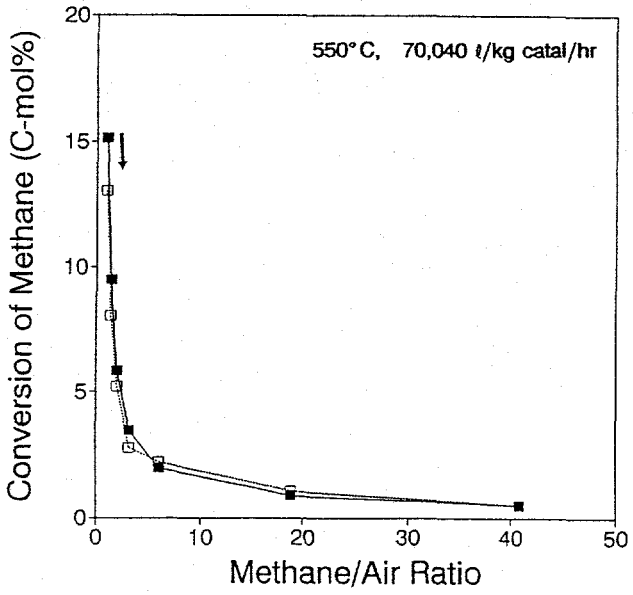

FIGURE 16. Effect on the conversion of CH_4 at 550°C over the 1 wt% $SO_4^{2-}/SrO/La_2O_3$ catalyst (0.100 g) as the CH_4/air reactant ratio was first increased (■) and then decreased (□). The flow rate was constant with GHSV = 70,040 ℓ/kg catal/hr at a total pressure of 0.1 MPa. The CH_4/air ratio was changed stepwise from 1.0 to 40.8 and then the procedure was reversed.

During the reverse process of decreasing the CH_4/air ratio stepwise back to 1, the CH_4 conversion increased in basically a reversible manner, as shown by the open symbols in Figure 16. Some deactivation was apparent at low reactant ratios, but it was rather small. This approximate reversibility is in contrast to the results obtained in the prior experiments at 550°C where the reactant gas flow rate (GHSV) was systematically decreased from 70,175 to 5,390 ℓ/kg catal/hr and then stepwise increased back to the original value while maintaining the CH_4/air reactant ratio at a constant value of 1 (see Figure 14). In that case, deactivation of atleast 20-25% was observed at all flow rates. As shown in Figure 16 for the current experiment, the CH_4 conversion exhibited much less deactivation upon completion of cycling the methane/air ratio.

As the CH_4/air ratio was varied, the C_2^+ hydrocarbon selectivity showed surprising behavior. As the reactant ratio was initially increased from 1.0 to 3.45, the selectivity toward C_2^+ hydrocarbons decreased very rapidly from ≈32 to 13 C-mol%, as shown in Figure 17A. However, as the CH_4/air ratio was further increased to 40.8, the C_2^+ selectivity reversed and increased quite linearly to over 50 C-mol%. The CO_x selectivity was the mirror image of the C_2^+ selectivity.

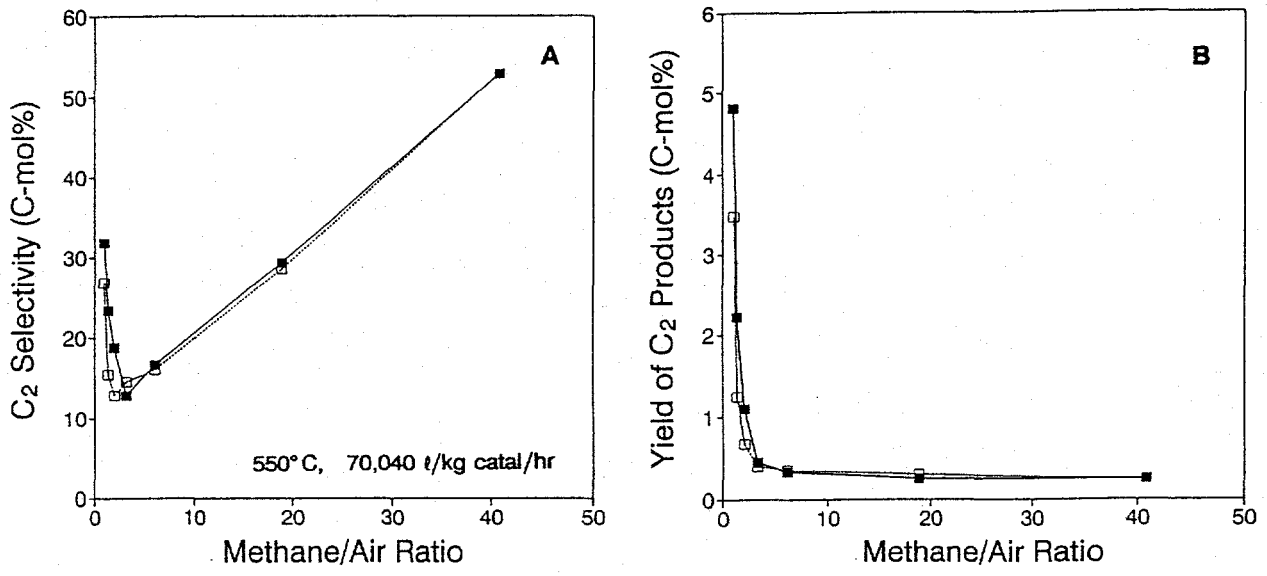

FIGURE 17. The effect of varying the CH_4/Air reactant ratio on the **[A]** C_2^+ hydrocarbon selectivity and the **[B]** C_2^+ %yield at 550°C over the 1 wt% SO_4^{2-}/1 wt% SrO/La_2O_3 catalyst at a constant GHSV = 70,040 ℓ/kg catal/hr at 0.1 MPa. The reactant ratio was first increased (■) and then decreased (□).

The subsequent stepwise decrease in the CH_4/air reactant ratio back to 1 resulted in rather reversible behavior. However, at the lowest ratios some loss of C_2^+ selectivity was observed. As shown in Figure 17A, the final C_2^+ selectivity obtained upon returning to the CH_4/air = 1.0 ratio was ≈85% of the initially observed selectivity with the fresh catalyst.

It is noted here that as the CH_4/air ratio increased, the methane conversion decreased, as shown in Figure 16 and the formation rates of both the C_2 hydrocarbons and the CO_x products were quite small at high methane/air ratios. This is also reflected in the %yields of the products. The %yield of the C_2^+ hydrocarbon products decreased very rapidly with increasing CH_4/air ratio, as shown by in Figure 17B, and this is a reflection of the conversion level of CH_4 (see Figure 16). While the CH_4/air ratio increased from 1.0 to 3.25, the %yield of CH_4 decreased by more than a factor of 10 (from 4.8 to 0.45 C-mol%). When the CH_4/air ratio reached its largest experimental value (40.8), the methane %yield was only 0.25 C-mol%.

Decreasing the CH_4/air ratio at 550°C as the second part of the cycle of the experiment, it was shown that the C_2 hydrocarbon productivity of the catalyst was nearly reversibility, as indicated in Figure 17B. However, some deactivation was evident at low reactant ratios, e.g. at the final ratio of CH_4/air = 1.0, the %yield of the C_2^+ hydrocarbons was ≈72% of the original value.

VI. Summary of Results

The experimental data presented here, further supported by the analyses described under Task 3, demonstrate the following:

1. The synthesis rate of the C_2 hydrocarbons by direct coupling of methane is significantly accelerated by the presence of sulfate (up to a factor of two),

2. An optimum sulfate doping level of ≈1% exists,

3. Under the reaction conditions employed in these studies, the C_2 selectivity increases as the conversion of methane increases,

4. The reaction kinetics indicate the same mechanism is operating for the La_2O_3, SrO/La_2O_3, and $SO_4^{2-}/SrO/La_2O_3$ catalysts,

5. The observed product selectivity is mainly controlled by the methane conversion level, which is determined in part by the availability of oxygen,

6. Carbonate poisoning of the catalyst is suppressed by the sulfate promoter, and

7. Carbonate deactivation of the catalyst is reversible.

TASK 2. Selective Methane Oxidation to Oxygenates

The direct conversion of methane to methanol and formaldehyde *via* partial oxidation is still a very challenging research area in heterogeneous catalysis. Many catalysts have been investigated for this process and review articles are available in the literature (4,60). Silica-supported V_2O_5 and MoO_3 have been studied extensively (23,25,36,61), and V_2O_5/SiO_2 was found to be one of the most active and selective catalysts for methane partial oxidation to formaldehyde by using either N_2O (23,61) or molecular oxygen (25,36) as oxidants. Besides steady-state catalytic tests, very few studies have focused on correlations between the catalyst structure and performance, as well as the nature of the active sites for methane partial oxidation.

It appears that silica is so far the only effective support for transition metal oxide catalysts for the selective conversion of methane to formaldehyde (50). Silica itself was shown to be quite selective to formaldehyde production, but it was not very active (51,54,56). However, there is no explanation for the special property of the silica support in the open literature. Transition metal oxide catalysts on other oxide supports have not been studied extensively for the catalytic partial oxidation of methane to methanol and formaldehyde. The reaction mechanisms are largely unknown, partly because of the lack of *in situ* analysis of the catalyst surfaces under reaction conditions. Recently, Koranne et al. (62) employed a transient isotope technique to study the carbon pathways for the partial oxidation of methane over V_2O_5/SiO_2 catalysts. The surface residence times and concentrations of various intermediates were obtained and a hypothesis about the reaction pathways was proposed, namely that different types of "sites" are involved in the formation of CH_2O, CO, and the C_2H_6 hydrocarbon, and these may correspond to vanadium oxide species in different redox states.

In the present study, a variety of catalysts consisting of redox transition metal oxides supported on silica were prepared and tested for activity and selectivity for converting methane to formaldehyde and methanol. Since it was found that vanadia catalysts exhibited the highest yields of these products, single-component supported vanadia catalysts (V_2O_5/SiO_2, V_2O_5/TiO_2, and V_2O_5/SnO_2) and three mixed oxide catalysts ($V_2O_5/TiO_2/SiO_2$, $V_2O_5/SnO_2/SiO_2$, and $V_2O_5/MoO_3/SiO_2$) were prepared and were tested for methane partial oxidation. Silica-supported vanadia catalysts using prepared using a variety of techniques and were tested in both single bed and double bed configurations. The influence of vanadia loading and specific oxide support were examined. In addition, the influence of steam in directing the conversion of methane toward oxygenates was investigated. As will be reported under Task 3, *in situ* Raman spectra were recorded for the first time during the methane partial oxidation reaction over these catalysts, and correlations between the surface vanadia structures and their catalytic performances were made. Mechanistic insight into the activation of methane and subsequent reaction for forming formaldehyde *via* partial oxidation over supported V_2O_5 catalysts is provided.

I. Supported Vanadia Catalysts for the Synthesis of Oxygenates

Experimental Methods. Amorphous SiO_2 (Cab-O-Sil EH-5, surface area = 380 m^2/g), treated with water to make it more dense, and TiO_2 (Degussa P-25 as received, surface area = 55 m^2/g) were generally utilized for making supported SiO_2 and TiO_2 catalysts. Other supports were also investigated, and the SnO_2 support was made from tin(II) acetate (Aldrich). After hydrolyzing tin(II) acetate with water, the sample was dried at room temperature, further dried at 120°C overnight and calcined in air at 450°C for six hr. The resultant SnO_2 support had a surface area of 20 m^2/g.

The incipient-wetness impregnation method with solutions of different precursors was used in preparing the supported catalysts for this study. A toluene solution of titanium(IV) isopropoxide ($Ti[OCH(CH_3)_2]_4$) (Alfa) was used for preparing the TiO_2/SiO_2 catalysts. A methanol solution of vanadium(V) triisopropoxide oxide ($VO[i\text{-}OC_3H_7]_3$) (Alfa) was used for making supported vanadium oxide catalysts. The above preparations were performed inside a glove box under a nitrogen atmosphere to avoid preoxidation by atmospheric moisture. SnO_2/SiO_2 samples were prepared from an aqueous solution of colloidal tin(IV) oxide (Alfa, 18 wt%) under ambient conditions. An aqueous solution of ammonium heptamolybdate, $(NH_4)_6Mo_7O_{24}\cdot 4H_2O$ (Matheson, Coleman and Bell), was used for the preparation of the supported molybdenum oxide catalysts. After impregnation, each catalyst was dried at room temperature at 120°C overnight and then calcined at 500°C for four hr under flowing air. The metal oxide loadings on the oxide supports were calculated based on the weight percentage of the deposited metal oxides.

A series of catalysts consisting of silica-supported V_2O_5, Cr_2O_3, MnO_2, Fe_2O_3, Cu_2O, MoO_3, WO_3, and Re_2O_7 were also prepared by using the aqueous impregnation method. The amorphous Cab-O-Sil EH-5 silica that was used as the support was first mixed with deionized water, and then the mixture was stirred and dried at 140°C so that the density of the silica was increased. The V_2O_5/SiO_2 catalyst was typically prepared by aqueous impregnation of ammonium metavandate (NH_4VO_3 from Aldrich) into the amorphous silica. For preparing other catalysts, $Cr(NO_3)_3$, $Mn(NO_3)_4$, $Fe(NO_3)_3$, iron(II) acetate, copper(I) acetate, and ammonium heptamolybdate were used. The resulting mixtures were thoroughly mixed by vigorous stirring at 60°C on a magnetic hot plate for 10-15 hr until a think paste was formed. The paste was then dried at 140°C overnight and calcined in air at 600°C for six hr. Oxidation of the catalysts during this latter treatment was not monitored.

Catalytic testing was carried out in a fixed-bed continuous flow quartz reactor (9 mm o.d.; 7 mm i.d.) in the temperature range of 400-630°C. Usually 25 to 200 mg of catalyst was used. A standard reactant mixture of methane and air (1.5/1.0 volume ratio) was used at ambient pressure, where the flow rates of the methane (Air Products and Chemicals, Inc.; ultra high purity grade) and air (JWS Technologies; zero grade) were controlled by calibrated Linde mass flowmeters. The principal products analyzed by on-line sampling *via* an automated heated sampling valve using a Hewlett Packard (HP) 5890 Series II gas

chromatograph (GC) were CO_2, C_2 hydrocarbons ($C_2H_6 + C_2H_4$) , CO and H_2O. The GC was equipped with two TCD detectors and Poraplot Q and molecular sieve 13A capillary columns, and it was coupled to an HP 3396 Series II recorder/integrator and a PC data station using ChromPerfect chromatographic software. Each analysis was carried out using temperature programming in the 50-150°C range using a 10°C/min temperature ramp. Formaldehyde was condensed from the exit stream with dual water scrubbers and quantitatively determined by iodometric titration (59). In the present research, the carbon balance between methane consumed and CH_2O, CO, CO_2, and C_2 hydrocarbons produced was always better than 90% and usually better than 95%.

As will be noted in some later experiments, steam was added to the reactant mixture by injection of distilled water into the heated volume preceding the catalyst bed by means of an ISCO liquid metering pump (Model 314). The steam was then collected with the condensible products after passing through the reactor, which were using water scrubbers or trapped at 0°C for subsequent analysis by GC/MS. The GC/MS formaldehyde analysis was calibrated by a series of standard solutions that were quantified by iodometric titration.

Comparison of Metal Oxide/Silica Catalysts. The transition metal catalysts that were prepared with loading levels of approximately 1 wt% were considered to be redox catalysts that were appropriate for methane partial oxidation. Table 5 compares the results obtained with the silica-supported catalysts using a CH_4/air = 1.5/1.0 reaction mixture at 600°C at ambient pressure and with a relatively moderate hourly space velocity (GHSV). Also shown for comparison are the results obtained with the empty reactor and with the reactor containing only quartz wool or the Cab-O-Sil support.

The data in Table 5 show that the V_2O_5/SiO_2 catalyst performed the best with respect to oxygenate yields. The Fe_2O_3/SiO_2, Cu_2O/SiO_2, MoO_3/SiO_2, and Re_2O_7/SiO_2 catalysts also gave appreciable space time yields of formaldehyde and methanol, although they were much less active than the V_2O_5/SiO_2 catalyst. The MoO_3/SiO_2 catalyst produced little CO_2 and exhibited notable selectivity to formaldehyde and methanol, but the activity of this catalyst was very low. Under the reaction conditions utilized, the Cr_2O_5/SiO_2 was the most active catalyst, but CO_2 was the dominant product, accompanied by CO. The data in Table 5 also indicate that gas phase free radical reactions were negligible since C_2 hydrocarbons were not formed. Since the Cab-O-Sil exhibited almost no catalytic activity, the data emphasize the important role played by the catalyst surface in oxygenate production.

Catalytic Activities and Selectivities of Supported Vanadia Catalysts. Since the vanadia/silica catalyst exhibited the highest productivities of formaldehyde and methanol, see Table 5, vanadia-based catalysts supported on silica, titania, and tin oxide were investigated in further detail. The catalysts studied and their observed methane conversions and product selectivities are summarized in Tables 6 and 7. In general, moderate-to-high reactant gas hourly space velocities (GHSV) were used so that the formaldehyde product could be removed effectively from the reaction zone without being further oxidized.

TABLE 5. The conversion of methane, space time yield (STY) of oxygenates, and product selectivities observed the partial oxidation of methane over Cab-O-Sil supported transition metal oxide catalysts (0.10 g) at 600°C and 0.1 MPa with CH_4/air = 1.5/1.0 reactant mixture at GHSV = 144,000 ℓ/kg catal/hr.

Catalyst	CH_4 Conv. (mol%)	CH_2O STY (g/kg/hr)	CH_3OH STY (g/kg/hr)	Selectivity (C mol%)			
				CH_2O	CH_3OH	CO	CO_2
Blank	0.1	0.0	0.0	0.0	0.0	0.0	100
Wool	0.01	0.0	0.0	0.0	0.0	0.0	100
Cab-O-Sil	0.02	0.0	0.0	100	0.0	0.0	0.0
V_2O_5/SiO_2	7.9	481	49	5.2	0.5	84.5	9.7
Cr_2O_3/SiO_2	10.4	18.2	0.0	0.2	0.0	19.9	79.9
MnO_2/SiO_2	4.3	32.1	0.0	0.6	0.0	29.8	69.6
Fe_2O_3/SiO_2	1.5	278	19.6	15.9	1.1	50.4	32.6
Cu_2O/SiO_2	1.5	185	18.2	10.6	1.0	45.7	42.7
MoO_3/SiO_2	0.05	29.4	18.8	50.5	30.3	13.4	5.7
WO_3/SiO_2	0.2	11.6	0.0	5.0	0.0	26.7	68.3
Re_2O_7/SiO_2	0.6	28.2	11.9	4.0	1.6	76.0	18.4

At the reaction conditions employed in this study, the contributions from the empty reactor and the pure silica support (Cab-O-Sil) were negligible for methane conversion. For the SiO_2 and MoO_3/SiO_2 catalyst, accurate analysis of the products other than formaldehyde was very difficult since methane conversions were extremely low. The TiO_2-containing catalysts were less active that the V_2O_5/SiO_2 catalysts, as well as SnO_2-containing catalysts. The SnO_2 support and the 1 wt% V_2O_5/SnO_2 catalyst were active (Table 6), but the dominant product formed was CO_2 (Table 7). Thus, SnO_2 tends to be a deep oxidation catalyst. Over the V_2O_5/SiO_2 catalysts, very high formaldehyde space time yields (STY >1 kg CH_2O/kg cat.hr) could be obtained, see Table 6, even though the single pass %yields (CH_4 conversion% x %CH_2O selectivity) were still quite low (< 2%). Under these reaction conditions, no significant production of methanol was observed.

TABLE 6. Methane conversion by air (CH_4/air = 1.5/1.0, 0.1 MPa) and formaldehyde productivity over supported metal oxide catalysts.

Catal. No.	Catalyst	Temp. (°C)	GHSV (ℓ/kg/hr)	CH_4 Conv. (%)	CH_2O STY (g/kg/hr)
1	SiO_2	630	70,000	0.05	24.3
2	2% MoO_3/SiO_2	630	70,000	0.08	37.9
3	1% V_2O_5/SiO_2	630	70,000	9.52	685
4	3% V_2O_5/SiO_2	580	140,000	6.86	1,022
5	5% V_2O_5/SiO_2	630	280,000	5.60	1,440
6	1% V_2O_5/ 3% MoO_3/SiO_2	630	70,000	8.47	675
7	TiO_2	630	70,000	1.55	17.6
8	3% TiO_2/SiO_2	630	70,000	0.31	27.6
9	1% V_2O_5/TiO_2	630	70,000	0.82	14.0
10	1% V_2O_5/ 3% TiO_2/SiO_2	630	70,000	1.07	101
11	3% V_2O_5/ 3% TiO_2/SiO_2	630	70,000	2.30	150
12	SnO_2	530	70,000	8.10	2.3
13	3% SnO_2/SiO_2	630	70,000	1.60	8.8
14	1% V_2O_5/SnO_2	530	70,000	7.60	---
15	1% V_2O_5/ 3% SnO_2/SiO_2	630	35,000	2.00	17.8

TABLE 7. Product selectivities observed for methane conversion by air (CH_4/air = 1.5/1.0, 0.1 MPa) over supported metal oxide catalysts.

Catal. No.	Catalyst	Selectivities (C-mol%)			
		CH_2O	C_2 HC	CO	CO_2
1	SiO_2	100	---	---	---
2	2% MoO_3/SiO_2	100	---	---	---
3	1% V_2O_5/SiO_2	15.7	1.7	76.4	6.3
4	3% V_2O_5/SiO_2	16.6	0.2	76.8	6.3
5	5% V_2O_5/SiO_2	13.5	-.2	81.3	4.3
6	1% V_2O_5/ 3% MoO_3/SiO_2	16.6	2.0	73.5	7.9
7	TiO_2	2.3	---	94.0	3.6
8	3% TiO_2/SiO_2	17.8	---	71.1	11.1
9	1% V_2O_5/TiO_2	3.3	1.2	73.0	22.5
10	1% V_2O_5/ 3% TiO_2/SiO_2	18.6	---	76.6	4.8
11	3% V_2O_5/ 3% TiO_2/SiO_2	12.5	---	82.2	5.3
12	SnO_2	0.1	---	8.9	90.4
13	3% SnO_2/SiO_2	1.1	13.7	8.7	76.3
14	1% V_2O_5/SnO_2	---	---	13.4	83.6
15	1% V_2O_5/ 3% SnO_2/SiO_2	3.9	---	77.2	18.9

The effect of reactant flow rate, and thus the resident time of the reactants over the catalyst, on the level of methane conversion to products was investigated over two of the vanadia catalysts. The conversion levels of methane as a function of contact time over the 1.0% and 3.0% V_2O_5/SiO_2 catalysts are shown in Figure 18. The data for the 1.0 wt% V_2O_5/SiO_2 catalyst were obtained at 630°C, while those for the 3.0 wt% V_2O_5/SiO_2 catalyst were obtained at 580°C because of the appreciably higher activity of the 3% V_2O_5 catalyst.

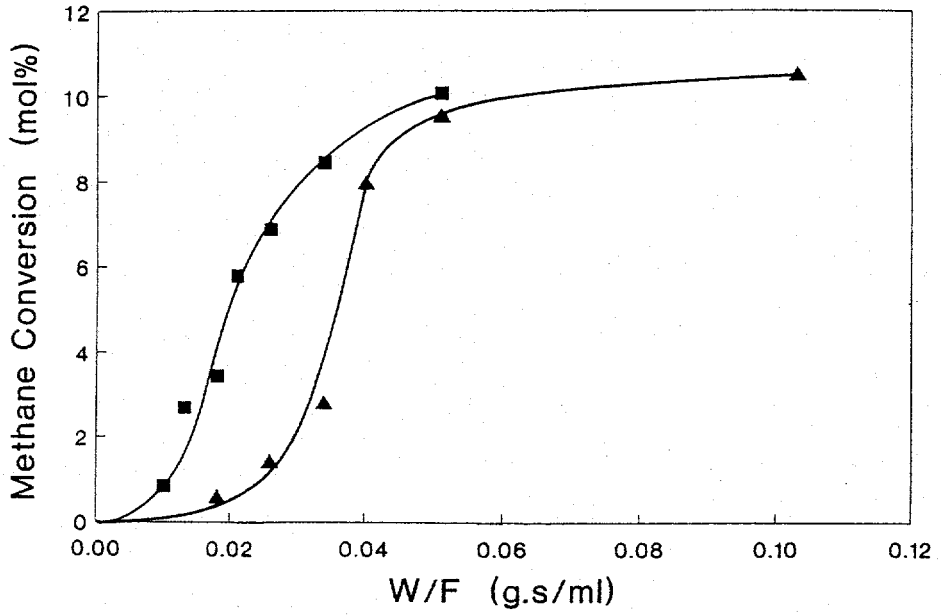

Figure 18. Conversions of methane from a reactant mixture of CH_4/air = 1.5/1.0 to products as a function of the reactant contact time over 1 wt% V_2O_5/SiO_2 (▲,630°C) and 3 wt% V_2O_5/SiO_2 (■,580°C) catalysts.

The relationship between product selectivity and activity of the vanadia catalysts was investigated. Figure 19 represents the formaldehyde selectivities as a function of methane conversion over four catalysts with different V_2O_5 loadings. As shown in Figure 19, the 1.0% V_2O_5/SiO_2 catalyst was tested at three different temperatures, and all of the data points were located on a single curve. The data demonstrated an inverse relationship between activity and selectivity, and this figure shows that as the methane conversion increased, the selectivity toward formaldehyde synthesize decreased. This figure shows that formaldehyde selectivity was very sensitive to the methane conversion level, which is well-recognized in the literature (4,36), and also very sensitive to the V_2O_5 loadings. On the other hand, the selectivity was rather insensitive to the reaction temperature, at least within the temperature range of 580-630°C. Koranne et al. (62) also reported a universal curve showing decreasing formaldehyde selectivity as the methane conversion increased in the 550-660°C temperature region where methane conversion was the primary factor for controlling selectivity rather than temperature.

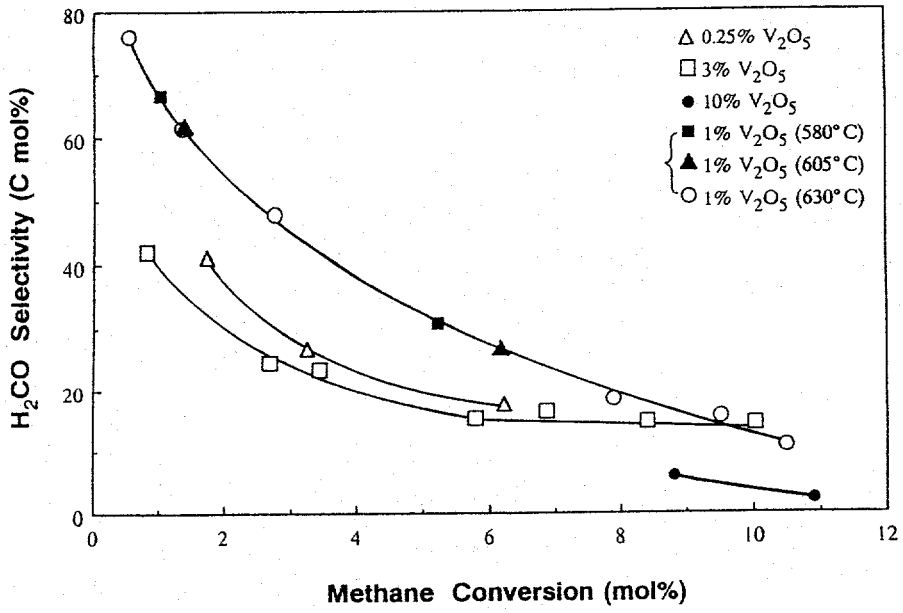

Figure 19. Formaldehyde selectivity *vs* methane conversion from CH_4/Air = 1.5/1.0 over different V_2O_5/SiO_2 catalysts, at 580°C except as noted.

To more directly determine the influence of the vanadia content of the catalysts on the product selectivity, the V_2O_5/SiO_2 catalysts were tested at temperatures where the methane conversion was maintained at ≈ 1%. Figure 20 shows the formaldehyde selectivity as a function of the vanadia loading of the silica support under these conditions.

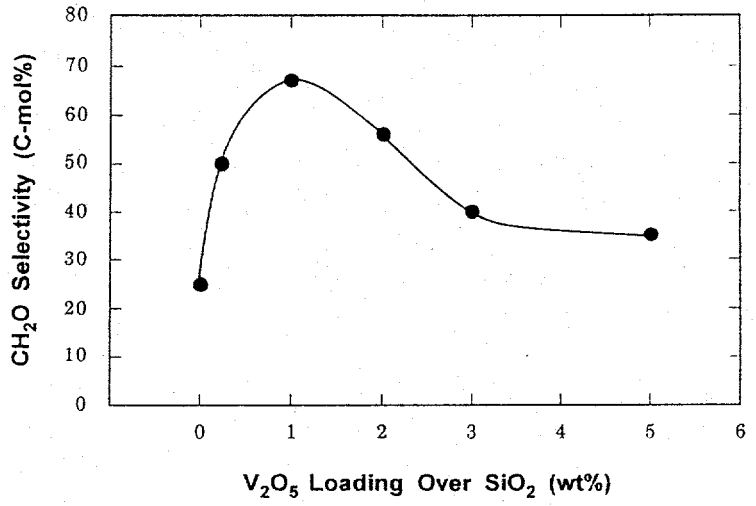

Figure 20. Formaldehyde selectivity as a function of the V_2O_5 loading of the silica support at a methane conversion level of ≈ 1 mol% from a CH_4/Air = 1.5/1.0 volume ratio reactant mixture.

Using a 2 wt% V_2O_5/SiO_2 catalyst, the apparent activation energy for conversion of methane to products was determined in the temperature range of 555 to 630°C. The methane conversion was limited to 1-2% by varying GHSV between 65,000 to 350,000 ℓ/kg cat.hr as the reaction temperature was progressively increased. The resultant Arrhenius plot obtained with this catalyst is shown in Figure 21, and the effective activation energy determined here was 29.2 kcal/mol. This value of apparent activation energy strongly indicates that the reaction was initiated by surface reactions. Interestingly, Figure 20 indicates the presence of an optimum V_2O_5 loading for methane partial oxidation to formaldehyde over the V_2O_5/SiO_2 catalysts, and over the doping range investigated, 1% V_2O_5 yielded the highest formaldehyde selectivity at constant methane conversion level.

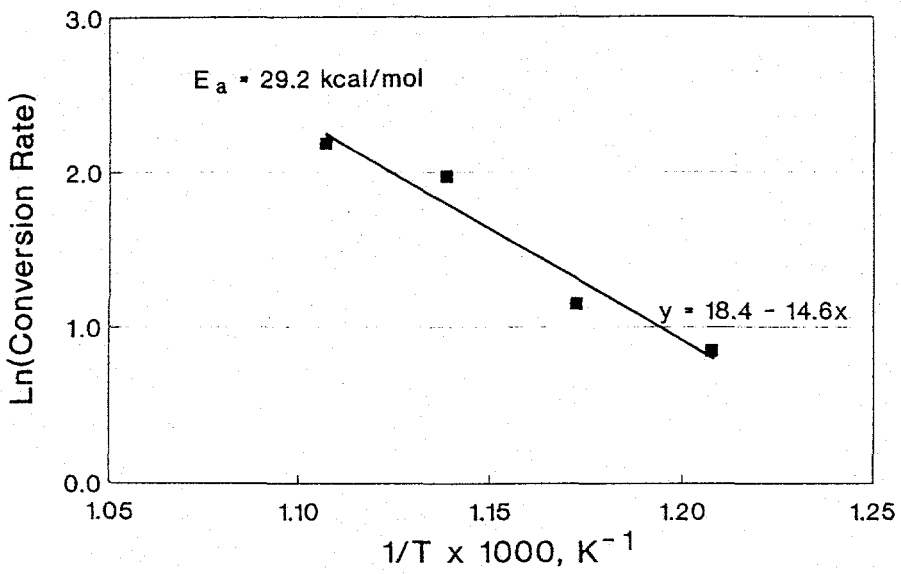

Figure 21. Arrhenius plot for methane conversion to products over a 2 wt% V_2O_5/SiO_2 catalyst using a CH_4/Air = 1.5/1.0 volume ratio reactant mixture.

Partial oxidations of methane are highly exothermic reactions (4). At high reaction temperatures, homogeneous gas phase reactions also contribute significantly to the overall partial oxidation reactions once the reactions are initiated over the catalyst surface (10). The level of methane conversions as a function of the contact times over the V_2O_5/SiO_2 catalysts at two V_2O_5 loadings were shown in Figure 18. At contact times below 0.04 sec, methane conversion exceeded the linear increase with increasing contact time expected for a differential reactor, which indicates that autocatalytic reactions occurred. At longer contact times, diffusion limitations caused the methane conversion to decrease. This autocatalytic property of methane partial oxidation over the V_2O_5/SiO_2 catalyst has not been explicitly noted in previous studies. There are two factors that could contribute to the autocatalytic behavior: (i) a hot spot may be able to form in the catalyst bed during the reaction and accelerate further the surface reactions due to the high exothermic nature of the partial oxidations or (ii) the gas phase free radical chain reaction could be initiated on the surface.

The presence of autocatalytic reactions makes it difficult to precisely determine the turnover frequency (TOF; methane molecules reacted/vanadium atom/sec) for methane activation and conversion over the V_2O_5/SiO_2 catalysts. Nevertheless, based on the fact that surface vanadium oxide species are molecularly dispersed and isolated over the SiO_2 support for loadings less than 10% V_2O_5 (see the laser Raman study in Task 3), the TOF of methane conversion was estimated by using the data obtained at methane conversions less than 2%. The estimates are given in Table 8, and these data indicate that the TOF for methane conversion did not change significantly as the V_2O_5 loading was increased from 0.25% to 5.0%. This suggests that methane activation only needs one type of active site, which increased linearly with the V_2O_5 content in the range studied here.

TABLE 8. Turnover frequencies (TOF) determined for methane conversion to products over V_2O_5/SiO_2 catalysts at 580°C and 0.1 MPa from a CH_4/Air = 1.5/1.0 reactant mixture.

V_2O_5 Content (wt%)	GHSV (ℓ/kg/hr)	CH_4 Conv. (mol%)	TOF (10^{-1} sec^{-1})
0.25	16,200	1.7	6.8
1.0	70,000	1.0	4.5
2.0	140,000	1.1	5.0
3.0	350,000	0.8	5.9
5.0	280,000	1.1	3.8

Discussion and Conclusions. The present study indicates that silica is the best support for the multivalent V_2O_5 catalyst for partial oxidation of methane to formaldehyde. Very high space time yields of formaldehyde (>1 kg CH_2O/kg cat.hr) have been achieved with the 1% V_2O_5/SiO_2 catalyst. Methane activation over this catalyst only needed a single active site whose concentration increased linearly with the V_2O_5 loadings up to atleast 5 wt%.

In examining other catalysts, the data in Table 6 clearly indicate that the 2% MoO_3/SiO_2 catalyst had an activity similar to that of the pure fumed silica support and was significantly less active than the V_2O_5/SiO_2 catalyst. The 1% V_2O_5/SiO_2 and 1% V_2O_5/3% MoO_3/SiO_2 catalysts exhibited almost identical catalytic activities and product selectivities for methane partial oxidation to formaldehyde. This indicates that V_2O_5 and MoO_3 were isolated species coexisting over the SiO_2 support without strong interactions and the catalytic activity was dominated by the surface vanadium oxide species. This conclusion is corroborated by the structural information obtained from Raman spectroscopy that will be presented in Task 3, which showed no interaction between the two transition metal oxides

The V_2O_5/TiO_2 catalyst, analogous to the V_2O_5/SiO_2 catalyst, is proposed to possess well-dispersed surface vanadia species over the TiO_2 support for low loadings. However, data in Table 6 reveal that for methane oxidation, the 1 wt% V_2O_5/SiO_2 catalyst was much more active than the 1 wt% V_2O_5/TiO_2 catalyst. Under the same reaction conditions, the methane conversion over the V_2O_5/SiO_2 catalyst was about one order of magnitude higher than over the V_2O_5/TiO_2. It is interesting that the catalytic performances of the 1 wt% V_2O_5/TiO_2 and the 1 wt%V_2O_5/3 wt% TiO_2/SiO_2 catalysts for methane oxidation are very similar, except that the latter catalyst exhibited a higher selectivity for formaldehyde production. These results are consistent with structural information that the vanadia overlayer is coordinated to the titania overlayer, which results in behavior similar to the V_2O_5/TiO_2 catalyst.

One striking observation (Table 6) was that the catalytic activities of the V_2O_5/TiO_2 catalyst and the bare TiO_2 support were very similar. However, the product selectivity patterns (Table 7) were quite different for these two systems. While methane oxidation over TiO_2 produced CO almost exclusively, a significant amount of CO_2 was produced over the V_2O_5/TiO_2 catalyst as well. In the absence of detailed mechanistic information, one can only suggest at this point that coupled redox systems, e.g. V(IV)/V(V)||Ti(IV)/Ti(III), may be responsible for the deep oxidation properties of the V_2O_5/TiO_2 catalyst.

The 1 wt% V_2O_5/SnO_2 catalyst exhibited a high catalytic activity for methane conversion (Table 6), but it only produced deep oxidation products CO_x, and predominantly CO_2 (Table 7). However, the catalytic activity of the 1 wt% V_2O_5/3 wt% SnO_2/SiO_2 catalyst was low and even lower than that of the 1 wt% V_2O_5/SiO_2 catalyst (Table 6). These catalytic results suggested a poisoning effect of the SnO_2 overlayer, which might have eliminated some of the active surface vanadia species on SiO_2 and reduced the catalytic activity. It is interesting to notice that over the mixed 1 wt% V_2O_5/3 wt% SnO_2/SiO_2 catalyst, the predominant product was CO instead of CO_2 as observed over the V_2O_5/SnO_2 catalyst. It is possible that CO was mainly formed *via* decomposition of the primary formaldehyde product accelerated by the supported SnO_2 overlayer on the SiO_2 surface.

Thus, it appears that vanadia is well-dispersed and present as a two-dimensional overlayer when supported on SiO_2, TiO_2, SnO_2, 3 wt% TiO_2/SiO_2, 3 wt% MoO_3/SiO_2 and 3 wt% SnO_2/SiO_2. The V_2O_5/SiO_2 catalyst is the most selective catalyst for the partial oxidation of methane by oxygen to form formaldehyde, but the catalytic performance was strongly dependent on vanadia coverage and an autocatalytic behavior was observed. At very low conversions, the formaldehyde activity increased linearly with vanadia coverage, indicating that isolated V^{5+} species were responsible for the active sites. Space time yields of 0.1-1.4 kg CH_2O/kg cat/hr and selectivities of 2-78% are reported herein for the V_2O_5/SiO_2 catalysts. Deep oxidation products, CO and CO_2, were principally produced over the V_2O_5/TiO_2 and V_2O_5/SnO_2 catalysts.

II. Double Bed Catalysts for Enhancing Methanol Formation

In direct conversion of methane to methanol and formaldehyde, research described in the current literature [3,4] has focused on developing a single catalyst that would be capable of both activating methane and generating methanol. In order to circumvent the difficulty of trying to accomplish two tasks using one catalyst, a different approach has been adopted in our research by using a double-layered catalyst bed. This provides for separate optimization of the two catalysts in the double-layered catalyst bed and greatly broadens the choices for the catalysts.

Experimental Procedures. The 1% $SO_4^{2-}/Sr/La_2O_3$ catalyst was prepared as summarized earlier in this report. The unsupported metal oxides ZrO_2, Y_2O_3, SrO, CuO, Fe_2O_3, MnO_2, Cr_2O_3, CaO, and MgO were obtained from Aldrich Chem. Co., Inc. and were calcined at 600°C for 6 hr. Amorphous SiO_2 (Cabosil EH-5, surface area = 380 m^2/g) was used as the support for the 1%Re_2O_7, MoO_3, and V_2O_5 catalysts used here. Except for the silica-supported 1% V_2O_5 catalyst that was prepared by using methanol solution of vanadium(V) triisopropoxide oxide ($VO[i\text{-}OC_3H_7]_3$) and amorphous SiO_2, the rest of the catalysts were prepared by aqueous impregnation. Loadings for all the catalysts tested are expressed in weight percentage.

The experiments were typically carried out both in the single-bed and the double-bed mode. The temperature range was 550-650°C and the gas hourly space velocity (GHSV) was 100,000-240,000 l/kg cat hr. Steam cofeeding, when utilized, was achieved by pumping distilled water into the heated volume preceding the catalyst bed with an ISCO liquid metering pump (model 314). The water was vaporized and the resulting steam was then mixed with the CH_4/air = 1.5 reagent gases. The rate of steam cofeeding was controlled at 19.6 ml/min by the metering pump in most experiments, and all the tubing leading into and out of the reactor was heated at about 150°C. This setup enabled the feeding of steam of up to several hundred Torr in the reagent gas mixture. All experiments were carried out at atmospheric pressure.

The analyses of the feed and product gases were done by using a Hewlett Packard 5890 gas chromatograph with a molecular sieve 13X column and a Chrompack Model 7550 PoraPLOT Q fused silica capillary column in parallel and coupled with two TCD detectors. The liquid products consisting of methanol, formaldehyde, and water were trapped by using an ice bath at 0°C and were separately analyzed by a Hewlett Packard 5970 MSD GC/MS instrument. More accurate analysis of formaldehyde was achieved by using an iodine titration method.

Methanol Production Over Various Metal Oxides. The direct conversion of methane to methanol is a multistep process possibly involving the generation of methyl radicals, their reaction with surface oxygen species to form methoxide ions, and the hydrolysis of the surface methoxide to form methanol. As the further loss of H-atoms from methyl radicals

formed during the reaction would be detrimental to the process, an oxide catalyst is preferred over a metal catalyst to avoid further dehydrogenation. The oxides should be able to provide an oxygen atom to the methyl radical and the resulting methoxide should be readily hydrolyzable, which indicates that an ionic-type bonding of the methoxide species to the surface is desirable. The oxide catalysts synthesized previously were studied in more detail, and additional metal oxide catalysts were also obtained and investigated.

Figure 22 shows the methanol space time yields over a variety of metal oxide catalysts at a GHSV of 72,000 l/kg hr. These results were obtained using the double bed reactor configuration. It is evident from the top part of the figure that supported V_2O_5 gave the highest methanol space time yield, which was nearly 100 g/kg cat.hr. In order to observe the results over the other oxides more closely, V_2O_5 was left out and the data were replotted on the scale of 0-12 g/kg cat/hr as shown in the bottom part of the figure. It is evident from the figure that the four other catalysts that gave significant methanol production were silica-supported Re_2O_7 and MoO_3 and unsupported Y_2O_3 and ZrO_2.

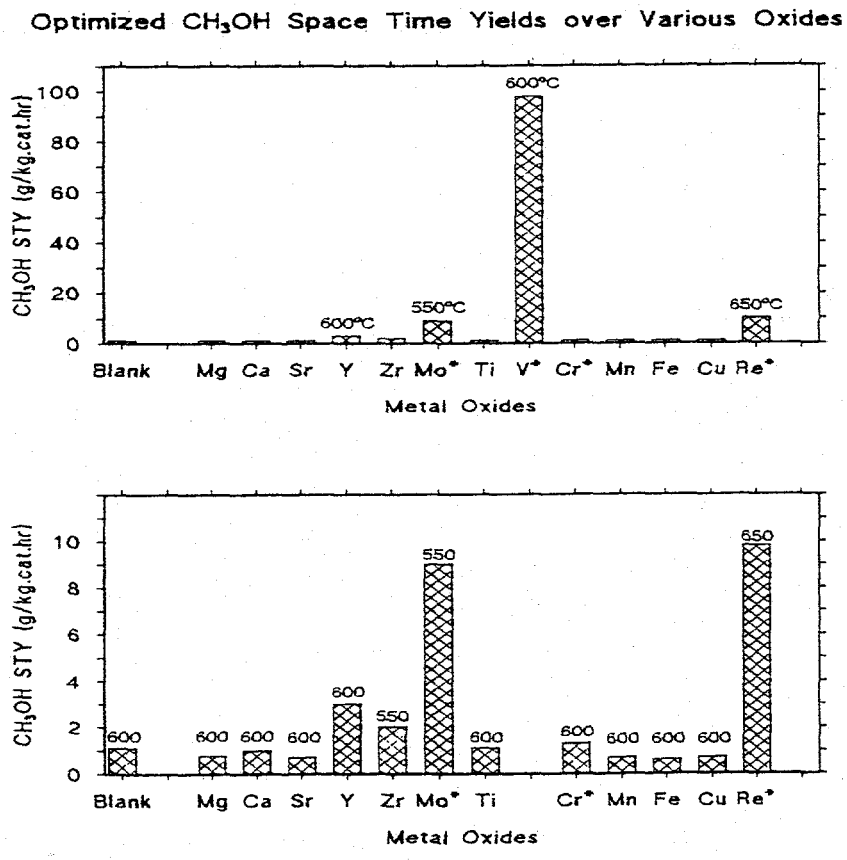

FIGURE 22. Space time yields of methanol obtained over various metal oxide catalysts in a double bed configuration, where * represents silica-supported catalysts. Experiments were carried out at 72,000 ℓ/kg.hr using 100 mg of 1 wt% $SO_4^{2-}/SrO/La_2O_3$ as the first-bed catalyst and with a ratio of CH_4/air/steam = 140/96/20 ml/min. The second bed size was 100 mg.

Comparison Between Single-bed and Double-bed Reactors. Both single-bed and double-bed experiments were carried out for all the catalysts tested, and the results showed a consistent enhancement of oxygenates production when the double-bed configuration was used. Figure 23 shows productivities of methanol over 1 wt% Re_2O_7/SiO_2 and 1 wt% MoO_3/SiO_2 and unsupported Y_2O_3 and ZrO_2 catalysts in both the single-bed and double-bed configuration. In the double bed configuration, the supported oxide catalysts exhibited the higher productivities of methanol, but these were still relatively low.

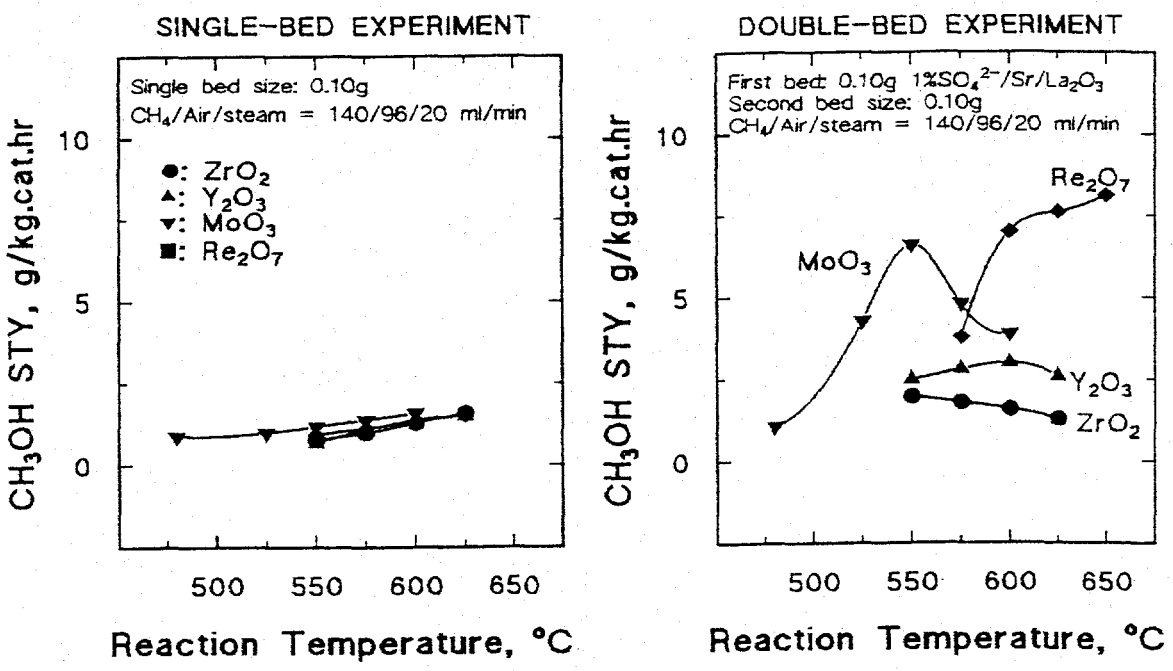

FIGURE 23. Comparison between CH_3OH space time yields over silica-supported Re_2O_7 and MoO_3 and unsupported Y_2O_3 and ZrO_2 catalysts in the single-bed and double-bed configurations using CH_4/air/steam = 1.5/1.0/0.2.

The activities of the silica-supported vanadia catalyst as a function of reaction temperature were determined in both the single bed and double bed configurations. Figure 24 shows the productivites of both methanol and formaldehyde produced by the $1\%V_2O_5/SiO_2$ catalyst, and it is shown that high activities were achieved. In both cases, the space time yields of methanol exhibited a maximum as a function of temperature, and that for the dual bed case was observed to occur at least 50°C lower that for the single bed test. In addition, the productivity of formaldehyde was much greater at lower temperatures in the dual bed configuration than for the single bed catalyst. These data demonstrated a positive contribution of the double bed reactor configuration in oxygenate production. The results are consistent with the role of the first catalyst layer as methyl radical generating catalyst and that of the second layer as the methyl radical trapping and methanol formation catalyst.

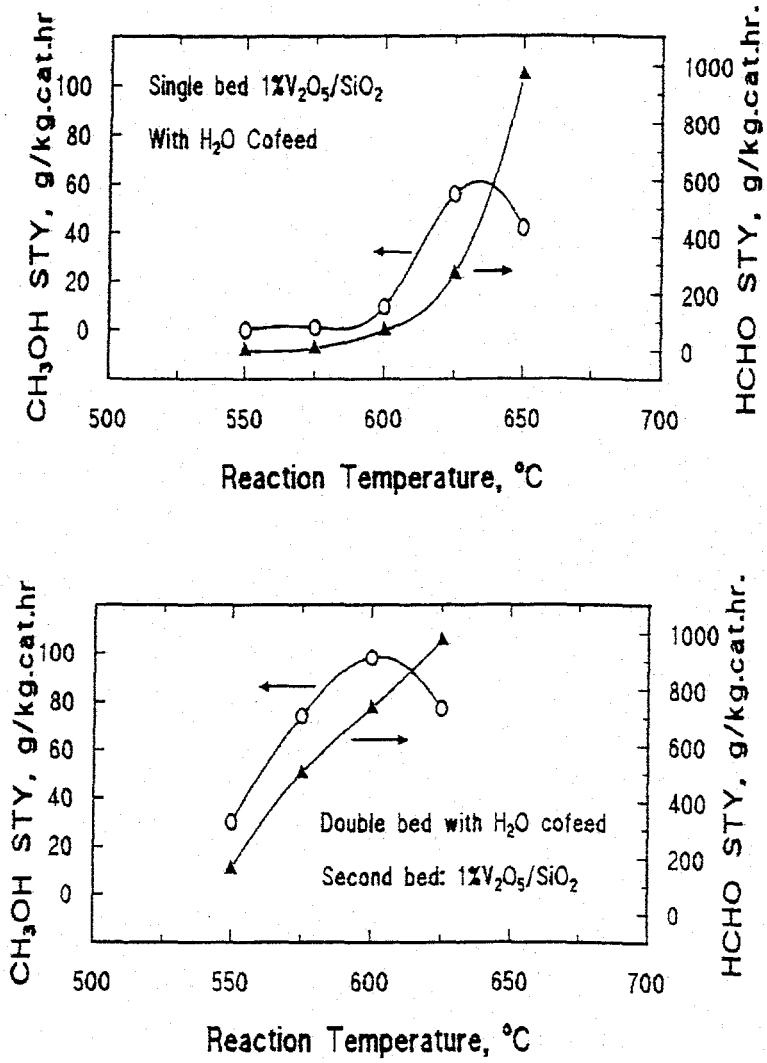

FIGURE 24. Effects of double-bed reactor configuration on the productivities of methanol and formaldehyde over 1 wt% V_2O_5/SiO_2 catalyst. Experiments were carried out at GHSV = 72,000 ℓ/kg.hr using 100 mg of 1 wt% $SO_4^{2-}/SrO/La_2O_3$ as the first-bed catalyst and with a reactant ratio of CH_4/air/steam = 140/96/20 ml/min. The second bed size was 100 mg.

The Role of Steam in Oxygenate Production Over Double-layer Catalysts. Pitchai and Klier [4] proposed that the role of steam in partial oxidation of methane to oxygenates was to hydrolyze the surface methoxide species formed during the reaction. Lunsford and co-workers [23] reported evidence for the formation of methoxide ions by using infrared spectroscopy over a silica-supported molybdenum catalyst. During previous work in this laboratory, the effect of steam cofeed at low methane conversion was investigated. This work was now extended to the study of the role of H_2O under relatively high methane conversions, in particular over the 1 wt% V_2O_5/SiO_2 catalyst because this catalyst currently gives the highest oxygenates yields under the double-bed reactor configuration.

It turned out that over this catalyst even at a methane conversion of about 15% the cofeeding of steam could still increase the oxygenate productivites, as depicted in Figure 25. The methanol production showed the biggest enhancement at 600°C, with the space time yield increasing from about 40 to nearly 100 g/kg cat./hr. The formaldehyde production also showed improvement with additional steam, but it followed a somewhat different trend. The production of methanol reached a maximum at around 600°C and then started dropping at higher temperature, while that of formaldehyde continued to increase within the temperature range of the experiment. This could be explained by fact that methanol is more readily oxidized than formaldehyde at higher temperatures and formaldehyde could be produced by oxidation of methanol. Thus, increasing temperature would gradually alter the selectivity from methanol to formaldehyde. The data indicate that in order to maximize the yield of methanol relative to that of formaldehyde, temperatures higher than 600°C should not be utilized, at least with this catalyst.

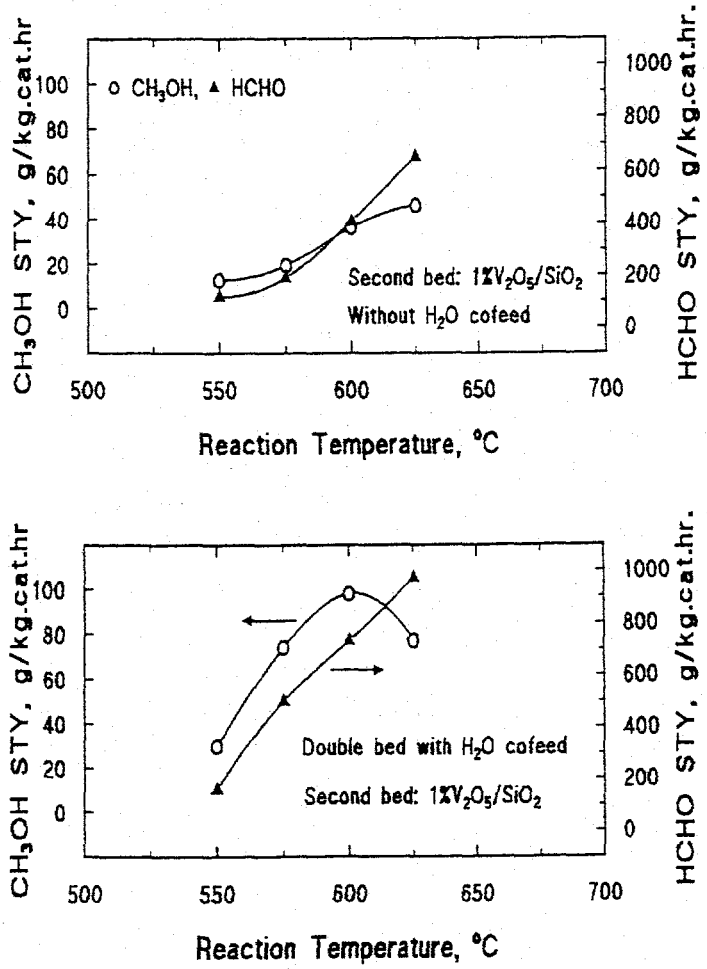

FIGURE 25. Effects of adding steam to the reactant mixture on the CH_3OH and HCHO space time yields over the 1 wt% V_2O_5/SiO_2 catalyst. Experiments were carried out at GHSV = 72,000 ℓ/kg.hr using 100 mg of 1% $SO_4^{2-}/SrO/La_2O_3$ as the first-bed catalyst and with reactant ratios of CH_4/air = 1.5/1.0 and CH_4/air/steam = 1.5/1.0/0.2. The second bed size was 100 mg.

Effect of Space velocity on Oxygenates Production. Hargreaves *et al.* [45] reported an increase in formaldehyde production with increasing total flow rate over a MgO catalyst. It can be inferred from those data that the survival of oxygenates required very short contact time in order to prevent their further oxidation. Experiments that varied both the total flow rate and the thickness of either layer of the double bed was carried out here in search of optimal reactor conditions. The study was carried out over a 1 wt% Re_2O_7/SiO_2 catalyst since this catalyst only produced minimal amounts of oxygenates in the single-bed reactor, and this made it easier to see the effect of a second bed. As shown in Figure 26, an increase of the total flow rate increased the productivites of both methanol and formaldehyde. At the same time the total level of methane conversion decreased.

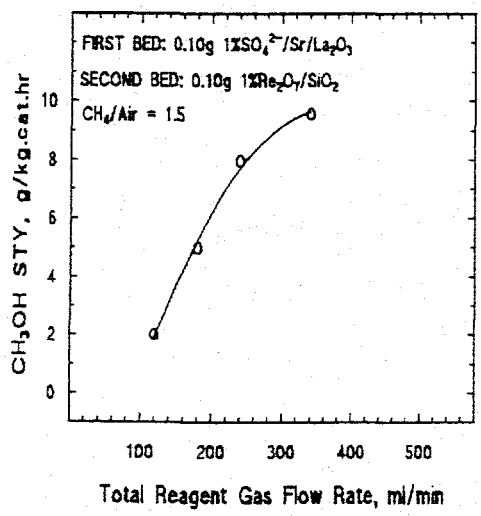

FIGURE 26. Effect of total flow rates on the CH_3OH space time yields over the 1 wt% Re_2O_7/SiO_2 catalyst. Experiments were carried out at 600°C using 100 mg of 1% $SO_4^{2-}/SrO/La_2O_3$ as the first-bed catalyst and with a reactant ratio of CH_4/air/steam = 1.5/1.0/0.2. The second bed size was 100 mg.

Figure 27 shows the results when the sizes of the first layer and the second layer of the bed were independently varied. It is evident that in both cases, the size of the beds can have either a positive or a negative impact on the yield of methanol. When the top layer, the methyl radicals generating bed, was very small and the contact time with this catalyst was short, the number of methyl radicals produced by the catalyst was small. Thus, the quantity of methanol formed over the second bed was small. As the size of the first catalyst bed was gradually increased, the formation of methanol was initially nearly linearly dependent on the size of the first bed. As the size of this bed increased and approached and exceeded that of the second bed, the proportion of methyl radicals that were oxidized to other products increased. Changing the size of the second bed, which is a methyl radicals trapping and methoxide hydrolysis bed, had a similar effect of increasing the space time yield of methanol.

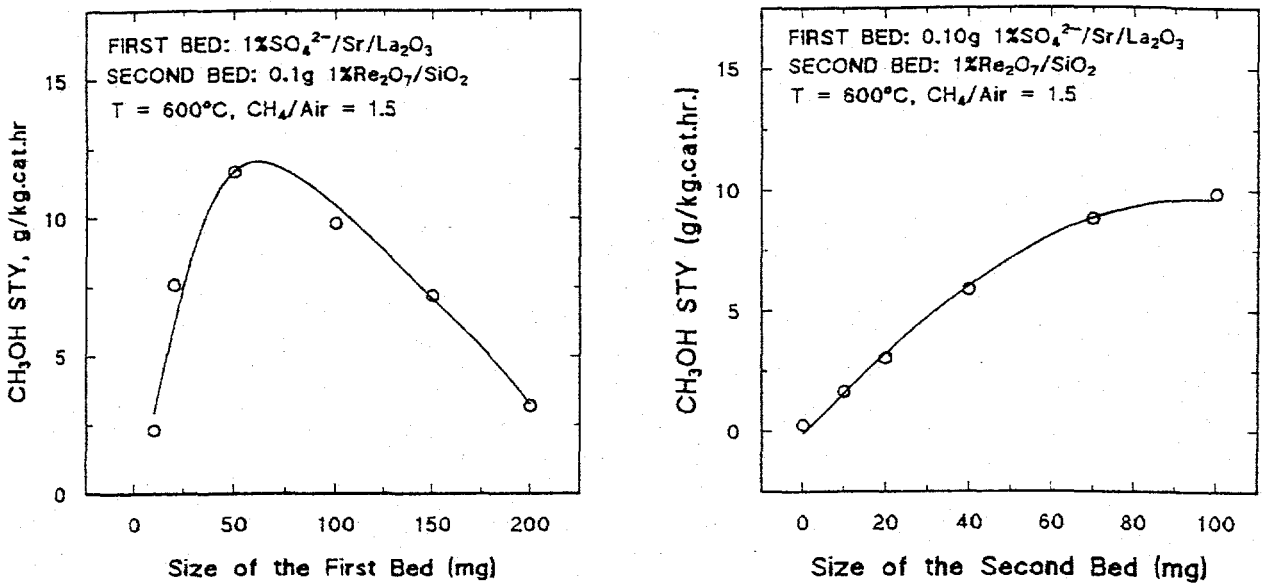

FIGURE 27. Effects of varying the first or second bed size, while maintaining the other constant, on the CH_3OH space time yields over the 1 wt% Re_2O_7/SiO_2 catalyst. Experiments were carried out at 600°C using 1 wt% $SO_4^{2-}/SrO/La_2O_3$ as the first-bed catalyst and with a reactant ratio of CH_4/air/steam = 1.5/1.0/0.2, at GHSV = 144,000 ℓ/kg.hr relative to the constant 0.100 g bed.

The Stability of the Double-Bed Catalysts. It was worthwhile to investigate the stability of the double bed catalyst pair of 1 wt% $SO_4^{2-}/SrO/La_2O_3$‖1 wt% V_2O_5/SiO_2, which previously had given the highest methanol space time yield in this work (nearly 100 g/kg cat·hr at 600°C). This catalyst test was carried out as a function of time on stream at ambient pressure (0.1 MPa). Again, the feed and product gases were analyzed by using a Hewlett Packard 5890 gas chromatograph with a molecular sieve 13X column and a Chrompack Model 7550 PoraPLOT Q fused silica capillary column in parallel and TCD detectors. In addition, the liquid methanol and formaldehyde products were trapped by using an ice bath at 0°C and were separately analyzed by a Hewlett Packard 5970 MSD GC/MS instrument.

As shown in Table 9, gradual deactivation of the double bed catalyst system was observed. Although the overall methane conversion decreased by 29% over a period of 72 hr, the space time yield of methanol decreased by 52% over the same period. Surprisingly, the formaldehyde productive did not change nearly as much.

TABLE 9. The conversions of methane and the space time yields of products formed over double bed catalysts with gaseous steam as cofeed. The first bed contained the 0.10 g 1%SO_4^{2-}/SrO/La_2O_3 catalyst and the second bed consisted of 0.10 g 1%V_2O_5/SiO_2. The reactant mixture consisted of CH_4/air/steam = 1.5/1.0/0.2 with GHSV = 76,500 ℓ/kg catal/hr for the dual bed system (or 153,000 ℓ/kg catal/hr relative to each bed). The reaction temperature was 600°C and the pressure was 0.1 MPa.

Time on stream, hr	CH_4 Conv., mol%	Space Time Yields, g/kg cat·hr (Selectivities, mol%)					CH_3OH /HCHO Molar Ratio
		C_2 HC	HCHO	CH_3OH	CO	CO_2	
2	14.4	2875 (39.7)	820 (5.5)	97.9 (0.6)	2688 (19.2)	7697 (35.0)	0.11
5	14.2	3427 (48.0)	771 (5.2)	91.6 (0.6)	2510 (18.2)	6077 (28.0)	0.11
11	13.1	3214 (48.8)	764 (5.6)	86.0 (0.6)	2479 (19.5)	5111 (25.6)	0.11
26	12.2	2876 (46.9)	854 (6.7)	70.6 (0.5)	1964 (16.6)	5416 (29.3)	0.07
29	11.4	2435 (42.5)	819 (6.9)	66.0 (0.5)	2170 (19.6)	5312 (30.5)	0.07
47	11.1	2498 (44.7)	786 (6.8)	60.4 (0.5)	1822 (16.8)	5266 (31.1)	0.07
58	10.6	2273 (42.6)	729 (6.6)	57.0 (0.5)	1962 (19.1)	5054 (31.2)	0.07
72	10.2	2194 (42.8)	741 (7.0)	46.7 (0.4)	1875 (18.9)	4816 (30.9)	0.06

The cause of the deactivation evidenced by the data in Table 9 has not been determined, but this should be investigated in the future. The stability of the SO_4^{2-}/SrO/La_2O_3 catalyst by itself with CH_4/air = 1/1 reactants during a 25 hr test was shown in Figure 9. It is possible that the presence of steam led to the loss of the sulfate promoter, resulting in lower production of methyl radicals and consequently of C_2 hydrocarbon products and oxygenates. However, since methanol and formaldehyde exhibited different

behavior, it is possible that the second bed was affected as well. The deactivation was possibly due to the gradual loss of vanadium from the second bed or to agglomeration of dispersed vanadium active centers into vanadia films or particles. In either case, this loss of dispersed active catalytic centers might be enhanced by the presence of steam in the reactant mixture. However, it is surprising to note that the space time yields of HCHO over the same time period hardly changed, and, in fact, the HCHO selectivity increased during the test. If vanadium were lost during the test, this result indicates that the formation of HCHO was not very sensitive to changes in the vanadium content on the catalyst, at least not within the range of vanadium content change of the experiment. These results might also indicate that higher vanadium content and/or higher concentration of dispersed vanadium active sites in the second bed catalyst might favor methanol formation more than HCHO formation. These are factors that should be studied in the future to optimize the double bed catalyst configuration for the direct synthesis of methanol from methane.

III. Xerogel Vanadia/Silica Catalysts for Selective Oxidation of Methane

Previous studies have shown that the oxidation of methane to methanol and formaldehyde over most oxide catalysts proceeds with appreciable activity only at high temperatures, but then only with low selectivities [4,60]. One reason for this is the secondary conversion of primary products to carbon dioxide. Higher selectivities of partially oxidized products such as methanol and formaldehyde might be achievable by using catalysts capable of activating methane at mild reaction conditions, but the low reactivity of methane makes this an extremely challenging task.

Among the numerous catalysts proposed for the partial oxidation of methane to formaldehyde, it was pointed out earlier in this report that silica-supported V_2O_5 catalyst was one of the most active and selective catalysts for partial methane oxidation by O_2 to formaldehyde [25,36,54]. In the previous section of this report, a process including feeding steam and/or using double catalyst bed was demonstrated for obtaining methanol over V_2O_5/SiO_2 catalysts. However, it is generally agreed that the interaction of the vanadia species with the silica support is relatively weak in catalysts prepared by impregnation of silica with a vanadium-containing precursor [63-65]. As a result of the weak interaction, the immobilized vanadia species tend to agglomerate when exposed to higher temperature. This behavior resulted in deactivation of the V_2O_5/SiO_2 catalysts in partial methane oxidation.

Baiker et al. [66] observed that finely dispersed vanadia species on silica could be stabilized in a silica matrix by employing a sol-gel process to prepare the catalysts. It was observed that in all mixed gel catalysts, the well-dispersed vanadia species were more stable at high temperature than those prepared by impregnation. Silica-based xerogels containing vanadium corresponding to the equivalent of 1.0 wt% to 25.0 wt% V_2O_5 were prepared by the sol-gel precess and investigated with regard to their structure and catalytic properties in selective partial oxidation of methane.

Preparation of Xerogel Catalysts. The V_2O_5-SiO_2 xerogels were prepared by a sol-gel synthesis using vanadium triisopropoxide oxide ($VO(OC_3H_7)_3$, Fisher) as precursor. The SiO_2 sol was first prepared by dissolving tetraethoxysilane ($Si(OC_2H_5)_4$, Fisher) in methanol (99.9%, Fisher) and combining it with a solution of deionized water and nitric acid (70%, Fisher), followed by stirring with a magnetic bar for 20 min for partial hydrolysis to occur. The SiO_2 sol was then mixed with vanadium triisopropoxide oxide diluted in methanol, after which the resulting transparent V_2O_5-SiO_2 sol was stirred for 15 min. Additional aqueous nitric acid was added to the V_2O_5-SiO_2 sol and a thick gel formed within 12 hr. The obtained gel was allowed to age at room temperature for an additional 10 hr. Subsequently, the V_2O_5-SiO_2 gel was dried at 50°C for 15 hr, at 120°C for 6 hr, and then calcined at 550°C for 4 hr. On the basis of 1 mol of tetraethoxysilane, the following substances were used: 2.76 mol of methanol, 0.66 mol of nitric acid, 7.8 mol of water, and an appropriate amount of vanadium triisopropoxide oxide that gave V_2O_5 contents of 1.0, 2.0, 3.0, 4.0, 5.0,

10.0, 20.0, and 25.0 wt% in the final V_2O_5-SiO_2 xerogels. The synthesis of a 15.0 wt% V_2O_5-SiO_2 xerogel was different from the above xerogels in the amount of employed water and nitric acid. Only 4.0 mol of water and 0.0001 mol of nitric acid on the basis of 1 mol of tetraethoxysilane was used for the preparation of 15.0 wt% V_2O_5-SiO_2 xerogel. The gel formed within 4 days.

A 0.05 wt% Pd-10.0 wt% V_2O_5-SiO_2 xerogel catalyst was synthesized by using the same method as that employed in the synthesis of V_2O_5-SiO_2 xerogel catalysts, but a mixture of $VO(OC_3H_7)_3$ and $Pd[(OCOCH_3)_2]_3$ in methanol was combined with a SiO_2 sol to form a Pd-V_2O_5-SiO_2 sol. The BET surface area and pore volume of the dried catalyst was 442 m^2/g and 0.31 cm^3/g, respectively.

Determination of the Surface Areas and Crystallinity of the Catalysts. All of the V_2O_5-SiO_2 xerogel catalysts were characterized by BET surface area measurements and X-ray powder diffraction (XRD). BET surface area and pore volume were measured with a commercial Gemini 2360 unit using nitrogen as the adsorbent. XRD patterns were obtained with an APD1700 automated powder diffractometer using a Cu K_α source. In XRD quantitative phase analysis, KCl was used as an inner standard. The peak areas for reflections $2\theta = 26.1°$ of V_2O_5 and $2\theta = 28.2°$ of KCl were measured to determine the amount of crystalline V_2O_5 in the xerogels. Pure vanadia was obtained by hydrolyzing $VO(OC_3H_7)_3$ in methanol followed by drying at 50°C for 10 hr, at 120°C for 6 hr, and calcining at 550°C for 6 hr.

Catalytic Testing. The low density V_2O_5-SiO_2 and Pd-V_2O_5-SiO_2 xerogel catalysts were pretreated in air at 550°C for 0.5 hr. Catalytic testing was carried out with a reactant stream of CH_4/air/steam = 150/100/56 ml/min at a pressure of 0.45 MPa. Typically, 0.10 g catalyst was packed in a downflow quartz reactor with quartz wool placed before and after the catalyst bed. In double-bed experiments, 0.10 g of 3.0 wt% and 0.10 g of 20.0 wt% V_2O_5-SiO_2 catalysts were packed in a quartz reactor with quartz wool placed before and after the catalyst bed. In one experiment, the 3.0 wt% V_2O_5-SiO_2 catalyst was the top catalyst (inlet portion of the reactor), while in a second experiment the 20.0 wt% V_2O_5-SiO_2 catalyst was the top catalyst.

The flow rates of methane and air were measured and controlled by mass-flow controllers (Brooks and Linde). The gases were preheated separately before entering the reactor. Water was injected into the reactant stream by means of an ISCO piston pump, and the water was vaporized in the preheater section of the reactor. The exhaust gas lines from the reactor to the GC and from the GC to the ice trap were heated to 150°C to prevent condensation of the products.

The exhaust gas was analyzed by a Varian 3700 gas chromatograph with helium as a carrier gas at a pressure of *ca.* 0.14 MPa with a flow rate of 30 ml/min using a Porapak Q column (2 m length x 1/8-in. o.d.) and a 5A zeolite column (2 m length x 1/8-in. o.d.) in

parallel and a thermal conductivity detector. The condensable products were trapped by using an ice bath at 0°C and were separately analyzed by a Hewlett Packard 5970 MSD GC/MS instrument. Data was collected and analyzed *via* an integrator and an on-line PC using ChromPerfect software.

Surface Areas and Crystallinities of the V_2O_5-SiO_2 Xerogel Catalysts. The BET surface areas and pore volumes of dried V_2O_5-SiO_2 xerogels containing 1.0, 2.0, 3.0, 4.0, 5.0, 10.0, 15.0, 20.0 and 25.0 wt% are listed in Table 10. The highest BET surface area was observed with the 1.0 wt% V_2O_5-SiO_2 xerogel, although the xerogels containing vanadia contents up to 25.0 wt% still remained a very high surface area. In contrast, a drastic decrease in surface area was observed by Baiker et al. [66] with vanadia-silica mixed gels prepared by another method when the vanadia content was 20.0 wt%. Therefore, the present synthesis process produced V_2O_5-SiO_2 xerogels with higher surface areas at higher vanadia contents.

TABLE 10. Surface areas and pore volumes of dried V_2O_5-SiO_2 xerogel catalysts.

V_2O_5 Content (wt%)	BET Surface Area (m^2/g)	Pore Volume (cm^3/g)
1.0	509	0.36
2.0	384	0.27
3.0	383	0.27
5.0	447	0.32
10.0	451	0.32
15.0	338	0.24
20.0	267	0.19
25.0	368	0.26

X-Ray diffraction patterns of V_2O_5-SiO_2 xerogel catalysts are presented in Figure 28. The patterns of catalysts containing the equivalent of 1.0, 2.0, 3.0, and 4.0 wt% vanadia showed only a broad peak characteristic for amorphous silica. A small sharp peak at 2θ =

31.0° was observed for 5.0 wt% V_2O_5-SiO_2 and several sharp reflections, such as $2\theta = 26.1°$ and $2\theta = 31.0°$, were observed for the catalysts with vanadia contents higher than 5.0 wt%. These sharp peaks were attributed to the existence of the crystalline V_2O_5 phase, which is well-recognized from the XRD pattern with a wide 2θ range for the 25.0 wt% V_2O_5-SiO_2 xerogel.

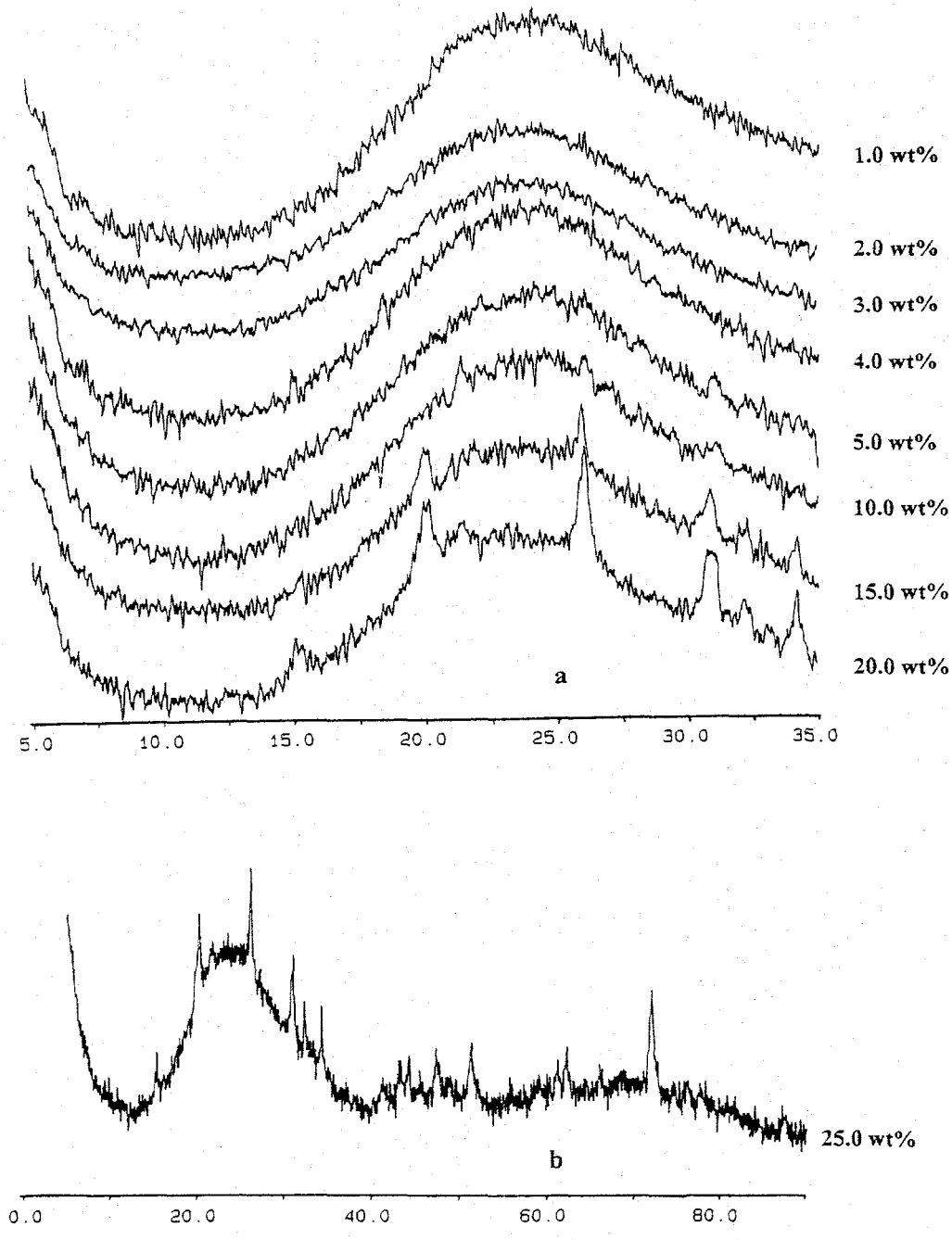

FIGURE 28. XRD patterns (in degrees 2θ) of V_2O_5-SiO_2 xerogels for (a) catalysts containing the equivalent of 1.0 to 20.0 wt% vanadia and (b) of 25.0 wt% vanadia.

Quantitative phase analysis using the intensity of the diffraction peaks yielded a measure of the amount of crystalline V_2O_5 *vs* the total *equivalent* amount of vanadia in the samples. From Figure 29, one can see that the straight line does not go through the origin but gives an intercept, corresponding to a critical dispersion capacity of vanadium within the silica matrix at about 4.0 wt% vanadia in V_2O_5-SiO_2 xerogels. When the content of V_2O_5 was below the critical dispersion capacity, no crystalline V_2O_5 could be detected by XRD, indicating that the V was finely dispersed within the matrix. This fine dispersion is proposed to be predominantly a monolayer dispersion of V_2O_5 on the surfaces of the silica particles, as suggested and confirmed by other researchers for the V_2O_5/SiO_2 catalysts prepared by impregnation [64,65]. However, it is possible that (a) there exists very small crystalline V_2O_5 within the silica matrix that cannot be detected by XRD, and (b) a small fraction of vanadium ions is in the V^{4+} state immobilized in the three-dimensional matrix of silica, as observed in V_2O_5-SiO_2 gels by electron spin resonance [66]. When the equivalent content of V_2O_5 exceeds this critical dispersion capacity, residual V_2O_5 will form its own crystalline phase mixed with the SiO_2 matrix. The amount of crystalline V_2O_5 increases with the total amount of V_2O_5.

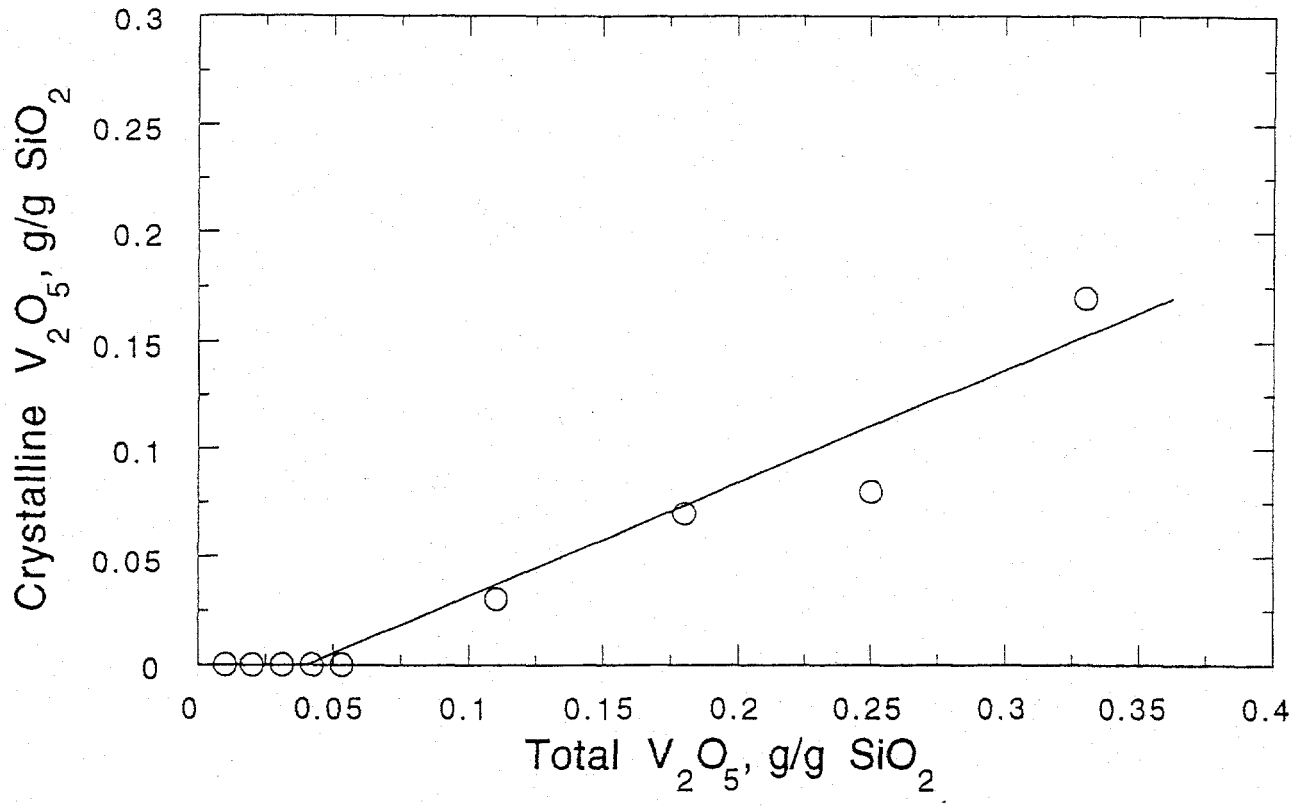

FIGURE 29. Amount of crystalline V_2O_5 *vs* total *equivalent* amount of vanadia that would be in the V_2O_5-SiO_2 xerogels if all vanadium were present as vanadia.

Catalyst Testing for Selective Oxidation of Methane. All of the V_2O_5-SiO_2 xerogels were tested for the selective oxidation of methane at a somewhat elevated reaction pressure. Table 11 presents the conversion of methane, the space time yields, and the selectivities of products for the V_2O_5-SiO_2 xerogel catalysts when using a reactant mixture of CH_4/air/steam = 1.5/1.0/0.56. For all catalysts, there were tendencies towards increasing the conversion of methane and the space time yields of methanol and formaldehyde but diminishing the selectivities to methanol and formaldehyde as the reaction temperature was progressively increased.

The conversion of methane at each temperature basically remained reasonable steady for each catalyst with different vanadia content except that 1.0 wt% V_2O_5-SiO_2 catalyst showed a very high methane conversion at 625°C and the 15.0 wt% V_2O_5-SiO_2 catalyst exhibited a very low methane conversion. The low activity of the 15.0 wt% V_2O_5-SiO_2 catalyst was probably due to its synthesis process, in which a smaller amount of deionized water and nitric acid was employed than for the rest of the catalysts, as mentioned previously. For a given methane conversion, the best methanol selectivity was exhibited with the catalysts having a low vanadium content, i.e with the catalysts containing vanadium equivalent to the range of 2.0-3.0 wt% vanadia content, and then decreased with increasing V_2O_5 content. The 2 wt% V_2O_5-SiO_2 catalyst gave the highest space time yield of methanol in the temperature range of 575-650°C. It was observed that the tendencies in the relationships between the yield and selectivity of formaldehyde and the vanadia content are in agreement with those observed by other researchers for silica-supported vanadia catalysts [27,62,67]. When the equivalent vanadia content exceeded 15.0 wt%, the selectivities and space time yields of methanol and formaldehyde fell to very small values or even to zero.

Table 12 reports the catalytic data of appropriate blank runs under our experimental conditions. The results show that the conversion of methane was negligible, smaller than 0.46 mol% up to the temperature of 650°C, while the space time yields of methanol and formaldehyde were less than 35.0 and 183 g/kg catal/hr, respectively. These results demonstrate the positive influence of the V_2O_5-SiO_2 xerogel catalysts in the partial oxidation of methane to oxygenates. However, it is still uncertain of the importance of the contribution of gas phase reaction to the production of oxygenates over V_2O_5-SiO_2 catalysts because the methyl radicals generated on the catalyst surface can leave the catalyst surface and undergo gas phase oxidation reactions forming methanol and formaldehyde. However, it is noted that C_2 hydrocarbons were not observed among the products (see Table 12).

TABLE 11. The conversion of methane and the space time yields and selectivities of products formed over 0.10 g V_2O_5-SiO_2 xerogel catalysts containing vanadium equivalent to 1.0-25.0 wt% V_2O_5. The reactant stream consisted of CH_4/air/steam (steam was added by injecting distilled water into the heated inlet line) = 150/100/56 ml/min with GHSV = 183,600 ℓ/kg catal/hr. Catalyst testing was carried out at the temperatures (Temp) indicated and at a pressure of 0.45 MPa.

V_2O_5 (wt%)	Temp (°C)	CH_4 Conv. (mol%)	Space Time Yield, g/kg cat/hr Selectivities (C mol%)					
			CH_3OH	HCHO	C_2H_4	C_2H_6	CO	CO_2
1.0	500	0.27	5.0 (1.6)	19.3 (6.8)	0.0 (0.0)	0.0 (0.0)	0.0 (0.0)	382 (91.6)
	550	0.42	9.1 (1.9)	169 (37.0)	0.0 (0.0)	0.0 (0.0)	0.0 (0.0)	409 (61.1)
	575	0.77	61.9 (8.1)	262 (36.6)	0.0 (0.0)	0.0 (0.0)	20.3 (3.0)	549 (52.3)
	600	4.25	92.7 (2.2)	456 (11.6)	86.8 (4.7)	302 (15.4)	1132 (30.9)	2031 (35.2)
	625	10.70	77.6 (0.7)	504 (4.9)	290 (6.0)	778 (15.1)	5420 (56.5)	2535 (16.8)
2.0	550	0.31	66.0 (19.7)	176 (56.0)	0.0 (0.0)	0.0 (0.0)	0.0 (0.0)	112 (24.3)
	575	1.10	145 (12.4)	109 (10.0)	0.0 (0.0)	141 (25.8)	0.0 (0.0)	829 (51.8)
	600	2.00	154 (7.2)	253 (12.6)	0.0 (0.0)	206 (20.6)	671 (36.0)	691 (23.6)
	625	3.06	213 (6.7)	309 (12.9)	64.4 (4.7)	166 (11.2)	1266 (45.8)	812 (18.7)
	650	4.87	213 (4.3)	328 (7.1)	46.2 (2.1)	220 (9.5)	2728 (63.0)	957 (14.1)

TABLE 11 (Continued). The conversion of methane and the space time yields and selectivities of products formed over 0.10 g V_2O_5-SiO_2 xerogel catalysts containing 1.0-25.0 wt% V_2O_5. The reactant stream consisted of methane/air/steam = 150/100/56 ml/min with GHSV = 183,600 ℓ/kg catal/hr. Catalyst testing was carried out at the temperatures indicated and at a pressure of 0.45 MPa.

V_2O_5 (wt%)	Temp (°C)	CH_4 Conv. (mol%)	Space Time Yield, g/kg cat/hr Selectivities (C mol%)					
			CH_3OH	HCHO	C_2H_4	C_2H_6	CO	CO_2
3.0	500	0.03	2.8 (7.9)	0.0 (0.0)	0.0 (0.0)	0.0 (0.0)	0.0 (0.0)	44.0 (92.2)
	550	0.28	66.5 (20.8)	176 (58.8)	0.0 (0.0)	0.0 (0.0)	0.0 (0.0)	89.2 (20.3)
	575	0.75	108 (12.3)	448 (54.4)	0.0 (0.0)	0.0 (0.0)	0.0 (0.0)	403 (33.3)
	600	1.15	99.9 (7.5)	542 (43.3)	0.0 (0.0)	0.0 (0.0)	425 (36.4)	235 (12.8)
	625	1.57	155 (8.5)	560 (32.8)	0.0 (0.0)	0.0 (0.0)	670 (42.1)	416 (16.6)
	650	1.91	181 (8.2)	533 (25.8)	0.0 (0.0)	0.0 (0.0)	966 (50.1)	483 (15.9)
5.0	500	0.08	11.0 (11.9)	35.6 (41.0)	0.0 (0.0)	0.0 (0.0)	0.0 (0.0)	59.8 (47.1)
	550	0.10	21.3 (18.1)	41.0 (37.2)	0.0 (0.0)	0.0 (0.0)	0.0 (0.0)	72.3 (44.7)
	575	1.25	19.9 (1.4)	150 (11.4)	0.0 (0.0)	0.0 (0.0)	0.0 (0.0)	1685 (87.2)
	600	1.67	50.9 (2.8)	301 (17.9)	0.0 (0.0)	0.0 (0.0)	0.0 0.0)	1959 (79.3)
	625	2.07	51.0 (2.3)	357 (17.0)	56.1 (5.7)	185 (17.6)	145 (7.4)	1535 (49.9)

TABLE 11 (Continued). The conversion of methane and the space time yields and selectivities of products formed over 0.10 g V_2O_5-SiO_2 xerogel catalysts containing 1.0-25.0 wt% V_2O_5. The reactant stream consisted of methane/air/steam = 150/100/56 ml/min with GHSV = 183,600 ℓ/kg catal/hr. Catalyst testing was carried out at the temperatures (Temp) indicated and at a pressure of 0.45 MPa.

V_2O_5 (wt%)	Temp (°C)	CH_4 Conv. (mol%)	Space Time Yield, g/kg cat/hr Selectivities (C mol%)					
			CH_3OH	HCHO	C_2H_4	C_2H_6	CO	CO_2
10.0	500	0.04	0.0 (0.0)	0.0 (0.0)	0.0 (0.0)	0.0 (0.0)	0.0 (0.0)	66.4 (100)
	575	1.05	52.4 (4.7)	154 (14.7)	0.0 (0.0)	0.0 (0.0)	128 (13.1)	1035 (67.5)
	600	1.24	51.4 (3.9)	349 (28.2)	0.0 (0.0)	0.0 (0.0)	47.3 (4.1)	1160 (63.8)
	625	1.50	76.6 (4.7)	495 (32.2)	0.0 (0.0)	139 (12.3)	46.8 (3.3)	1077 (47.6)
	650	1.19	103 (8.1)	183 (15.4)	0.0 (0.0)	95.7 (16.1)	93.2 (8.4)	909 (52.1)
15.0	500	0.02	0.0 (0.0)	0.0 (0.0)	0.0 (0.0)	0.0 (0.0)	0.0 (0.0)	24.2 (100)
	550	0.09	7.0 (6.8)	21.0 (21.9)	0.0 (0.0)	0.0 (0.0)	0.0 (0.0)	100 (71.3)
	575	0.25	11.3 (4.0)	29.5 (11.2)	0.0 (0.0)	0.0 (0.0)	0.0 (0.0)	327 (84.8)
	600	0.31	14.7 (4.1)	34.0 (14.3)	0.0 (0.0)	0.0 (0.0)	0.0 (0.0)	280 (80.0)
	625	0.32	11.3 (0.5)	30.0 (1.4)	0.0 (0.0)	0.0 (0.0)	0.0 (0.0)	494 (98.2)
	650	0.34	18.7 (4.7)	21.4 (5.8)	0.0 (0.0)	0.0 (0.0)	0.0 (0.0)	488 (89.5)

TABLE 11 (Continued). The conversion of methane and the space time yields and selectivities of products formed over 0.10 g V_2O_5-SiO_2 xerogel catalysts containing 1.0-25.0 wt% V_2O_5 The reactant stream consisted of methane/air/steam = 150/100/56 ml/min with GHSV = 183,600 ℓ/kg catal/hr. Catalyst testing was carried out at the temperatures (Temp) indicated and at a pressure of 0.45 MPa.

V_2O_5 (wt%)	Temp (°C)	CH_4 Conv. (mol%)	Space Time Yield, g/kg cat/hr Selectivities (C mol%)					
			CH_3OH	HCHO	C_2H_4	C_2H_6	CO	CO_2
20.0	500	0.02	0.0 (0.0)	0.0 (0.0)	0.0 (0.0)	0.0 (0.0)	0.0 (0.0)	23.8 (100)
	550	0.04	0.0 (0.0)	0.0 (0.0)	0.0 (0.0)	0.0 (0.0)	0.0 (0.0)	49.7 (100)
	575	0.09	0.0 (0.0)	10.5 (10.7)	0.0 (0.0)	0.0 (0.0)	0.0 (0.0)	128 (89.3)
	600	0.35	0.0 (0.0)	12.0 (3.3)	0.0 (0.0)	0.0 (0.0)	0.0 (0.0)	516 (96.7)
	625	3.2	0.0 (0.0)	16.7 (0.6)	0.0 (0.0)	0.0 (0.0)	0.0 (0.0)	4222 (99.4)
	650	4.26	2.8 (0.1)	15.2 (0.4)	0.0 (0.0)	0.0 (0.0)	0.0 (0.0)	6437 (99.6)
25.0	500	0.00	0.0 (0.0)	0.0 (0.0)	0.0 (0.0)	0.0 (0.0)	0.0 (0.0)	0.0 (0.0)
	550	0.11	0.0 (0.0)	0.0 (0.0)	0.0 (0.0)	0.0 (0.0)	0.0 (0.0)	175 (100)
	575	0.0	0.0 (0.0)	0.0 (0.0)	0.0 (0.0)	0.0 (0.0)	0.0 (0.0)	0.0 (0.0)
	600	2.28	2.9 (0.1)	161.3 (6.6)	0.0 (0.0)	0.0 (0.0)	0.0 (0.0)	3349 (93.3)
	625	2.60	3.1 (0.1)	224.8 (8.5)	0.0 (0.0)	0.0 (0.0)	36.8 (1.5)	3496 (89.2)
	650	3.43	11.7 (0.3)	144.5 (4.2)	0.0 (0.0)	0.0 (0.0)	935.2 (29.1)	3358 (66.4)

TABLE 12. The conversion of methane and the space time yields* and selectivities of products formed [A] over a quartz wool bed and [B] in a blank reactor from CH_4/air/steam = 150/100/56 ml/min with GHSV = 183,600 l/kg catal/hr. Testing was carried out at 0.45 MPa at the temperatures (Temp) indicated.

Test	Temp (°C)	CH_4 Conv. (mol%)	Space Time Yield, g/kg cat/hr (Selectivities, C mol%)					
			CH_3OH	HCHO	C_2H_4	C_2H_6	CO	CO_2
[A]	550	0.00	0.0 (0.0)	0.0 (0.0)	0.0 (0.0)	0.0 (0.0)	0.0 (0.0)	0.0 (0.0)
	600	0.13	3.4 (2.3)	131 (95.1)	0.0 (0.0)	0.0 (0.0)	0.0 (0.0)	5.3 (2.6)
	625	0.05	3.2 (5.9)	40.1 (79.4)	0.0 (0.0)	0.0 (0.0)	0.0 (0.0)	10.8 (14.6)
	650	0.46	21.8 (4.2)	152 (31.3)	0.0 (0.0)	0.0 (0.0)	0.0 (0.0)	13.3 (1.89)
[B]	550	0.00	0.0 (0.0)	0.0 (0.0)	0.0 (0.0)	0.0 (0.0)	0.0 (0.0)	0.0 (0.0)
	600	0.13	7.0 (4.8)	124 (89.9)	0.0 (0.0)	0.0 (0.0)	0.0 (0.0)	10.7 (5.3)
	625	0.20	20.0 (8.8)	184 (86.0)	0.0 (0.0)	0.0 (0.0)	0.0 (0.0)	16.2 (5.2)
	650	0.13	35.0 (24.1)	92.6 (67.9)	0.0 (0.0)	0.0 (0.0)	0.0 (0.0)	16.0 (8.0)

*Here, the same dimensional unit was utilized as was used for the previous testing in order to compare the product productivities with those obtained over a catalyst bed.

Table 13 gives the catalytic results over the 2.0 wt% V_2O_5/SiO_2 catalyst prepared by impregnation under the same experimental conditions as used in the catalytic testing of the 2.0 wt% V_2O_5-SiO_2 xerogel catalyst. As can be seen from Table 11 and Table 13, the methane conversion for the V_2O_5-SiO_2 xerogel catalyst was lower than that for the supported V_2O_5/SiO_2 catalyst. However, It is especially noted that the methanol productivity and selectivities over the V_2O_5-SiO_2 xerogel catalyst were much higher than those for the

supported V_2O_5/SiO_2 catalyst prepared by impregnation. On the other hand, the supported V_2O_5/SiO_2 catalyst exhibited high productivity and selectivity toward formaldehyde and carbon monoxide. These results suggest that the active site(s) of the V_2O_5-SiO_2 xerogel catalyst for production of methanol is probably more stable at higher temperature than that of the supported V_2O_5-SiO_2 catalyst. A similar result was observed in the selective reduction of nitric oxide with ammonia over mixed V_2O_5-SiO_2 gel catalyst [66].

TABLE 13. The conversion of methane and the space time yields and selectivities of products formed over 0.10 g 2.0 wt% V_2O_5/SiO_2 catalyst prepared by impregnation. The reactant stream consisted of CH_4/air/steam = 150/100/56 ml/min with GHSV = 183,600 ℓ/kg catal/hr. Catalyst testing was carried out at the temperatures indicated and at a pressure of 0.45 MPa.

Temp. (°C)	CH_4 Conv. (mol%)	Space Time Yield, g/kg cat/hr (Selectivities, C mol%)					
		CH_3OH	HCHO	C_2H_4	C_2H_6	CO	CO_2
550	0.31	18.7 (5.0)	282 (80.4)	0.0 (0.0)	0.0 (0.0)	0.0 (0.0)	74.9 (14.6)
575	0.57	73.0 (11.5)	505 (84.6)	0.0 (0.0)	0.0 (0.0)	0.0 (0.0)	34.6 (4.0)
600	7.62	152 (2.0)	1170 (16.4)	36.8 (1.1)	70.4 (2.0)	4651 (69.7)	938 (8.9)
625	9.05	140 (1.6)	1652 (19.7)	135 (3.5)	145 (3.5)	4970 (63.6)	1015 (8.3)
650	9.86	116 (1.2)	1340 (14.8)	184 (4.4)	261 (5.8)	5419 (64.2)	1273 (9.6)

To probe the effect of sample size on the catalytic results, a larger portion of a xerogel catalyst was loaded into the reactor. The methane conversion and product selectivities of the 2.0 wt% V_2O_5-SiO_2 xerogel catalyst with a 0.30 g loading in the reactor, but employing the same reactant flow rates (in ml/min) as utilized in the previous experiments, are shown in Table 14. The net effect is a lower GHSV and a higher contact time of the reactants. As compared to the results obtained with a 0.10 g loading of the catalyst (Table 11), the 0.30 g loading exhibited a much higher methane conversion with an enhanced selectivity to CO but much lower space time yields and selectivities of methanol. Note that CO_2 formation

remained low. Two factors affect the changes in the methane conversion, product yields, and selectivities when a large amount of the catalyst is loaded in the reactor. One is an increase of the thickness of the catalyst bed and a longer residence time, which will cause an increase in methane conversion but a decrease in oxygenate selectivities due to the secondary oxidation of oxygenates. Another factor is that the decrease of GHSV makes a negative contribution to the space time yields of oxygenates.

TABLE 14. The conversion of methane and the space time yields and selectivities of products formed over 0.30 g of the 2.0 wt% V_2O_5-SiO_2 xerogel catalyst. The reactant stream consisted of CH_4/air/steam = 150/100/56 ml/min with GHSV = 61,200 l/kg catal/hr. Catalyst testing was carried out at the temperatures indicated and at a pressure of 0.45 MPa.

Temp. (°C)	CH_4 Conv. (mol%)	Space Time Yield, g/kg cat/hr (Selectivities, C mol%)					
		CH_3OH	HCHO	C_2H_4	C_2H_6	CO	CO_2
550	2.80	18.1 (1.5)	62.0 (5.5)	0.0 (0.0)	0.0 (0.0)	954 (90.3)	50.2 (3.0)
575	8.94	63.1 (2.3)	221 (8.4)	0.0 (0.0)	6.0 (0.5)	1896 (77.3)	447 (11.6)
600	10.21	63.7 (2.1)	343 (11.9)	3.6 (0.3)	18.8 (1.3)	1949 (72.3)	518 (12.2)
650	11.00	71.3 (2.1)	276 (8.8)	47.0 (3.2)	152.6 (9.7)	2048 (69.8)	298 (6.5)

Double Bed Catalytic Testing of V_2O_5-SiO_2 Catalysts. To probe the effect of bulk vanadia on the product selectivitiy and activity, testing was carried out utilizing two catalysts in sequence to form a bed in the tubular reactor, where the catalysts contained different quantities of vanadium. Table 15 presents the catalytic results for selective oxidation of methane over a double-catalyst bed consisting of 3.0 and 20.0 wt% V_2O_5-SiO_2 xerogels. When the 20.0 wt% V_2O_5-SiO_2 catalyst was used as the first bed and the 3.0 wt% V_2O_5-SiO_2 catalyst as the second bed, significantly higher space time yields of methanol and formaldehyde were observed in the temperature range of 575-625 °C, as compared to the case where the 3.0 wt% V_2O_5-SiO_2 catalyst was employed as the first bed and the 20.0 wt%

catalyst as the second bed. The difference in the space time yields of methanol was remarkably large between the two double-bed configurations, especially at the higher reaction temperatures. The difference in the space time yields observed for formaldehyde was also significant.

TABLE 15. The conversion of methane and the space time yields and selectivities of products formed over a double catalyst bed of **[A]** 0.10 g of 20 wt% V_2O_5-SiO_2 as the first bed and 0.10 g of 3 wt% V_2O_5-SiO_2 as the second bed and **[B]** 0.10 g of 3 wt% V_2O_5-SiO_2 as the first bed and 0.10 g of 20 wt% V_2O_5-SiO_2 as the second bed. The reactant stream consisted of CH_4/air/steam = 150/100/56 ml/min with total GHSV = 91,800 ℓ/kg cat/hr (corresponding to 183,600 ℓ/kg cat/hr for each individual catalyst bed). Catalyst testing was carried out at the temperatures indicated and at a pressure of 0.1 MPa.

Catalyst (Double-Bed)	Temp. (°C)	CH_4 Conv. (mol%)	Space Time Yield, g/kg cat/hr Selectivities (C mol%)			
			CH_3OH	HCHO	CO	CO_2
[A]: 20 wt% V_2O_5-SiO_2‖3 wt% V_2O_5-SiO_2	550	0.03	3.1 (18.9)	12.5 (81.1)	0.0 (0.0)	0.0 (0.0)
	575	0.70	23.4 (5.7)	152.4 (39.9)	158.0 (44.4)	55.9 (10.0)
	600	1.25	28.8 (4.0)	266.2 (39.3)	312.2 (49.3)	74.2 (7.5)
	625	1.11	18.6 (2.9)	125.1 (20.9)	312.8 (55.9)	178.2 (20.3)
[B]: 3 wt% V_2O_5-SiO_2‖20 wt% V_2O_5-SiO_2	550	0.07	1.9 (4.7)	27.5 (73.7)	5.2 (14.8)	4.0 (7.2)
	575	0.49	5.1 (1.9)	94.8 (36.7)	139.7 (58.0)	13.1 (3.5)
	600	0.97	2.2 (0.40)	85.2 (16.6)	310.9 (64.8)	137.4 (18.2)
	625	1.57	1.9 (0.2)	72.7 (8.9)	535.1 (70.5)	250.3 (20.9)
	650	1.83	3.0 (0.3)	99.4 (10.4)	512.7 (57.3)	450.6 (32.1)

As previously shown, the 20.0 wt% V_2O_5-SiO_2 xerogel contained a large amount of detectable crystalline V_2O_5. The data presented here further suggest that the existence of crystalline V_2O_5 in the catalysts remarkably diminished the space time yields of methanol and formaldehyde due to its strong ability for further oxidation of methanol and formaldehyde to carbon oxides at higher temperatures. In the case of 20.0 wt% V_2O_5-SiO_2 catalyst as the second bed, some of the methanol and formaldehyde formed in the first bed was further oxidized on the surface of crystalline V_2O_5 in the second catalyst bed. The results also showed that methanol was more easily oxidized than formaldehyde on the surfaces of V_2O_5 at 575-650°C.

Pd-Modified V_2O_5-SiO_2 Catalyst. Palladium readily activates methane, and to probe its effect on the conversion and selectivity of the selective oxidaiton of methane over the xerogel catalysts, a V_2O_5-SiO_2 xerogel catalyst was prepared that contained a small quantity of Pd. The results given in Table 16 show that small amounts of methanol and formaldehyde could be produced from a reactant stream of CH_4/air/steam = 150/100/56 ml/min over a 0.05 wt% Pd-10.0 wt% V_2O_5-SiO_2 xerogel catalyst. The results showed that the Pd-modified V_2O_5-SiO_2 xerogel catalyst was more active than the binary V_2O_5-SiO_2 xerogel catalysts. For example, complete oxygen conversion was achieved at 600°C and ambient pressure for the Pd-V_2O_5-SiO_2 catalyst, while this conversion level was not observed for the V_2O_5-SiO_2 catalysts. However, addition of Pd to the V_2O_5-SiO_2 xerogel catalyst significantly decreased the selectivities to oxygenates, and the product selectivity was shifted toward CO_2 and CO. Therefore, under the reaction conditions employed, addition of Pd to the xerogel catalyst was not beneficial for the selective oxidation of methane to form methanol and formaldehyde.

TABLE 16. The conversion of methane and the space time yields and selectivities of products formed over 0.10 g 0.05 wt% Pd-10.0 wt%V_2O_5-SiO_2 xerogel catalyst. The reactant stream at 0.1 MPa consisted of CH_4/air/steam = 150/100/56 ml/min with GHSV = 183,600 l/kg catal/hr.

Temp. (°C)	CH_4 Conv. (mol%)	Space Time Yield, g/kg cat/hr (Selectivities, C mol%)			
		CH_3OH	HCHO	CO	CO_2
500	0.06	1.6 (2.5)	9.7 (16.0)	0.0 (0.0)	72.7 (81.6)
550	0.24	3.0 (1.1)	19.7 (7.8)	0.0 (0.0)	336.0 (91.1)
600	11.9	11.7 (0.1)	20.4 (0.2)	7821 (74.4)	4179 (25.3)

Conclusions. Catalysts consisting of V_2O_5-SiO_2 xerogels containing the equivalent of 1.0-25.0 wt% vanadia were synthesized by a sol-gel process and had high surface areas. Crystalline V_2O_5 was not observed by X-ray powder diffraction (XRD) in the xerogels containing 1.0, 2.0, 3.0, and 4.0 wt% vanadia, indicating that the vanadium phase was finely dispersed within or on the silica matrix. However, the crystalline V_2O_5 phase could be detected by XRD when the vanadia content exceeded 5.0 wt%.

Catalytic testing showed that for a given methane conversion, the best selectivity to methanol was obtained with catalysts having a vanadium content corresponding to 2.0-3.0 wt% vanadia content. The 2.0 wt% V_2O_5-SiO_2 catalyst gave the highest space time yield of methanol in the temperature range of 575-650°C. When the vanadia contents exceeded 15.0 wt%, the yields of methanol and formaldehyde decreased to very small amounts, even to zero. The decrease in the space time yields and selectivities of oxygenates with an increase in vanadia content may be attributed to the existence of the bulk-like vanadia, which catalyzes the secondary oxidation of oxygenates to carbon oxides.

Appropriate blank runs under our experimental conditions were also carried out. The results showed that the conversion of methane was negligible, smaller than 0.46 mol% up to 650°C at a pressure of 0.45 MPa with a space time yield of methanol less than 35.0 g/kg catal/hr and a space time yield of formaldehyde smaller than 183.5 g/kg catal/hr. As compared to the 2.0 wt% V_2O_5/SiO_2 catalyst prepared by impregnation, the 2.0 wt% V_2O_5-SiO_2 xerogel catalyst exhibited a lower methane conversion but higher selectivities to methanol and formaldehyde. The space time yield of methanol given by the 2.0 wt% V_2O_5-SiO_2 xerogel catalyst at 625-650°C is higher than that given by the supported 2.0 wt% V_2O_5/SiO_2 catalyst.

Double catalyst bed experiments were carried out using two V_2O_5-SiO_2 catalysts having different vanadia content. Much higher space time yields of methanol and formaldehyde were observed over a double catalyst bed with 0.1 g 20.0 wt% V_2O_5-SiO_2 xerogel as the first bed and 0.1 g 3.0 wt% V_2O_5-SiO_2 xerogel as the second bed than when 0.1 g 3.0 wt% V_2O_5-SiO_2 xerogel was employed as the first bed and 0.1 g 20.0 wt% V_2O_5-SiO_2 xerogel as the second bed. This indicates that in the latter case the oxygenates produced over the first catalyst bed of the 3.0 wt% V_2O_5-SiO_2 were readily further oxidized as they passed the second catalyst bed of the 20.0 wt% V_2O_5-SiO_2, which contained a large quantity of crystalline vanadia. The data demonstrate a deleterious effect of the crystalline vanadia in the V_2O_5-SiO_2 xerogel catalysts on the space time yields of oxygenates, especially methanol.

In an additional experiment, a Pd-modified V_2O_5-SiO_2 xerogel catalyst was prepared and catalytically tested. The results showed that addition of palladium (0.05 wt% Pd) into a 10 wt% V_2O_5-SiO_2 xerogel greatly enhanced the activity for methane oxidation but significantly diminished the selectivities to the target oxygenates, methanol and formaldehyde.

TASK 3. Catalyst Characterization and Optimzation

I. Chemical and Physical Characterization of SrO/La_2O_3-Based Catalysts

The preparation and catalytic testing of $SO_4^{2-}/SrO/La_2O_3$ catalysts were described under TASK 1 (page 16). Additional experiments have been carried out with the sulfated catalysts, e.g. additional temperature programming studies and variation of pretreatment conditions. They give further evidence that the formation and decomposition of surface carbonate on these catalysts play an important role in controlling the activity and selectivity under the reaction conditions employed here. Surface and bulk analyses of these catalysts were carried out, and some of the results are presented in Table 17.

TABLE 17. Chemical and Surface Analysis of SrO/La_2O_3-Based Catalysts

Sample	Sulfate (wt%)	Carbonate (wt%)	BET Area (m^2g^{-1})
(A) Before Reaction			
1 wt% SrO/La_2O_3	---	3.30	10.36
1 wt% $SO_4^{2-}/SrO/La_2O_3$	0.93	4.35	16.17
(B) Pretreatment only at 800°C (for 1 hr in Air or He); no reaction			
1 wt% $SO_4^{2-}/SrO/La_2O_3$ (Air)	0.96	---	15.18
1 wt% $SO_4^{2-}/SrO/La_2O_3$ (He)	0.93	---	13.15
(C) After Reaction (500 → 700 → 500°C; GHSV = 70,000 $\ell\ kg^{-1}hr^{-1}$; CH_4/Air = 1/1)			
1 wt% SrO/La_2O_3		7.50	7.03
1 wt% $SO_4^{2-}/SrO/La_2O_3$	0.36	5.35	8.20
(D) After Reaction at 550°C with Low GHSV (70,000 → 5,400 $\ell\ kg^{-1}hr^{-1}$; CH_4/Air = 1/1)			
1 wt% $SO_4^{2-}/SrO/La_2O_3$	0.87	15.35	

Notes: (1) The chemical analysis were carried out by Galbraith Laboratories, Inc.
(2) The BET areas were measured with a Micrometrics Gemini-2360 instrument.

The analyses after the brief pretreatment of the sulfated catalysts at 800°C (**B**) that were carried out in air or under helium indicate that sulfate was not lost from the catalysts and that the surface areas were maintained. After experiments carried out under reductive environments with reaction temperatures higher than 600°C, this was not the case (**C**). For catalysts analyzed to-date that were utilized under those reaction conditions, it was found that sulfate was lost from the catalyst and that the surface areas had decreased significantly. In addition, appreciably increased levels of carbonate were generally observed in those catalysts.

Examination of the catalysts after testing indicated that both contained more carbonate than they did in the pretreated state and both had experienced significant loss of surface area, as shown in Table 17 (sections **A** and **C**). In addition, the sulfated catalyst has lost a significant portion of the sulfate dopant. It was shown separately that pretreatment at 800°C in air or in He did not result in lost of sulfate and the lost of surface area was not particularly significant, as shown in section **B** of Table 17. Thus, it is likely that the instability of the $SO_4^{2-}/SrO/La_2O_3$ catalyst during the CH_4/air testing cycle that reached 700°C was caused by the reducing atmosphere resulting from the high methane conversion level and depletion of gas phase oxygen that might promote the transformation of sulfate to a volatile component at the high temperature, resulting in loss of the acidic dopant. The somewhat lower activity and %yield of C_2 hydrocarbon products could be due to the partial loss of surface area of both catalysts.

II. *In Situ* Raman Study of Methane Activation over the SrO/La_2O_3 Catalysts

In situ laser Raman spectroscopy was used for the first time with these SrO/La_2O_3 systems to explore the mechanism for the promoting effect of the sulfate on the SrO/La_2O_3 catalysts for methane activation. It is known that the surface carbonates play important roles for the partial oxidation of methane over strong basic metal oxide catalysts [68,69]. It has been reported that carbon dioxide, produced as a by-product during the coupling reaction, rapidly poisons the SrO catalyst by forming $SrCO_3$ [58]. Indeed, it was observed that when added to the reaction mixture, carbon dioxide strongly inhibited the $\bullet CH_3$ radical production over the SrO/La_2O_3 catalyst [70]. However, the surface species on these catalysts have not been monitored by *in situ* spectroscopic techniques under the coupling reaction condition employed with these catalysts.

Methodology for *In Situ* Raman Spectrocopy. The *in situ* Raman spectrometer system consisted of a quartz cell and sample holder (schematically shown in Figure 30), a triple-grating spectrometer (Spex, Model 1877), a photodiode array detector (EG&G, Princeton Applied Research, Model 1420), and an argon ion laser (Spectra-Physics, Model 165). The sample holder was made from a metal alloy, and a 100-200 mg sample disc was held by the cap of the sample holder. The sample holder was mounted onto a ceramic shaft and was rotated by a DC motor at a speed of 1000-2000 rpm. The quartz cell containing the sample holder assembly, Figure 30, was surrounded by a cylindrical heating coil that was used to heat the sample at a controlled temperature, which was monitored by an internal thermocouple. The quartz cell was capable of operating up to 600°C, and the reaction gas was introduced into the cell at a rate of 100-300 ml/min at atmospheric pressure.

The 514.5 nm line of the Ar+ laser, with 10-100 mW of power, was focused on the sample disc in a right-angle scattering geometry. An ellipsoid mirror collected and reflected the scattered light into the filter stage of the spectrometer to reject the elastically scattered component. The resulting filtered light, consisting primarily of the Raman component of the scattered light, was collected with an EG&G intensified photodiode array detector that was coupled to the spectrometer and was thermoelectrically cooled to -35°C. The photodiode array detector was scanned with an EG&G optical multichannel analyzer (Model OMA III 1463). The Raman spectra under reaction conditions were initially obtained by the following procedures: the Raman spectra of the dehydrated samples were collected after heating the sample to 500°C in a flow of pure oxygen gas (Linde Specialty Grade, 99.99% purity) for 30 min. A flowing gas mixture of CH_4/O_2 (10/1 vol%) was then introduced into the cell and the Raman spectra were collected again upon reaching steady state reaction conditions. After the above treatments, the sample was further sequentially treated with pure oxygen gas and pure methane gas at 500°C for one hr in each case. The Raman spectra were recorded in the 100-1200 cm^{-1} region with overall resolution better than 1 cm^{-1}.

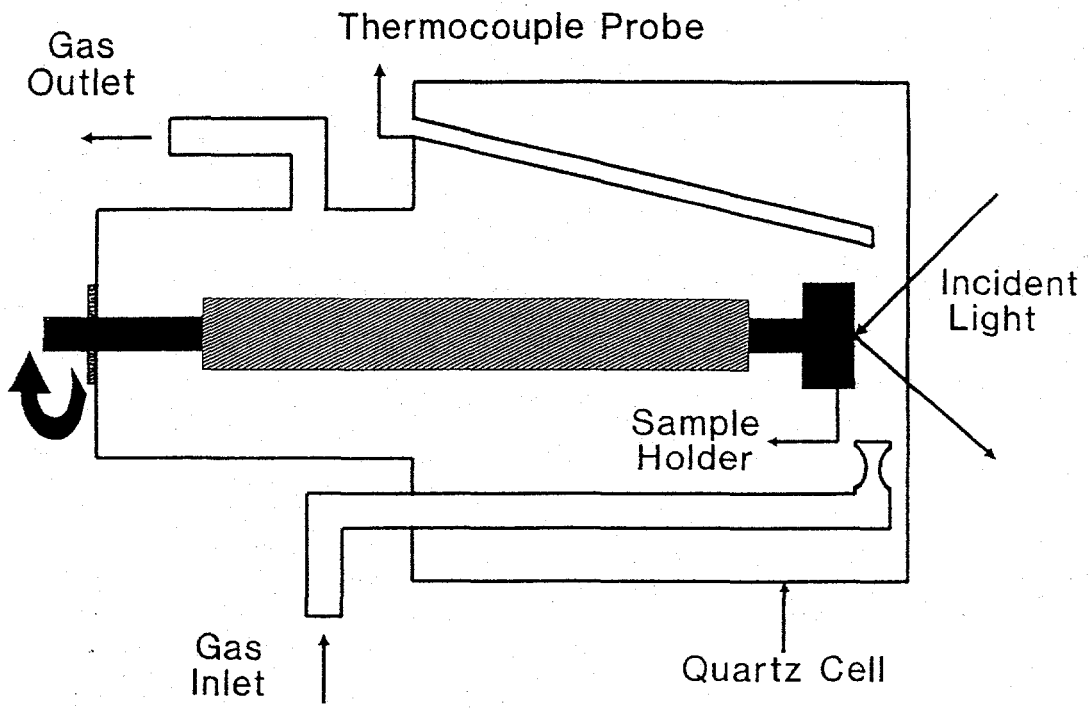

FIGURE 30. Schematic representation of the *in situ* cell used to obtain the Raman spectra of catalyst samples being tested for the selective oxidation of methane under continuous flow conditions.

Experimental Results. Raman spectra of the standard synthetic compounds $SrCO_3$ and $La_2(CO_3)_3$ were recorded. The breathing mode (symmetric stretch, ν_1) [71] of $SrCO_3$ was observed at 1070 cm^{-1} and the bending mode (ν_3) was at 699 cm^{-1}, while those for the $La_2(CO_3)_3$ were observed at Raman shifts of 1087 cm^{-1} (ν_1) and 741 cm^{-1} (ν_3), respectively. The corresponding bands for bulk natural mineral strontianite ($SrCO_3$) were observed at 1075 and 700 cm^{-1}, respectively [72]. Raman bands below 500 cm^{-1} are due to lattice vibrations, and they will not be discussed further.

In the ambient environment, oxides can adsorb and react with carbon dioxide to form carbonates. This is illustrated in Figure 31, where samples of SrO and La_2O_3 were left exposed to the atmosphere before obtaining the Raman spectra of the samples under ambient conditions. According to "standard" spectra of carbonate compounds, as discussed above, the 1087 cm^{-1} and 1072 cm^{-1} Raman bands in Figure 31 were assigned to the ν_1 breathing modes of the $La_2(CO_3)_3$ and $SrCO_3$, respectively. These Raman band frequencies indicate that the carbonates formed over these catalyst surfaces are bulk compounds [71] rather than true surface species with a double C=O bond, in which case higher frequency Raman bands (>1300 cm^{-1}) should be observed. Lattice vibrations due to the oxide materials are evident. The strong band at 405 cm^{-1} observed with lanthana was used to normalize the intensities of Raman spectra of the SrO/La_2O_3 and $SO_4^{2-}/SrO/La_2O_3$ catalysts to be described.

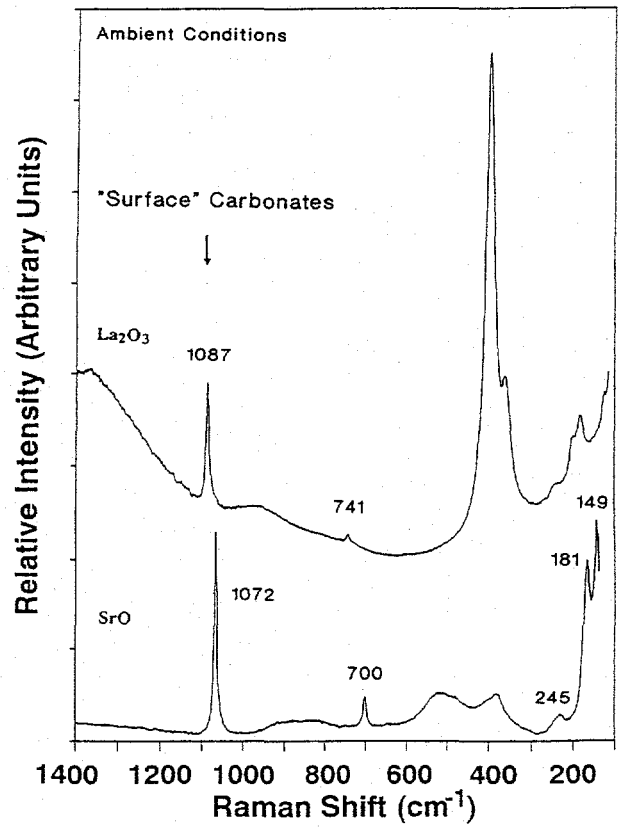

FIGURE 31. Raman spectra of SrO and La_2O_3 samples that were exposed to the ambient atmosphere, which show the formation of bulk carbonates in or on the oxide materials.

An *in situ* laser Raman study of the SrO/La_2O_3-based catalysts was carried out with the analysis/reaction cell maintained at 500°C. The spectra of the 1 wt% SrO/La_2O_3 (A), 1 wt% SO_4^{2-}/1 wt% SrO/La_2O_3 (B), and 2 wt% SO_4^{2-}/1 wt% SrO/La_2O_3 (C) catalysts that were obtained with the samples in flowing air (flow rate ≈ 100 ml/min) at 500°C are shown in Figure 32. As the sulfate content of the samples increased from 0% to 2%, the band at ≈992 cm^{-1}, assignable to the SO_4^{2-} anion, appeared and increased in intensity. At the same time, the bands at ≈1086 and ≈1068 cm^{-1} appeared to diminish in intensity. Upon changing the gas flow to a mixture of methane and air (CH_4/air ≈ 1.2, total flow rate ≈ 120 ml/min), spectra in the 600-1400 cm^{-1} spectral region were again obtained, as shown in Figure 32 (spectral A'-C'). Very similar spectra were obtained for the two reaction environments.

Considering the results shown in Figure 32, it appears that surface-doping with sulfate inhibited the overall formation of the carbonates. In accord with these observations and with the catalytic activities determined here, Aika and Aono [58] observed much lower activity for $SrCO_3$ as compared with SrO for the activation of methane. The inhibition of the formation of $SrCO_3$ by surface sulfate could be directly contributing to the promoting effect of sulfate on the SrO/La_2O_3 catalysts for methane coupling reactions occurring in the low temperature regions being studied.

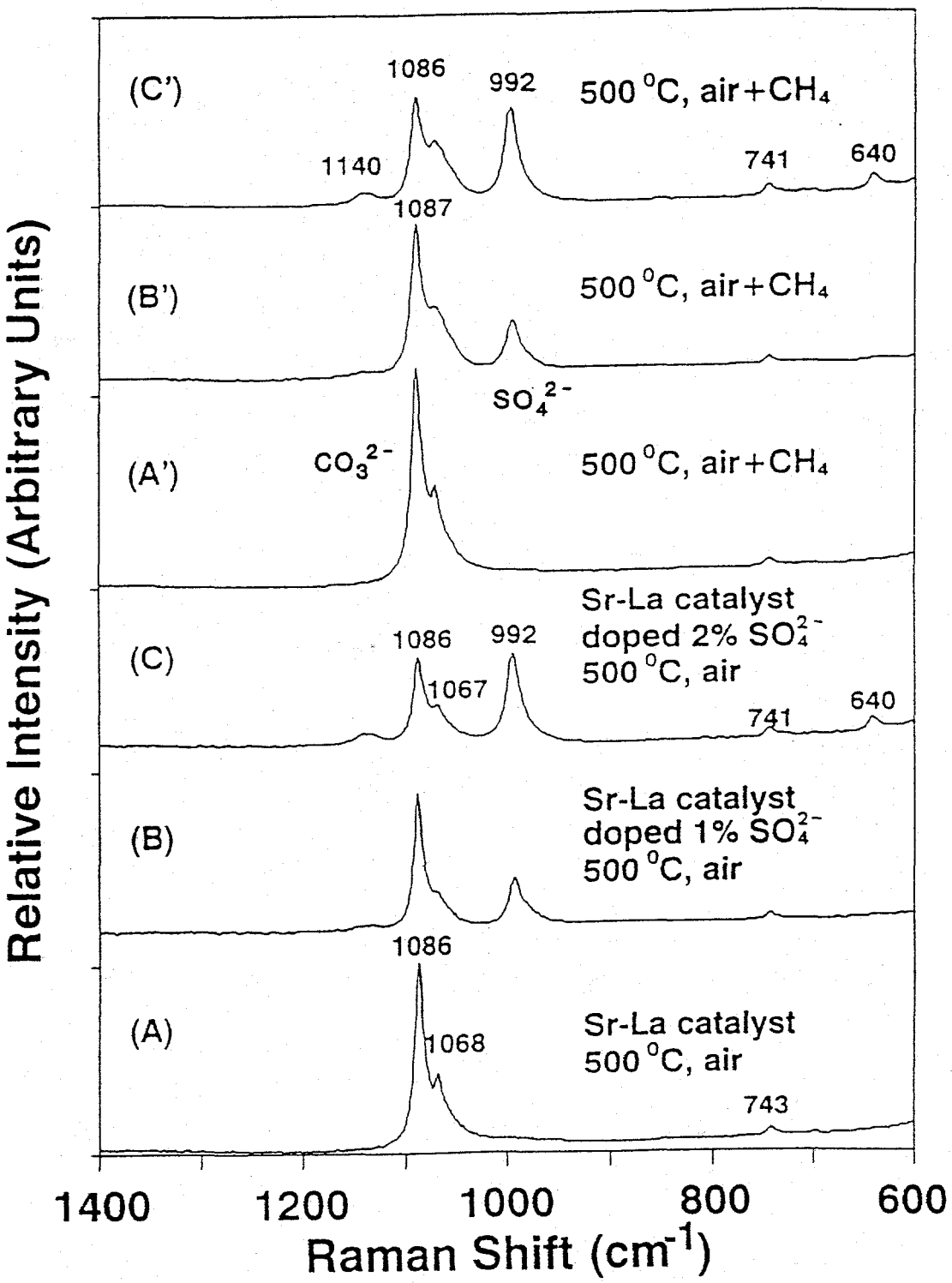

FIGURE 32. *In situ* laser Raman spectra of the 1 wt% SrO/La_2O_3, 1 wt% $SO_4^{2-}/SrO/La_2O_3$, and 2 wt% $SO_4^{2-}/SrO/La_2O_3$ catalysts at 500°C with flowing air (A-C) and in a mixture of flowing methane and air (CH_4/air ≈ 1.2) (A'-C').

Spectra A'-C' in Figure 32 were recorded under the reaction conditions indicated ≈30 min after the introduction of the reaction mixture. These *in situ* spectra suggest that sulfates remained on the catalyst surfaces during the coupling reactions and that slightly more carbonates were formed under methane coupling at mild temperatures, i.e. 500°C, in comparison to calcination conditions depicted in Figure 32(A-C). Figure 33 shows the difference spectra between the spectral sets A'-A, B'-B and C'-C in Figure 32. Figure 33 indicates that the carbonates formed during the coupling reactions are different from those formed on SrO, La_2O_3, and the SrO/La_2O_3 catalyst. For the SrO/La_2O_3 catalyst, it appears that $La_2(CO_3)_3$ was the principal carbonate produced. On the other hand, for the sulfate-promoted catalysts, it is evident that $SrCO_3$ or other forms of carbonates were also formed in addition to the formation of the $La_2(CO_3)_3$.

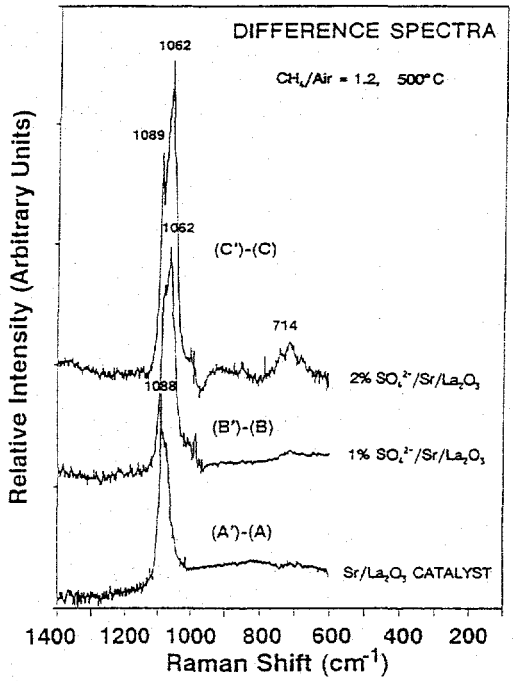

FIGURE 33. The corresponding difference Raman spectra of A'-A, B'-B, and C'-C, where the individual spectra were shown in Figure 32.

The assignment of the band at 1062 cm^{-1} is uncertain, but it appears to arise from a shoulder on the 1068 cm^{-1} band that causes broadening of the band. One origin of this band could be distorted amorphous-like $SrCO_3$. A second possibility might be that the 1062 cm^{-1} band arises from the formation of another type of lanthanum carbonate, where it would be a more stable form and could benefit the methane oxidative coupling reactions [68]. Sulfate may be able to promote the formation of this type of carbonate while inhibiting $SrCO_3$ formation, and thus promoting the catalytic performance of the SrO/La_2O_3 catalysts. Further *in situ* spectroscopy studies are needed to gain a better understanding of the surface chemistry involved in enhancement of methane activation, as well as retardation of methane activation and conversion, over SrO/La_2O_3 catalysts.

III. *In situ* Raman Spectroscopy Investigation of Supported Vanadium Oxide Catalysts During the Partial Oxidation of Methane to Formaldehyde

The vanadia/silica catalysts exhibit high activities toward the selective oxidation of methane to oxygenates, but the catalysts and the catalytic process has not been optimized over these catalysts. To provide input for this to occur, knowledge of the active state of the vanadia is needed. The V_2O_5/SiO_2 catalyst has been extensively characterized by Raman spectroscopy [39,73], ^{51}V NMR spectroscopy [39,74], as well as XANES/EXAFS [40]. These studies revealed that under dehydrated conditions, the V_2O_5/SiO_2 catalyst possesses a surface vanadium oxide species with an isolated mono-oxo tetrahedral vanadate structure. Similar surface vanadia structures were found over different catalyst supports such as TiO_2, Al_2O_3, and ZrO_2 [75-77], but polymeric tetrahedral vanadate structures were also present on these oxide supports. No *in situ* characterization studies have yet been undertaken under methane oxidation reaction conditions.

In situ Raman spectra were recorded for the first time during the methane partial oxidation reaction over these catalysts, and correlations between the surface vanadia structures and their catalytic performances were made. The Raman spectrometer system and the experimental procedures utilized were discussed in the previous section of this report. Mechanistic insight into the activation of methane and subsequent reaction for forming formaldehyde *via* partial oxidation over supported V_2O_5 catalysts is provided.

Raman Studies of Dehydrated Catalysts. The Raman spectra of the dehydrated SiO_2 support and the silica-supported MoO_3, V_2O_5, and V_2O_5/MoO_3 catalysts are shown in Figure 34. The SiO_2 support possessed Raman features at ~450 and ~800 cm^{-1} (Si-O-Si siloxane linkages), ~600 and ~487 cm^{-1} (three-fold and four-fold siloxane rings), ~970 cm^{-1} (surface silanol groups), and a very weak band at ~1050 cm^{-1} (the antisymmetric mode of the siloxane linkages) [78,79]. Upon impregnation of 3 wt% MoO_3 and 1 wt% V_2O_5 on the SiO_2 support, followed by dehydration, strong Raman bands appeared at ~986 and ~1037 cm^{-1} that are characteristic of the surface molybdenum oxide species possessing a highly distorted MoO_5 structure and the surface vanadium oxide species possessing a tetrahedral VO_4 structure, respectively [28,39,80,81]. For the 1 wt% V_2O_5/3 wt% MoO_3/SiO_2 sample, the surface vanadium oxide (Raman band at ~1037 cm^{-1}) and surface molybdenum oxide (Raman band at ~986 cm^{-1}) species coexist as isolated species on the SiO_2 support.

The Raman spectra of the surface vanadium oxide species on dehydrated TiO_2, SiO_2, and 3 wt% TiO_2/SiO_2 are presented in Figure 35. The Raman peak position of 1029 cm^{-1} for the 1 wt% V_2O_5/3 wt% TiO_2/SiO_2 sample strongly suggests that the vanadium oxide species were largely associated with the titania surface layer, as previously indicated [82].

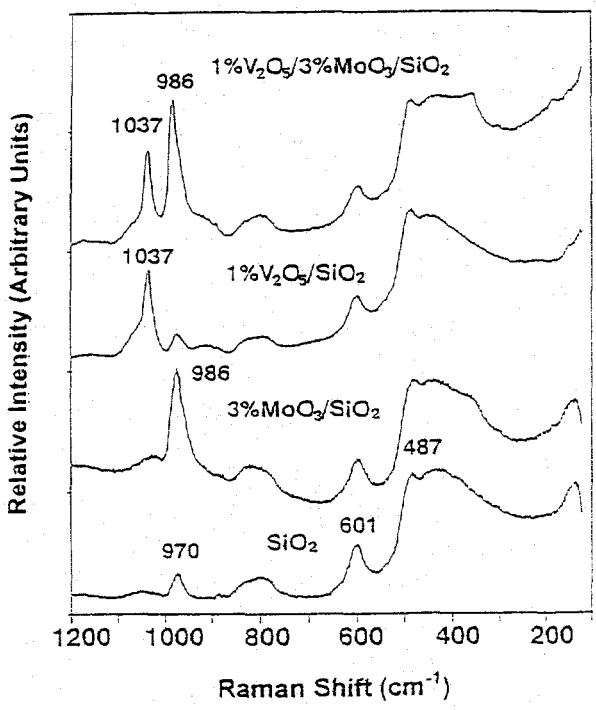

FIGURE 34. Raman spectra of SiO_2, 3 wt% MoO_3/SiO_2, 1 wt% V_2O_5/SiO_2, and 1 wt% V_2O_5/3 wt% MoO_3/SiO_2 under dehydration conditions of 250°C in flowing O_2.

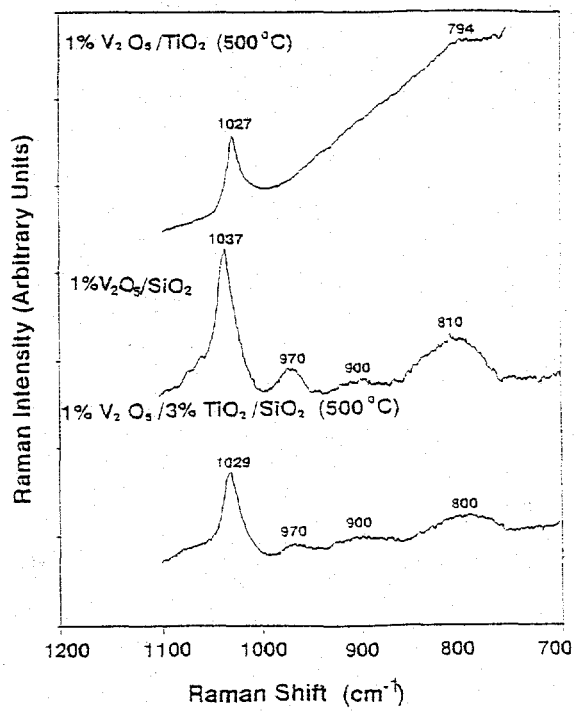

FIGURE 35. Raman spectra of 1 wt% V_2O_5/TiO_2, 1 wt% V_2O_5/SiO_2, and 1 wt% V_2O_5/3 wt% TiO_2/ SiO_2 catalysts dehydrated at 500°C.

The laser Raman spectra of thermally dehydrated SnO_2, 1 wt% V_2O_5/SnO_2, and 1 wt% V_2O_5/3% SnO_2/SiO_2 are presented in Figure 36. The SnO_2 as a support possessed a strong Raman band at 622 cm^{-1} that was characteristic of the symmetric stretching mode of an octahedral SnO_6 structure. The weak and broad Raman bands in the 650-800 cm^{-1} and 200-600 cm^{-1} region are characteristic of asymmetric modes of the octahedral SnO_6 structure and bending modes of the Sn-O-Sn linkages. Upon doping of 1 wt% V_2O_5 onto the SnO_2, additional Raman bands appeared at ~1027 and ~900 cm^{-1}, which are characteristic of "surface" vanadium oxide species possessing monomeric VO_4 and polymeric-type $[VO_3]_n$ structures, respectively. The additional new Raman band at ~830 cm^{-1} is probably due to the formation of a V_x-Sn_y-O_z compound [83,84]. For the 1 wt% V_2O_5/3 wt% SnO_2/SiO_2 catalyst sample, SnO_2 apparently formed a surface tin oxide overlayer on the silica support as suggested by the absence of any Raman features of bulk SnO_2, and vanadium oxide formed isolated surface VO_4 species with a terminal V=O bond that gave rise to the peak at ~1039 cm^{-1} [39].

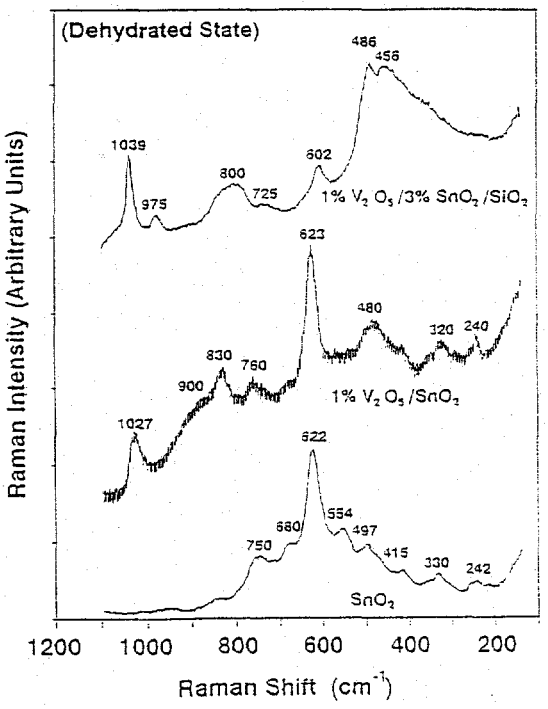

Figure 36. Raman spectra of dehydrated SnO_2 (450°C), 1 wt% V_2O_5/SnO_2 (500°C), and 1 wt% V_2O_5/3 wt% SnO_2/SiO_2 (500°C) catalysts.

In Situ Raman Studies. The Raman spectra of 1 wt% V_2O_5 supported on SiO_2, TiO_2, SnO_2, and 3 wt% TiO_2/SiO_2 were recorded during methane oxidation at 500°C, utilizing the procedures described in the Methods section, and are shown in Figures 37-40. The background due to the SnO_2 support was subtracted from the 1.0 wt% V_2O_5/SnO_2 sample in Figure 39. Upon oxygen gas treatment, dehydrated surface monomeric VO_4 species with a Raman band in the 1027-1034 cm^{-1} region were predominantly present on all the samples,

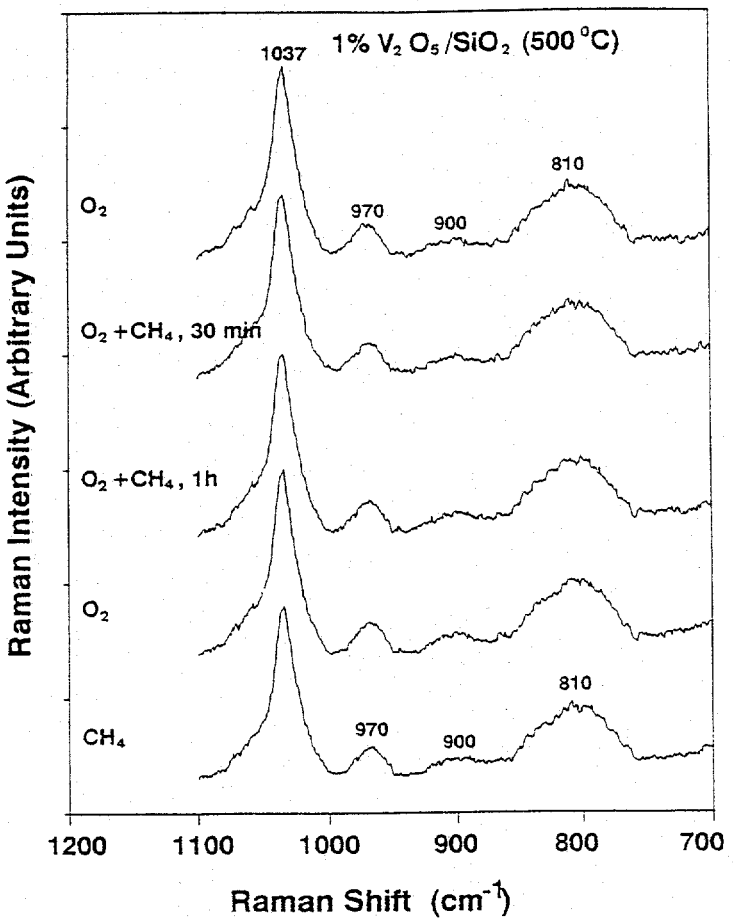

FIGURE 37. *In situ* Raman spectra of the 1 wt% V_2O_5/SiO_2 catalyst obtained after sequential treatments at 500°C in flowing O_2, CH_4/O_2 (10/1) reactant mixture, and CH_4.

and the surface polymeric $[VO_3]_n$ species with a broader Raman band at ~900 cm^{-1} were primarily present on the SnO_2 support. An additional Raman band at ~830 cm^{-1} appeared only in the V_2O_5/SnO_2 system, indicating the formation of a V_x-Sn_y-O_z compound mentioned earlier [83-84].

Under methane oxidation reaction conditions, Raman intensities of the surface vanadium oxide species decreased in the V_2O_5/TiO_2 (Figure 38) and V_2O_5/SnO_2 (Figure 39) systems due to the reduction of the surface vanadium oxide species under the reducing methane oxidation environment (excess methane), but no significant changes were observed in the V_2O_5/SiO_2 (Figure 37) and $V_2O_5/TiO_2/SiO_2$ (Figure 40) catalyst systems. In the case of the SnO_2-supported catalyst, reduction resulted in a reduced surface V(IV) phase characterized by a weak and broad band at 855 cm^{-1} (cf. Figure 39). The original surface vanadium(V) oxide species was restored by flowing pure oxygen into the cell and reoxidizing the reduced surface vanadium phase (Figure 39).

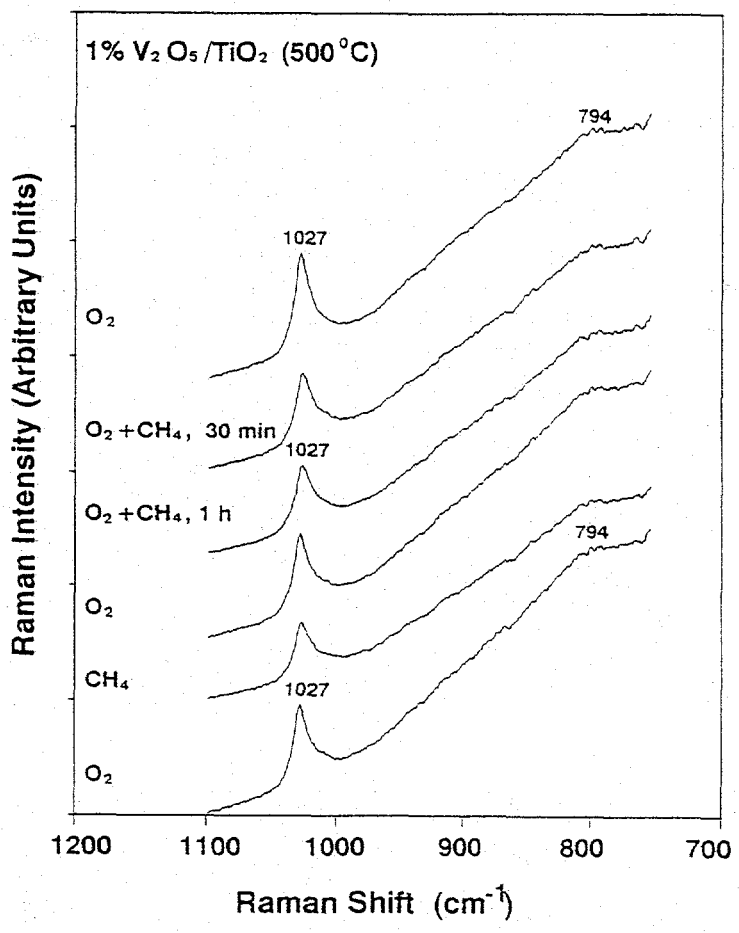

FIGURE 38. *In situ* laser Raman spectra of the 1 wt% V_2O_5/TiO_2 catalyst obtained after sequential treatments at 500°C in flowing O_2, CH_4/O_2 (10/1) reactant mixture, and CH_4.

The *in situ* Raman spectra obtained under the reaction conditions (Figure 37) show that the pentavalent vanadium oxide moieties were the predominant species on the silica support, and even under a pure flowing methane atmosphere there was no observable reduction of the surface vanadium(V) oxide species. Generally, the V=O stretching vibration frequency appears in the 950-1000 cm^{-1} region for the monomeric oxovanadium(IV) complexes [85]. Upon reduction from the V(V) state to a lower oxidation state, the 1035 cm^{-1} V=O band intensity should be reduced in the Raman spectrum (see Figures 38 and 39 for V_2O_5/TiO_2 and V_2O_5/SnO_2, respectively). The lack of significant reduction of the 1035 cm^{-1} band with the SiO_2-supported catalyst does not imply that the surface vanadium does not undergo a redox cycle, e.g. between V(V) and V(IV), but it does mean that the dynamic redox potential of vanadium in V_2O_5/SiO_2 is shifted toward V(V) compared to the other systems studied, V_2O_5/TiO_2 and V_2O_5/SnO_2, under otherwise identical reaction conditions. It, therefore, appears that stability of pentavalent vanadia is a key factor controlling the selectivity of methane oxidation to formaldehyde.

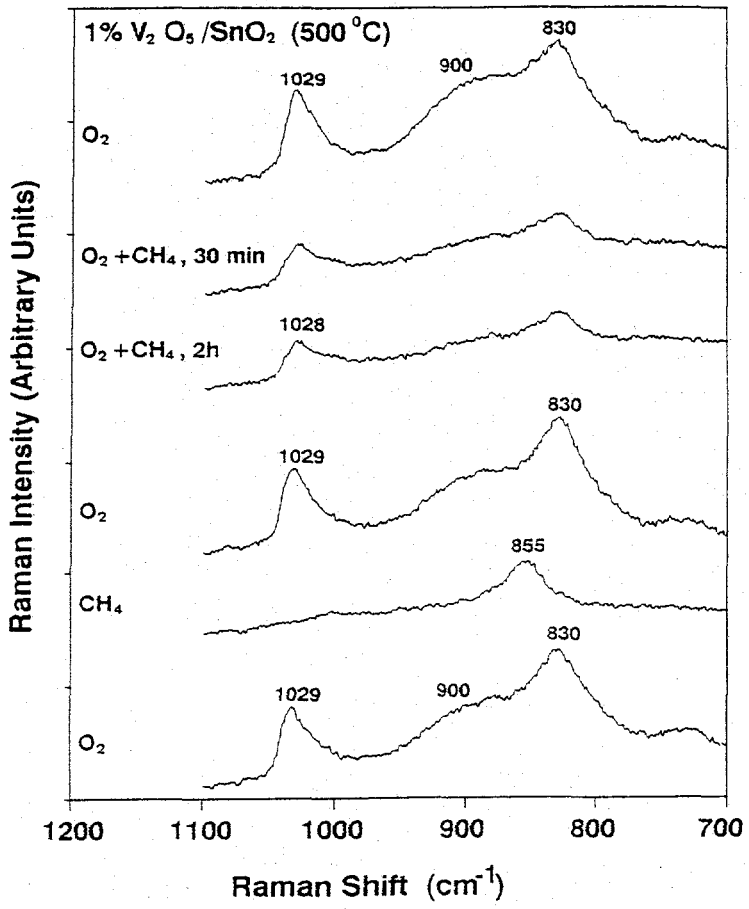

FIGURE 39. *In situ* laser Raman spectra of the 1 wt% V_2O_5/SnO_2 catalyst obtained after sequential treatments at 500°C in flowing O_2, CH_4/O_2 (10/1) reactant mixture, and CH_4.

It is interesting that the catalytic performances (Table 6) of the 1 wt% V_2O_5/TiO_2 and the 1 wt% V_2O_5/3 wt% TiO_2/SiO_2 catalysts for methane oxidation are very similar, except that the $V_2O_5/TiO_2/SiO_2$ catalyst exhibited a higher selectivity for formaldehyde production. These results are consistent with the structural information that the vanadia overlayer is coordinated to the titania overlayer, which results in behavior similar to the V_2O_5/TiO_2 catalyst. *In situ* laser Raman spectra for V_2O_5/TiO_2 (Figure 38) indicate that the surface vanadium(V) oxides were appreciably reduced (30%) under the reaction conditions employed. The reduced surface vanadium oxide species do not exhibit the 1027 cm^{-1} Raman band attributed to the stretching mode of the terminal V=O bond of vanadium(V) oxide and resulted in the intensity reduction of this Raman band. These reduced species were reoxidized to the vanadium(V) oxide under a pure oxygen environment at elevated temperature (here shown for 500°C reoxidation). There is evidence that a significant amount of reduced vanadium oxide species coexisted with the V(V) species under the steady-state reaction condition. *In situ* Raman spectra of the 1 wt% V_2O_5/3 wt% TiO_2/SiO_2 system

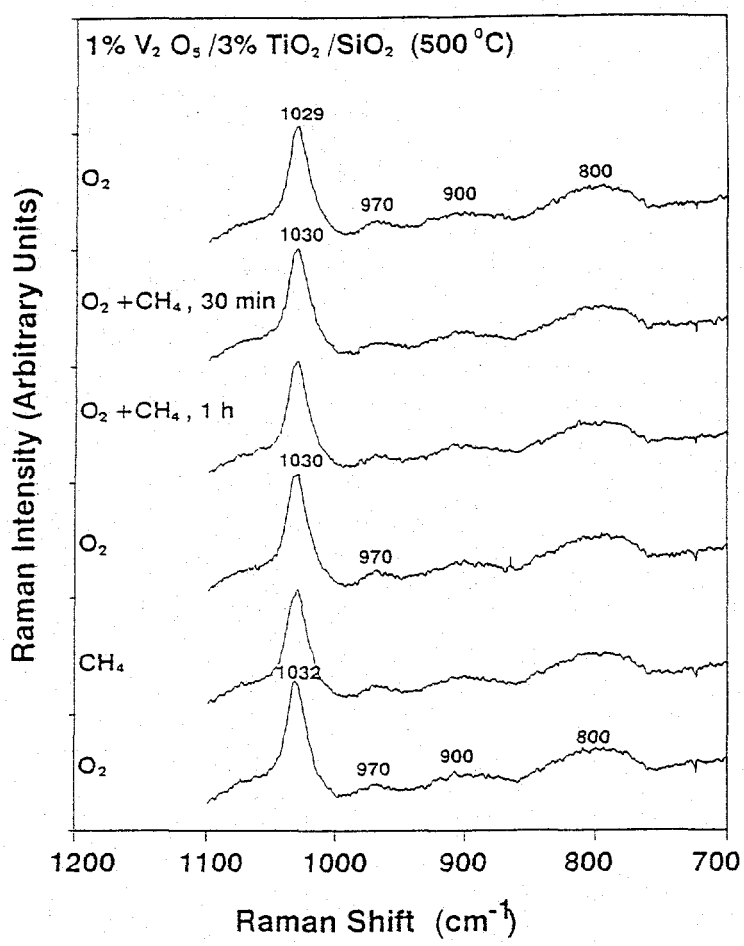

FIGURE 40. *In situ* Raman spectra of 1 wt% V_2O_5/3 wt% TiO_2/SiO_2 catalyst obtained after sequential treatments at 500°C in flowing O_2, CH_4/O_2 (10/1) reactant mixture, and CH_4.

(Figure 40) suggest that the surface V_2O_5 species were quite stable under reaction conditions, as in the case of the 1% V_2O_5/SiO_2 catalyst, and remain fully oxidized. One striking observation (Table 6) was that the catalytic activities of the V_2O_5/TiO_2 catalyst and the bare TiO_2 support were very similar. However, the product selectivity patterns were quite different for these two systems. While methane oxidation over TiO_2 produced CO almost exclusively, a significant amount of CO_2 was produced over the V_2O_5/TiO_2 catalyst as well. In the absence of detailed mechanistic information, one can only suggest at this point that coupled redox systems, e.g. V(IV)/V(V)||Ti(IV)/Ti(III), may be responsible for the deep oxidation properties of the V_2O_5/TiO_2 catalyst.

Data in Table 6 show that the catalytic activity for methane activation was extremely high for the 1 wt% V_2O_5/SnO_2; however, it only produces deep oxidation products CO_x, and predominantly CO_2. *In situ* Raman study demonstrated (Figure 39) that the V_2O_5 species were largely reduced (55%) under the methane oxidation reaction conditions employed here.

Similar to the V_2O_5/TiO_2 catalyst, coupled redox systems of V(IV)/V(V)||Sn(IV)/Sn(II) could be promoting deep oxidation of methane to CO_2. However, for the 1% V_2O_5/3% SnO_2/SiO_2 catalyst, the catalytic activity for the methane oxidation was low and even lower than that of the 1% V_2O_5/SiO_2 catalyst (Table 6). Dispersed vanadium(V) oxide species on the SiO_2 surface were suggested by the presence of the Raman band corresponding to the stretching vibration of the terminal V=O bond at 1039 cm^{-1} (Figure 36). However, the catalytic results suggested a poisoning effect of the SnO_2 overlayer, which might have eliminated some of the active surface vanadia species on SiO_2 and reduced the catalytic activity. It is interesting to notice that over the mixed 1% V_2O_5/3% SnO_2/SiO_2 catalyst, the predominant product was CO instead of CO_2 as observed over the V_2O_5/SnO_2 catalyst. It is possible that CO was mainly formed *via* decomposition of the primary formaldehyde product accelerated by the supported SnO_2 overlayer on the SiO_2 surface.

Mechanistic Considerations. In the research field of selective partial oxidation of hydrocarbons, it is always essential to identify the nature of the active sites that determine the catalytic activity and the product selectivities. For propylene oxidation, Sachtler and De Boer [86] correlated the catalytic selectivity with the catalyst reducibility. They found that the higher was the reducibility of the catalysts, the higher the activity and lower the selectivity. Bielanski and Haber [87] explained the selectivity patterns by postulating that lattice oxygen (nucleophilic) was responsible for partial oxidation, while adsorbed ionic or radical oxygen species (electrophilic) caused total oxidation.

Recently, Koranne et al. [62] proposed reaction pathways for methane oxidation over V_2O_5/SiO_2 catalysts based on isotope transient kinetic studies and suggested three types of active sites: S1, a site with high oxygen insertion and H-abstraction capabilities; S2, a site with intermediate oxygen insertion and H-abstraction capabilities; and S3, a site with low oxygen insertion capability and with high H-abstraction capability. They have further suggested [62] that these sites may merely be the same "site" but in different oxidation states. It would be very interesting to provide experimental evidence for characterizing the nature of these active sites and determining how they vary with catalyst composition and reaction conditions.

The present Raman study provides some fundamental details about the properties of the active sites for methane activation and product selectivity. For the V_2O_5/SiO_2 catalyst in the dehydrated state, the vanadium(V) oxide is bound to the SiO_2 surface *via* V-O-Si bridging bonds and possesses a terminal V=O double bond. These bridging and double bonded oxygen functionalities can be viewed as surface lattice oxygens (nucleophilic) [87]. The bond order of the V=O bond was found to vary only by a very small amount over different supports [73]. Therefore, the V=O bond is not likely to be responsible for the activity differences observed for V_2O_5 over different catalyst supports. Furthermore, *in situ* Raman study has shown that the V=O bond is very stable under the reaction conditions in the case of V_2O_5/SiO_2. Consequently, it is reasonable to argue that the terminal V=O bond is not the active center for activating the methane molecule.

However, the catalytic data certainly showed that the methane oxidation activity was a direct result of the V_2O_5 loading and was dependent on the specific oxide support. The bridging oxygen (V-O-Support, e.g. V-O-Si) bond strength is expected to vary with the support and could be responsible for the differences observed for the V_2O_5 catalysts on different supports. These bridging bonds could be one of the determining factors for the initial activity of the catalysts for the methane activation. Once the methane conversion proceeds, some vanadium(V) oxide species will be reduced to the lower oxidation states and provide the sites for oxygen adsorption to form undesirable electrophilic oxygen species [87]. The population of these reduced species should depend on the catalyst support. The present *in situ* Raman studies clearly show that these reduced species are not favored over the SiO_2 surface and are much more prevalent over the TiO_2 and SnO_2 supports under the reaction conditions employed. The stability trend of the reduced vanadium oxides over these catalysts is $V_2O_x/SnO_2 > V_2O_x/TiO_2 > V_2O_x/SiO_2$ (where $x < 5$). This catalyst reducibility trend correlates quite well with the CO_2 selectivity trend and in the reverse order to that of the formaldehyde selectivity. Upon increasing methane conversion, formaldehyde selectivity decreased and CO selectivity increased monotonically over the V_2O_5/SiO_2 catalysts. It is evident that the CO mostly arises from the decomposition of formaldehyde by further H-abstraction. On the other hand, there is no simple correlation between the selectivities to CO and CO_2, which indicates that these two carbon oxides could be formed through two parallel reaction pathways instead of the sequential reactions $CH_2O \rightarrow CO \rightarrow CO_2$.

A different pathway needs to be invoked over pure SiO_2, which also produced formaldehyde as well as C_2 hydrocarbons at low methane conversions and elevated temperatures. A parallel reaction pathway for formaldehyde and C_2 hydrocarbon production was previously proposed [56]. Unlike the V_2O_5/SiO_2 and MoO_3/SiO_2 catalysts that were capable of converting the methyl radical to formaldehyde instead of C_2 hydrocarbons, over the SiO_2 surface methyl radicals once formed are most likely to couple in the gas phase to produce ethane. In a recent dual catalyst bed study, it was demonstrated that methyl radicals generated by a first SrO/La_2O_3 catalyst bed could be converted to formaldehyde over a second bed consisting of MoO_3/SiO_2 [47]. In fact, at very low methane conversions (i.e. <1%), the selectivities to formaldehyde were previously reported to approach 100% over MoO_3/SiO_2 and V_2O_5/SiO_2 catalysts [25,36]. This agrees with the selectivities shown in Table 7 for very low conversions of methane over SiO_2 and MoO_3/SiO_2 catalysts.

A very unique property of the SiO_2 support is its low surface acidity. In comparison with other common supports like TiO_2, gamma-Al_2O_3, and ZrO_2 that all have quite high densities of surface Lewis acid sites, pure SiO_2 is almost free of Lewis acid sites [88]. This could be another underlying cause of the major differences between SiO_2 and TiO_2 supports, giving rise to the relatively higher selectivity to formaldehyde over pure SiO_2 and SiO_2-supported catalysts, while the Lewis acid sites on TiO_2 promote the formation of CO. In a double bed experiment performed by Spencer [25] where a MoO_3/SiO_2 catalyst bed was followed by gamma-Al_2O_3, it was noticed that the formaldehyde produced by the upstream MoO_3/SiO_2 catalyst was decomposed by the downstream gamma-Al_2O_3 bed. A double bed

experiment carried out here using an upstream V_2O_5/SiO_2 bed followed by a TiO_2 bed has also shown that TiO_2 is very active for decomposing formaldehyde to carbon monoxide. This is very probably due to the Lewis acidity of the TiO_2 surface.

Conclusions. *In situ* Raman spectra showed that methane alone could not reduce the surface vanadia species and methane conversion required the simultaneous presence of oxygen. This suggests that methane was activated by active sites on the silica surface created upon the dispersion of vanadium(V) oxide. The *in situ* Raman studies strongly suggest that V=O is not the active site for the initial activation of the methane molecule. TiO_2-based catalysts produced mostly CO, while the very active SnO_2-supported catalysts formed almost exclusively CO_2. It is evident that under reaction conditions, TiO_2 - and SnO_2 -supported catalysts were largely reduced by the reactant mixture and favored the deep oxidation of methane. There is no simple correlation of the catalyst activity with reducibility of the supported vanadia catalysts studied. However, the CO_2 selectivity tended to increase with the increasing reducibility of the catalysts.

IV. Static Solid State ^{51}V NMR Analysis of the V_2O_5-SiO_2 Xerogel Catalysts

The differences in the yields and selectivities of oxygenates formed *via* oxidation of methane over silica-supported vanadia catalysts as a function of the V_2O_5 content (e.g. see Table 11) can be attributed to the changes in the structure of the active vanadium component. It is well-known that the partial oxidation of hydrocarbons on oxide catalysts involves a redox mechanism in which the catalyst is partially reduced by the hydrocarbon and then reoxidized by gas-phase oxygen [87,89,90] to form oxygenated products. At low vanadium content, the vanadium is present on the silica support in the form of tetrahedral surface V species, as indicated by ^{51}V nuclear magnetic resonance (NMR), laser Raman spectroscopy, and TPR [67,91,92]. Thus, it was suggested that the tetrahedral surface V species is an active site for methane oxidation on supported V_2O_5/SiO_2 catalysts prepared by impregnation [93].

As mentioned above, vanadia in the V_2O_5-SiO_2 xerogels containing low vanadia contents is also well-dispersed within or on the silica matrix, likely as a surface V species. It is expected that the structure and behavior of vanadia in the xerogel catalysts during partial oxidation of methane to methanol are similar to those of vanadia in the supported V_2O_5/SiO_2 catalysts prepared by impregnation. As discussed earlier in this report, it can be proposed that methane is first activated by the surface V species to form a surface methoxy intermediate, which is then hydrolyzed by water to produce methanol. The bridging oxygens of the surface VO_n species can possibly play a direct role in the partial oxidation of methane because these oxygens are more labile than terminal oxygens once the surface V species is reduced [94].

The space time yields and selectivities of oxygenates should increase with an increase in vanadia content at a low vanadia contents because more dispersed vanadia can provide more active sites. On the other hand, the amount of bulk-like vanadia also increased with V_2O_5 content. It is known that vanadia does not disperse well on the surface of a silica support. As was shown in Figure 28, some crystalline V_2O_5 could be observed by XRD in the 5.0 wt% V_2O_5-SiO_2 xerogel. Due to the lack of sensitivity of XRD in detecting very small crystalline particles, it is quite possible that microcrystalline vanadia was also present in the xerogels containing 3.0 and 4.0 wt% vanadia content.

Solid-state ^{51}V NMR studies of supported V_2O_5/SiO_2 catalysts prepared *via* a different method indicated the presence of microcrystalline vanadia species even at very low vanadia loadings, such as in a 1.6 wt% catalyst [92]. The bulk-like vanadia of the crystalline V_2O_5 has an octahedral structure, which is suggested as an active site for further oxidation of formaldehyde to CO and CO_2 [89]. It was also observed that pure V_2O_5 showed a much higher activity for partial oxidation of methanol than the 1.0 wt% supported V_2O_5/SiO_2 catalyst [73]. The turnover frequency of methanol oxidation catalyzed by pure V_2O_5 was ten times greater than that catalyzed by the 1.0 wt% supported V_2O_5/SiO_2 catalyst.

Therefore, the decreases in methanol and formaldehyde selectivities with an increase in vanadia content may be attributed to the further oxidation of oxygenates on bulk-like vanadia. ^{51}V NMR analyses of the xerogel catalysts prepared here have been carried out to characterize the state of vanadium in the V_2O_5-SiO_2 xerogel catalysts.

Solid state ^{51}V NMR is a powerful approach for studies of the local environments of ^{51}V nuclei in vanadia-supported catalysts due to the fact that the ^{51}V nucleus (I = 7/2) has a 99.76% natural abundance, a large magnetic moment, and short spin-lattice relaxation times. The direct proportionality of the NMR peak area to the number of nuclei makes this method an effective technique for quantitative studies. In recent years, solid state ^{51}V NMR has been widely used to characterize vanadia-based solid catalysts, e.g. V_2O_5/Al_2O_3, V_2O_5/TiO_2, V_2O_5/ZrO_2, V_2O_5/SnO_2, V_2O_5/MgO, V_2O_5/TiO_2-ZrO_2, $Rh/V_2O_5/SiO_2$, $V_2O_5/AlPO_4$, and V_2O_5-$K_2S_2O_7$, and the results of those studies have been discussed in a review paper [95]. V_2O_5/SiO_2 catalysts prepared *via* impregnation were investigated by Lapina et al. [95] and Koranne et al. [92], and two NMR peaks at *ca.* -300 and -550 to -600 ppm were observed in the spectra of the V_2O_5/SiO_2 catalysts. Attempts have been made to assign the former peak to the octahedral V species of crystalline V_2O_5 and the latter to VO_4 tetrahedral surface species by comparing the peak positions with those of model compounds with established vanadium symmetries [95,96].

Following synthesis and catalytic testing of the V_2O_5-SiO_2 xerogel catalysts, static solid state ^{51}V NMR spectra of 1.0, 2.0, 3.0, 4.0, 5.0, 10.0, 15.0, and 20.0 wt% V_2O_5-SiO_2 xerogels were obtained at 78.93 MHz on a General Electric Model GN-300 spectrometer, which was equipped with a Nicolet 2090-IIIA high-speed digital oscilloscope and a 7-mm MAS-NMR Doty probe. The measurements were carried out with a simple one-pulse sequence (Bloch decay) with a pulse width of 1 μs, a preacquization delay of 10 sec, a dwell time of 0.5 μs, a relaxation delay of 5-10 sec, 4,000 data points, and 3840 scans for each sample. Prior to Fourier transform analysis, a line broadening factor of 600 Hz was applied. All chemical shifts were referenced against liquid $VOCl_3$. Prior to analysis, the V_2O_5-SiO_2 xerogel samples were dehydrated by calcination at 550°C for 4 hr, cooling in a desiccator containing dehydrated 4A zeolite, followed by transfer to an NMR sample holder in a glove box with a flow of dry nitrogen. Hydrated samples were obtained by exposing the dehydrated samples to the ambient atmosphere for a couple of days or wetting with water followed by drying at 120°C for 1 hr.

Experimental Results. Figure 41 shows the static solid state ^{51}V NMR spectra of dehydrated V_2O_5-SiO_2 xerogel catalyst samples as a function of vanadia content. For 1.0 and 2.0 wt% V_2O_5-SiO_2 xerogels, only peak A with $\delta \approx$ -510 ppm was observed. When the content of vanadium in the samples equaled or exceeded the equivalent of 3.0 wt% vanadia, a new peak (B) with $\delta \approx$ -280 ppm appeared in the spectra. Peak B increased with an increase in vanadia content. Previous studies conducted by other researchers [92,95] have indicated that peak A could be attributed to tetrahedral V surface species and peak B to octahedral V sites in crystalline V_2O_5. The use of a short pulse length (1 μs) and a long

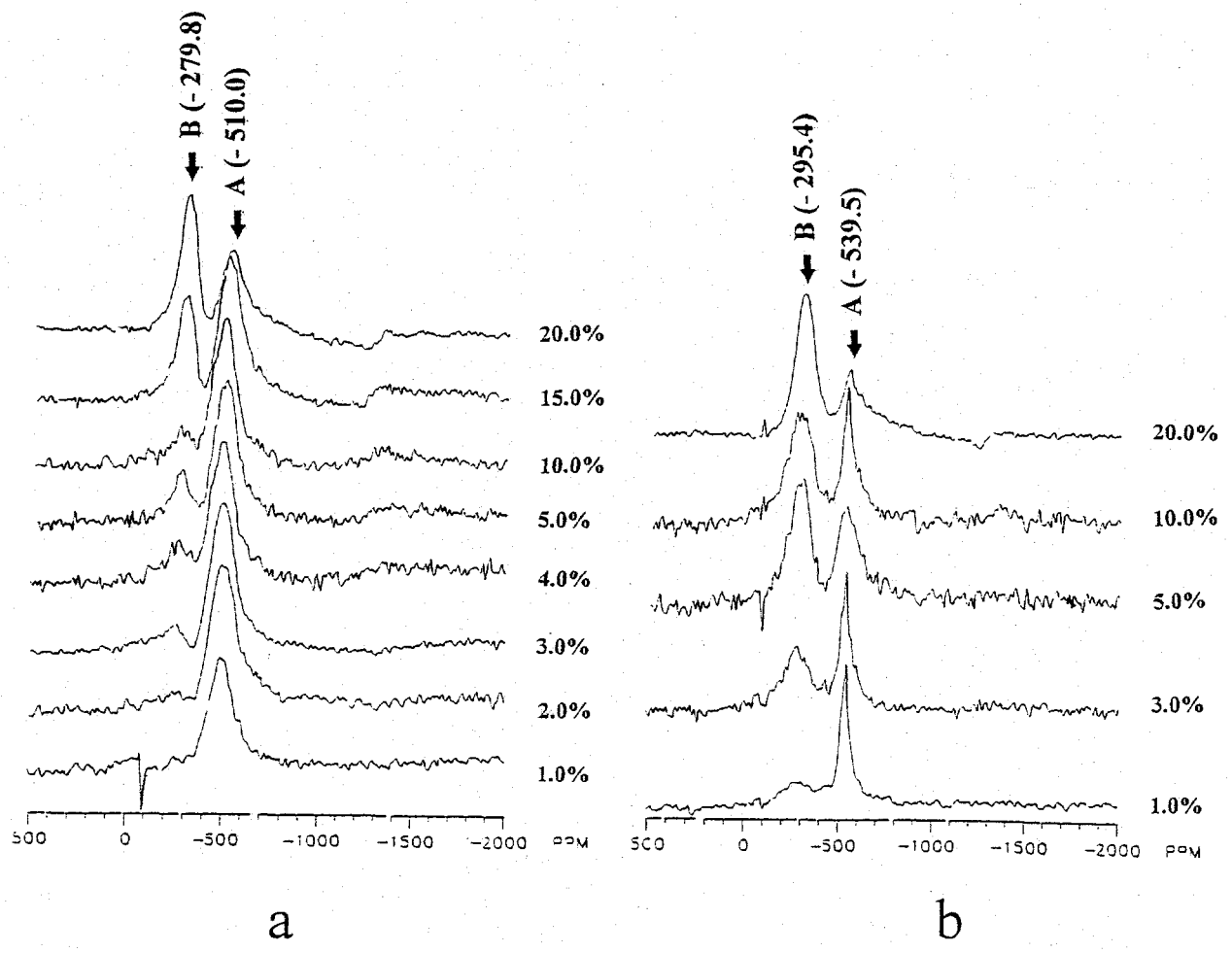

FIGURE 41. Static solid state ^{51}V NMR spectra of (a) dehydrated V_2O_5-SiO_2 xerogel catalysts and (b) samples after hydration by exposure to the ambient atmosphere for a few days.

relaxation delay (5 to 10 sec) provides for reliable determination of signal fractions from peak intensities. The signal fractions and calculated compositions of two kinds of the V species are shown in Table 18, indicating that the dispersed V species increased with the increase of total vanadia content up to a critical dispersion capacity of *ca.* 9.5 wt%.

These results coincide well with the catalytic testing data observed here (Table 11) for V_2O_5-SiO_2 xerogel catalysts, which showed that the 2.0 wt% V_2O_5-SiO_2 xerogel catalyst gave the highest space time yields of and selectivities to methanol and formaldehyde in the partial methane oxidation. The 2.0 wt% V_2O_5-SiO_2 catalyst possessed more tetrahedral V surface species acting as active sites for partial methane oxidation than the 1.0 wt% V_2O_5-SiO_2 catalyst. However, for the catalysts containing more than 3.0 wt% vanadia, the presence of crystalline V_2O_5 increased the oxidation of methanol and formaldehyde by secondary reactions to carbon oxides, although these catalysts contained more dispersed

Table 18. Relative ^{51}V NMR signal areas and compositions of two V species in V_2O_5-SiO_2 xerogel catalysts.

V_2O_5 (wt%)	Dehydrated Samples					Hydrated Samples	
	Signal Fraction (%)*		V Species #			Signal Fraction (%)*	
	Peak A	Peak B	Dispersed V_2O_5 (wt%)	Crystalline V_2O_5 (wt%)	Crystalline V_2O_5 (g V_2O_5/ g SiO_2)	Peak A	Peak B
1.0	100	0.0	1.0	0.0	0.000	67.3	32.7
2.0	100	0.0	2.0	0.0	0.000	--	--
3.0	81.7	18.3	2.5	0.5	0.005	45.9	54.1
4.0	78.6	21.4	3.1	0.9	0.009	--	--
5.0	76.7	23.3	3.8	1.2	0.012	48.0	52.0
10.0	78.6	21.4	7.9	2.1	0.021	40.7	59.3
15.0	63.6	36.4	9.5	5.5	0.058	--	--
20.0	45.7	54.3	9.1	10.9	0.122	37.7	62.3

*Estimated error = ±10%.
#Calculated from the relative ^{51}V NMR signal areas.

species than that in the 2.0 wt% xerogel catalyst. Therefore, an important issue for preparation of V_2O_5-SiO_2 catalysts is to design a suitable process not only to create a large amount of V surface species but also to avoid the formation of crystalline V_2O_5 in the final catalysts.

Water adsorption of V_2O_5-SiO_2 xerogels increased the signal intensity of peak B but decreased the intensity of peak A, suggesting that the tetrahedral surface V species interacted with water molecules to form distorted octahedral V sites, as reported previously for other for V_2O_5/SiO_2 catalysts studied by solid state NMR, EPR and IR [95-97]. It was also found that peak A did not disappear even though the V_2O_5-SiO_2 samples remained in the air for a few days or were wetted with water. Even with exposure to excess water , the results indicate that some of the tetrahedral V species in V_2O_5-SiO_2 xerogel samples did not changed their coordination environment after water adsorption.

There is a possibility that a small fraction of the vanadium ions is immobilized in the silica matrix in the V^{4+} state, as previously known in V_2O_5-SiO_2 gels [66]. The V^{4+} species has a tetrahedral coordination with oxygen atoms, which makes a contribution to peak A but does not interact with water molecules. However, Table 18 shows that the signal fraction of peak A in the hydrated samples was almost 50%, implying existence of another type of tetrahedral surface V species that was not readily coordinated by water molecules. This type of tetrahedral surface V species has been observed in V_2O_5/Al_2O_3 catalysts at low surface coverage by other researchers using EXAFS/XANES and NMR [40,96].

Calculation of Reaction TurnOver Numbers for the Xerogel Catalysts. Using only the portion of vanadium present as tetrahedral (surface dispersed) species (see Table 18), the turnover numbers (T.O.N.) for methane conversion to products and of the formation of methanol and formaldehyde over these catalysts (see Table 11) have been calculated, and they are given in Table 19.

TABLE 19. The calculated turnover numbers (T.O.N.), along with methane conversions, obtained with the V_2O_5/SiO_2 xerogel catalysts containing 1.0-20.0 wt% vanadia. The reaction mixture consisted of CH_4/air/steam = 1.5/1.0/0.56 with GHSV = 183,600 ℓ/kg catal/hr. Catalyst testing was carried out at the temperatures indicated and at a pressure of 0.45 MPa.

V_2O_5 (wt%)	Temp (°C)	CH_4 Conv. (mol%)	Turnover Numbers (10^{-2} sec^{-1})		
			CH_4	CH_3OH	HCHO
1.0	550	0.42	4.27	0.08	1.58
	575	0.77	7.80	0.64	2.86
	600	4.25	43.2	0.95	5.01
	625	10.70	109	0.76	5.32
2.0	550	0.31	1.58	0.31	0.88
	575	1.10	5.61	0.70	0.56
	600	2.00	10.2	0.73	1.29
	625	3.06	15.6	1.05	2.01
	650	4.87	24.8	1.06	1.76

TABLE 19 (Continued). The calculated turnover numbers (T.O.N.), along with methane conversions, obtained with the V_2O_5/SiO_2 xerogel catalysts containing 1.0-20.0 wt% vanadia. The reaction mixture consisted of CH_4/air/steam = 1.5/1.0/0.56 with GHSV = 183,600 ℓ/kg catal/hr. Catalyst testing was carried out at the temperatures indicated and at 0.45 MPa.

V_2O_5 (wt%)	Temp (°C)	CH_4 Conv. (mol%)	Turnover Numbers (10^{-2} sec^{-1})		
			CH_4	CH_3OH	HCHO
3.0	550	0.28	1.14	0.24	0.67
	575	0.75	3.06	0.38	1.66
	600	1.15	4.69	0.35	2.03
	625	1.57	6.41	0.54	2.10
	650	1.91	7.79	0.64	2.01
5.0	550	0.10	0.27	0.05	0.10
	575	1.25	3.36	0.13	0.38
	600	1.67	4.48	0.13	0.80
	625	2.07	5.56	0.13	0.90
10.0	575	1.05	1.36	0.06	0.20
	600	1.24	1.60	0.06	0.45
	625	1.50	1.94	0.09	0.62
	650	1.19	1.56	0.12	0.24
20.0	550	0.04	0.05	0.0	0.0
	575	0.09	0.10	0.0	0.01
	600	0.35	0.39	0.00	0.01
	625	3.2	3.59	0.00	0.02
	650	4.26	4.78	0.00	0.02

The turnover numbers for the 1.0-5.0 wt% V_2O_5/SiO_2 xerogel catalysts at approximately 1 mol% methane conversion are tabulated in Table 20. This level of conversion was principally observed at a reaction temperature of 575°C. The turnover numbers are expressed as molecules of methane converted per dispersed V atom, where the number of vanadium atoms was determined from NMR analyses as previously noted. While there is scatter in this data, the turnover numbers suggest that methane activation and conversion needs only one type of active site. At higher vanadia contents (>5 wt% V_2O_5), the observed turnover numbers were appreciably lower at reaction temperatures such as 575-600°C, indicating that the active tetrahedral vanadium species in these samples were less available for activation of methane. This lower activity of dispersed V sites as the concentration of this tetrahedrally coordinated type of species increases might be due to polymerization of the active surface-held V to form less active dimers, trimers, etc.

TABLE 20. Turnover numbers for methane conversion to products over V_2O_5/SiO_2 xerogel catalysts from a CH_4/air/steam = 1.5/1.0/0.56 volume ratio reactant mixture with GHSV = 183,600 ℓ/kg catal/hr at 0.45 MPa.

V_2O_5 (wt%)	% Dispersed V[a]	Dispersed V (wt% V_2O_5)	Temp. (°C)	CH_4 Conv. (mol%)	T.O.N. (10^{-2} sec^{-1})
1.0	100	1.0	575	0.77	7.80
2.0	100	2.0	575	1.10	5.61
3.0	81.7	2.5	575	0.75	3.06
3.0	81.7	2.5	600	1.15	4.69
5.0	76.7	3.8	575	1.25	3.36

[a]Expressed as equivalent %V_2O_5, calculated from the intensities of the ^{51}V NMR signal assignable to a T_d environment relative to the total intensities of the ^{51}V peak.

CONCLUSIONS

Significant progress has been made in the direct selective conversion of methane to C_2 hydrocarbons, formaldehyde, and methanol under moderate reaction conditions. Each of these products have been formed in very high space time yields or in the highest space time yield reported to-date in the literature, as described below. Different catalysts and engineering concepts were developed and utilized in synthesizing these three different products, but optimization of the synthesis processes has not yet been carried out.

To form **C_2 hydrocarbons** directly from methane, it was found that sulfate doping of the strongly basic SrO/La_2O_3 catalyst doubled the conversion and improved the selectivity in the oxidative coupling of CH_4 to C_2 hydrocarbons. At reaction tempertures that are moderate for oxidative coupling, e.g. 550°C with CH_4/air = 1/1 at GHSV = 70,000 ℓ/ kg catal/hr, the sulfate doping showed a maximum effect at 1 wt% SO_4^{2-} concentration. For this catalyst, the C_2 space time yield at 550°C was 72 mol/kg catal/hr (>2 kg/kg catal/hr) with 20% CH_4 conversion and 50% C_2 selectivity. The sulfated catalysts showed high catalytic stability under these reaction conditions, with no deactivation observed during a 25 hr test. The C_2 hydrocarbon product selectivity increased with CH_4 conversion for catalysts of all compositions, including undoped catalysts, and all testing sequences between 500 and 700°C, supporting the same principal synthesis mechanism for all samples. At lower GHSV (down to 5,400 ℓ/ kg catal/hr), carbonate build-up, supported by characterization studies, partially poisoned the $SO_4^{2-}/SrO/La_2O_3$ catalyst at 550°C, but the deactivation was reversed by increasing the reaction temperature above 580°C at GHSV = 70,000 ℓ/ kg catal/hr.

It has been shown here that significant progress has been made toward the goal of selectively oxidizing methane directly to **formaldehyde**, thereby by-passing the high temperature steam reforming and methanol synthesis steps that are part of the current technology of producing formaldehyde. It was demonstrated that vanadia supported on high surface area silica (Cab-O-Sil) exhibited high catalytic activities and selectivities from CH_4/air = 1.5/1.0 reaction gas mixtures at moderate temperatures, e.g. 600°C, and space time yields of >1 kg formaldehyde/kg catal/hr were achieved (see Table 6). The conversion of methane to products was limited by the availability of oxygen, and the influence of the CH_4/O_2 reactant ratio on the oxygenate product selectivity needs to be investigated.

As pointed out in the Introduction, it was earlier proposed that a role of steam during partial oxidation reactions with methane should be to react with surface methoxide species to form methanol [4,23]. The results shown here with the double bed catalyst configuration are consistent with this, where the first catalyst generates methyl radicals and the second catalyst bed acts as the methyl radical trapping and oxygenate-forming catalyst. The additional H_2O present over the second catalyst bed because of the injected steam enhanced the productivity of **methanol**, as well as of formaldehyde (e.g. see Figure 25). Indeed, using

a double bed catalyst system ($SO_4^{2-}/SrO/La_2O_3 \| V_2O_5/SiO_2$) with steam present significantly increased the productivity of methanol as compared wiht a single bed V_2O_5/SiO_2 catalyst or using the double bed catalyst without the presence of steam in the reactant mixture (see Figure 24 and 25). The space time yield of methanol reached 100 g/kg catal/hr.

The principal reactions envisaged for this dual catalyst system are schematically illustrated by Equations (16)-(21), where $\square_o$ represents an oxygen vacancy and Reactions (18) and (21) occur in parallel.

$$2\,CH_4 + 0.5\,O_2 \rightarrow 2\,{}^{\bullet}CH_3 + H_2O \qquad \textit{First catalyst layer} \qquad (16)$$

$$2\,{}^{\bullet}CH_3 + 2\,M^{(n+1)+}O^{2-} \rightarrow 2\,M^{n+}(OCH_3)^- \qquad (17)$$

$$2M^{n+}(OCH_3)^- + 2H_2O \rightarrow 2M^{n+}(OH)^- + 2CH_3OH \qquad (18)$$

$$2\,M^{n+}(OH)^- \rightarrow M^{n+}O^{2-} + M^{n+}\square_o + H_2O \qquad (19)$$

$$M^{n+}O^{2-} + M^{n+}\square_o + 0.5\,O_2 \rightarrow 2\,M^{(n+1)+}O^{2-} \qquad (20)$$

$$2M^{n+}(OCH_3)^- + 1.5\,O_2 \rightarrow 2M^{(n+1)+}O^{2-} + 2HCHO + H_2O \qquad (21)$$

Second catalyst layer

The high space time yields of formaldehyde achieved in this research are shown in Figure 42 as a comparison of the results obtained by others, including those of Sun et al. [56] with a silica catalyst and of Parmallana et al. [54] with a vanadia/silica catalyst. As indicated out, HCHO productivities of >1.2 kg/kg catal/hr have been achieved over the silica-supported vanadia catalysts, although higher selectivities are needed. Thus, significant progress has been made in the challenging task of directly synthesizing HCHO, and CH_3OH, from CH_4.

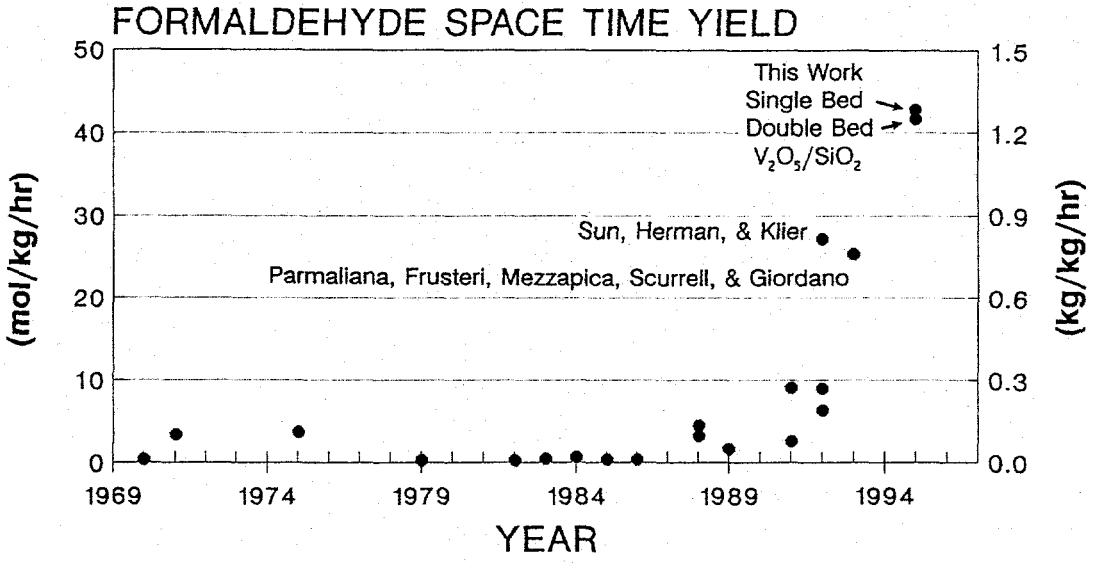

FIGURE 42. Comparisons of the space time yields of formaldehyde achieved here by direct methane oxidation over V_2O_5/SiO_2 catalysts in continuous flow reactors with the productivities reported earlier (see also Figures 1 and 4).

ACKNOWLEDGEMENTS

Partial support of this research by the AMOCO Corporation is gratefully acknowledged. We appreicate the input and discussions with M. M. Bhasin of Union Carbide Corporation, and equipment provided by Union Carbide Corporation is also gratefully acknowledged. We appreciate the direction given by the catalyst testing experiments of Isabel Di Cosimo and the contributions of J.-M. Jehng, H. Hu, and I. E. Wachs in carrying out the laser Raman experiments and data analysis. Guidance for this research project was provided by Rodney Malone of U.S. DOE-METC.

LIST OF PUBLICATINS TO-DATE

"Oxidative Coupling of Methane Over Sulfated Sr/La_2O_3 Catalysts," J. Sárkány, Q. Sun, R. G. Herman, and K. Klier, Preprint, Div. Pet. Chem., ACS, **39(2)**, 226-230 (1994).

"Oxidative Coupling of Methane Over Sulfated SrO/La_2O_3 Catalysts," J. Sárkány, Q. Sun, J. I. Di Cosimo, R. G. Herman, and K. Klier, in "*Methane and Alkane Conversion Chemistry*," ed. by M. M. Bhasin and D. N. Slocum, Plenum Press, New York, 31-38 (1995).

"Partial Oxidation of Methane by Molecular Oxygen Over Supported V_2O_5 Catalysts: A Catalytic and *in situ* Raman Spectroscopy Study," Q. Sun, J.-M. Jehng, H. Hu, R. G. Herman, I. E. Wachs, and K. Klier, in "*Methane and Alkane Conversion Chemistry*," ed. by M. M. Bhasin and D. N. Slocum, Plenum Press, New York, 219-226 (1995).

"Direct Conversion of Methane to Methanol and Formaldehyde Over a Double-Layered Catalyst Bed in the Presence of Steam," C. Shi, Q. Sun, H. Hu, R. G. Herman, K. Klier, and I. E. Wachs, J. Chem. Soc., Chem. Commun., 663-664 (1996).

"*In situ* Raman Spectroscopy During the Partial Oxidation of Methane to Formaldehyde over Supported Vanadium Oxide Catalysts," Q. Sun, J.-M. Jehng, H. Hu, R. G. Herman, I. E. Wachs, and K. Klier, J. Catal., **165**, 91-101 (1997).

"Development of Active Oxide Catalysts for the Direct Oxidation of Methane to Formaldehyde," R. G. Herman, Q. Sun, C. Shi, K. Klier, C.-B. Wang, H. Hu, I. E. Wachs, and M. M. Bhasin, Catal. Today, (1997); in press.

"Preparation, Characterization, and Catalytic Properties of V_2O_5/SiO_2 Xerogels for Selective Oxidation of Methane to Oxygenates," C.-B. Wang, C. Shi, Q. Sun, R. G. Herman, K. Klier, and J. E. Roberts, J. Catal.,; manuscript under revision.

"Partial Oxidation of Methane to Oxygenates Over Transition Metal Oxide Catalysts in the Presence of Steam," C. Shi, C.-B. Wang, Q. Sun, R. G. Herman, and K. Klier, manuscript under preparation.

REFERENCES

1. Keller, G. E. and Bhasin, M. M., J. Catal., **73** (1982) 9.

2. Foster, N. R., Appl. Catal., **19** (1985) 1.

3. Gesser, H. D., Hunter, N. R., and Prakash, C. B., Chem. Rev., **85(4)** (1985) 235.

4. Pitchai, R. and Klier K., Catal. Rev.-Sci. Eng., **28** (1986) 13.

5. Scurrell, M. S., Appl. Catal., **32** (1987) 1.

6. Lee, J. S. and Oyama, S. T., Catal. Rev.-Sci. Eng., **30** (1987) 249.

7. Hutchings, G. J., Scurrell, M. S., and Woodhouse, J. R., Chem. Soc. Rev., **18** (1989) 251.

8. Lunsford, J. H., Catal. Today, **6** (1990) 235.

9. Lunsford, J. H., in "*Natural Gas Conversion*" (Studies in Surface Science and Catalysis, Vol. 61), ed. by A. Holmen, K.-J. Jens, and S. Kolboe, Elsevier, New York, (1991) 3.

10. Mackie, J. C., Catal. Rev.-Sci. Eng., **33** (1991) 169.

11. Amenomiya, Y., Birss, V. I.,Goledzinowski, M., Galuska, J., and Sanger, A. R., Catal Rev.-Sci. Eng., **32** (1990) 163 .

12. Hamid, H. B. A. and Moyes, R. B., Catal. Today, **10** (1991) 267.

13. Forlani, O. and Rossini, S., Mat. Chem. Phys., **31** (1992) 155.

14. Krylov, O. V., Catal. Today, **18** (1993) 209.

15. Zhang, Z., Verykios, X. E., and Baerns, M., Catal. Rev.-Sci. Eng., **36** (1994) 507.

16. Holm, M. M. and Reichl, E. H., Fiat Report No. 1085, U.S. Office of Miliary Government for Germany (March 31, 1947).

17. Cullis, C. F., Keene, D. E., and Trimm, D. L., J. Catal., **19** (1970) 378.

18. Mann, R. S. and Dosi, M. K., J. Chem. Technol. Biotechnol., **29** (1979) 467.

19. Dowden, D. A. and Walker, G. T., U.K. Patent 1,244,001 (Aug. 25, 1971); assigned to ICI, England.

20. Stroud, H. J. F., U.K. Patent 1,398,385 (June 18, 1975); assigned to British Gas Corp.

21. Liu, R.-S., Iwamoto, M., and Lunsford, J. H., J. Chem. Soc., Chem. Commun., (1982) 78.

22. Iwamoto, M., Japan. Kokai Tokkyo Koho 5,892,629 (June 2, 1983).

23. Liu, H.-F., Liu, R.-S., Liew, K. Y., Johnson, R. E., and Lunsford, J. H., J. Am. Chem. Soc., **106** (1984) 4117.

24. Khan, M. M. and Somorjai, G. A., J. Catal., **91** (1985) 263.

25. Spencer, N. D., J. Catal., **109** (1988) 187.

26. Spencer, N. D., Pereira, C. J., and Grasselli, R. K., J. Catal., **126** (1990) 546.

27. Kennedy, M., Sexton, A., Kartheuser, B., Mac Giolla Coda, E., McMonagle, J. B., and Hodnett, B. K., Catal. Today, **13** (1992) 447.

28. Hu, H., Wachs, I. E., and Bare, S. R., J. Phys. Chem., **99** (1995) 10897.

29. de Boer, M., van Dillen, A. J., Koningsberger, D. C., Geus, J. W., Vuurman, M. A., and Wachs, I. E., Catal. Letters, **11** (1991) 227.

30. Cornac, M., Janin, A., and Lavalley, J. C., Polyhedron, **5** (1986) 183.

31. Banares, M. A., Hu, H., and Wachs, I. E., J. Catal., **150** (1994) 407.

32. Banares, M. A., Spencer, N. D., Jones, M. D., and Wachs, I. E., J. Catal., **146** (1994) 204.

33. Kasztelan, S., Payen, E., and Moffat, J. B., J. Catal., **112** (1988) 320.

34. Banares, M. A., Hu, H., and Wachs, I. E., J. Catal., **155** (1995) 249.

35. Rocchiccioli-Deltcheff, C., Amirouche, M., Che, M., Tatibouet, J. M., and Fournier, M., J. Catal., **125** (1990) 2892.

36. Spencer, N. D. and Pereira, C. J., J. Catal., **116** (1989) 399.

37. Iwamoto, M., Japan. Kokai Tokkyo Koho 5,892,630 (June 2, 1983).

38. Lee, I. and Ng, K. Y. S., Preprints, Div. Fuel Chem., ACS, **33(3)** (1988) 403.

39. Das, N., Eckert, H., Hu, H., Wachs, I. E., Walzer, J. F., and Feher, F. J., J. Phys. Chem., **97** (1993) 8240.

40. Yoshida, S. Tanaka, U., Nishimura, Y., Mizutani, H., and Funabiki, T., Proc. 9th Intern. Congr. Catal., **3** (1988) 1473.

41. Oyama, T., Went, G. T., Lewis, K. B., Bell, A. T., and Somorjai, G. A., J. Phys. Chem., **93** (1989) 6786.

42. Anderson, J. R. and Tsai, P., J. Chem. Soc., Chem. Commun., (1987) 1435.

43. Sojka, Z., Herman, R. G., and Klier, K., in *"Preprints Supplement, Symp. on Methane Activation, Conversion, and Utilization,"* PACIFICHEM '89, Intern. Chem. Congr. of Pacific Basin Societies, Honolulu, HI, (1989) 7.

44. Sojka, Z., Herman, R. G., and Klier, K., J. Chem. Soc., Chem. Commun., (1991) 185.

45. Hargreaves, J. S. J., Hutchings, G. J., and Joyner, R. W., Nature (London), **348** (1990) 428.

46. Hargreaves, J. S. J., Hutchings, G. J., and Joyner, R. W., Appl. Catal., **77** (1991) N18.

47. Sun, Q., Di Cosimo, J. I., Herman, R. G., Klier, K., and Bhasin, M. M., Catal. Letters, **15** (1992) 371.

48. DeBoy, J. M. and Hicks, R. G., Ind. Eng. Chem. Res., **27** (1988) 1577.

49. DeBoy, J. M. and Hicks, R. G., J. Catal., **113** (1988) 517.

50. Kasztelan, S. and Moffat, J. B., J. Chem. Soc., Chem. Commun., (1987) 1663.

51. Kastansa, G. N., Tsigdinos, G. A., and Schwank, J., Appl. Catal., **44** (1988) 33.

52. Kastansa, G. N., Tsigdinos, G. A., and Schwank, J., J. Chem. Soc., Chem. Commun., (1988) 1298.

53. Ahmed, S. and Moffat, J. B., Appl. Catal., **58** (1990) 83.

54. Parmaliana, A., Frusteri, F., Miceli, D., Mezzapica, A., Scurrell, M. S., and Giordano, N., Appl. Catal., **78** (1991) L7.

55. Matsumura, Y., Hashimoto, K., and Moffat, J. B., Catal. Letters, **13** (1992) 283.

56. Sun, Q., Herman, R. G., and Klier, K., Catal. Letters, **16** (1992) 251.

57. Dautzenberg, F. M., in "*Preprints, Symp. on Methane Activation, Conversion, and Utilization*," PACIFICHEM '89, Intern. Chem. Congr. of Pacific Basin Societies, Honolulu, HI, Paper No. 170, (1989) 163.

58. Aika, K. I. and Aono, K., J. Chem. Soc., Faraday Trans., **87** (1991) 1273.

59. Romijn, G., Z. Anal. Chem., **36** (1877) 19; Walker, J. F., "*Formaldehyde,*" 3rd Ed., Reinhold Publ. Corp., New York, (1964) 489.

60. Brown, M. J. and Parkyns, N. D., Catal. Today, **8** (1991) 305.

61. Zhen, K. J., Mark, C. H., Lewis, K. B., and Somorjai, G. A., J. Phys. Chem., **94** (1985) 501.

62. Koranne, M. M., Goodwin, J. G., Jr., and Marcelin, G., J. Phys. Chem., **97** (1993) 673.

63. Haber, J., Kozowska, A., and Kozowski, R. J., J. Catal., **102** (1986) 52 .

64. Roozeboom, F., Mittelmeijer-Hazeleger, M. C., Moulijn, J. A., Medema, J., de Beer, V. H., and Gellings, P. J., J. Phys. Chem., **84** (1980) 2783 .

65. Kijenski, J., Baiker, A., Glinski, M., Dollenmeier, P., and Workaun, A., J. Catal., **101** (1986) 1.

66. Baiker, A., Dollenmeier, P., Glinski, M., Reller, A., and Sharma, V. K., J. Catal., **111** (1988) 273.

67. Miceli, D., Arena, F., Parmaliana, A., Scurrell, M. S., and Sokolovskuu, V., Catal. Lett., **18** (1993) 283.

68. Taylor, R. P. and Schrader, G. L., Ind. Eng. Chem. Res., **30** (1991) 1016.

69. Conway, S. J., Greig, J. A., and Thomas, G. M., Appl. Catal. A, **86** (1992) 199.

70. Xu, M.-T. and Lunsford, J. H., Catal. Lett., **11** (1991) 295.

71. Nakamoto, K., "*Infrared and Raman Spectra of Inorganic and Coordination Compounds,*" 4th. ed., John Wiley & Sons, Inc. (1986).

72. Herman, R. G., Bogdan, C. E., Sommer, A. J., and Simpson, D. R., Appl. Spectrosc., **41** (1987) 437.

73. Deo, G. and Wachs, I. E., J. Catal., **129** (1991) 307.

74. Taouk, B., Guelton, M., Grimblot, J., and Bonnelle, J. P., J. Phys. Chem., **92** (1988) 6700.

75. Vuurman, M. A., Wachs, I. E., and Hirt, A., J. Phys. Chem., **95** (1991) 8781.

76. Vuurman, M. A., and Wachs, I. E., J. Phys. Chem., **96** (1992) 5008.

77. Deo, G., Wachs, I. E., and Haber, J., Crit. Rev. Surf. Chem., **4(3/4)** (1994) 141.

78. Tallant, D. R., Bunker, B. C., Brinker, C. J., and Balfe, C. A., in *"Better Ceramics Through Chemistry II,"* ed. by C. J. Brunker, D. E. Clark, and D. R. Ulrich, Materials Research Society, Pittsburgh, PA, (1986) 261.

79. Varshal, B. G., Denisov, V. N., Marvin, B. N., Parlova, G. A., Podobedov, V. B., and Sterin, K. E., Opt. Spectrosc. (USSR), **47** (1979) 344.

80. Roark, R. D., Kohler, S. D., Ekerdt, J. G., Kim, D. S., and Wachs, I. E., Catal. Lett., **16** (1992) 77.

81. de Boer, M., van Dillen, A. J., Koningsberger, D. C., Geus, J. W., Vuurman, M. A., and Wachs, I. E., Catal. Lett., **11** (1991) 227.

82. Jehng, J. M. and Wachs, I. E., Catal. Lett., **13** (1992) 9.

83. Pomonis, P. J. and Vikerman, J. C., Disc. Faraday Soc., **72** (1982) 247.

84. Ono, T., Nakagawa, Y., and Kubokawa, Y., Bull. Chem. Soc. Jpn., **54** (1981) 343.

85. Pasquali, M., Marchetti, F., Floriani, C., and Merlino, S., J. Chem. Soc., Dalton, (1977) 139.

86. Sachtler, W. M. H. and de Boer, N. D., Proc. 3rd. Intern. Congr. Catal.-*1964*, Amsterdam, **1** (1965) 252.

87. Bielanski, A. and Haber, J., Catal. Rev. Sci. Eng., **19** (1979) 1.

88. Datka, J., Turek, A. M., Jehng, J. M., and Wachs, I. E., J. Catal., **135** (1992)186 .

89. Snyder, T. P. and Hill, Jr., C. G., Catal. Rev.-Sci. Eng., **31** (1989) 43.

90. Sokolovskii, V. D., Catal. Rev.-Sci. Eng., **32** (1990) 1.

91. Wachs, I. E., Chem. Eng. Sci., **45** (1990) 2561.

92. Koranne, M. M., Goodwin, Jr., J. G., and Marcelin, G., J. Catal., **148** (1994) 369.

93. Koranne, M. M., Goodwin, Jr., J. M., and Marcelin G., J. Catal., **148** (1994) 388.

94. Weber, R. S., J. Phys. Chem., **98** (1994) 2999.

95. Lapina, O. B., Mastikhin, V. M., Shubin, A. A., Krasilnikov, V. N., and Zamaraev, K. I., Prog. NMR Spectrosc., **24** (1992) 457.

96. Eckert, H. and Wachs, I. E., J. Phys. Chem., **93** (1989) 6796.

97. Norayana, M., Narasimha, C. S., and Kevan, L., J. Catal., **79** (1983) 237.